AIAA 2020-2021 Undergraduate Team Design RFP

Light Attack Aircraft: Team Chimera

KU Aerospace Engineering Department

Justin Gassmann
#1144049

Connor Kinkade
#977208

Benett Miller
#2047399

Tyler Miller
#1081653

Hunter Ryll
#1082991

Cole Williams
#1083432

Faculty Advisor: Dr. Ronald Barrett #022393

Table of Contents

List of Figures

[1] Chimera Logo Header, Ref. 1

List of Tables

List of Symbols

Symbols	Description	Units
a	Acceleration	(ft/s^2)
AR	Aspect Ratio	(~)
b	Wingspan	(ft)
c	Thrust Specific Fuel Consumption	(lb/lb/hr)
C	Chord Length	(ft)
C_L	Coefficient of Lift	(~)
d	Diameter	(in)
D	Drag	(lbs)
IE	Impact Energy	(ft-lbf)
L	Lift	(lbs)
P	Power	(hp)
S	Wing Area	(ft^2)
SR	Specific Range	(nmi/lb)
t	Time	(s)
T	Thrust	(lb)
V	Airspeed	(knots)
W	Weight	(lb)
X	Horizontal Position	(ft)
Z	Vertical Position	(ft)

Greek Symbols	Description	Units
γ	Flight Path Angle	Degrees

Subscripts	Description
cr	Cruise
crew	Crew
E	Empty
F	Fuel
j	Jet
L	Landing
loiter	Loiter
pl	Payload
r	root
t	tip
tfo	Trapped Fuel and Oil
TO	Takeoff

Abbreviations	Description
AAA	Advanced Aircraft Analysis
AEO	All Engines Operative
AO	Ancillary Objective
APEX	Armor Piercing Explosive
BASS	Ballistically Aeromechanically Stable Sabot
CEP	Circular Errors Probability
ConOps	Concept of Operations
FOD	Foreign Object Debris/Foreign Object Damage
IR	Infrared

LA ..... Light Attack
LAAR..... Light-Attack/Armed Reconnaissance
LARA..... Light Armed Reconnaissance Aircraft
MK ..... Mark
O..... Objective
OEI..... One Engine Inoperative
R..... Requirement
RFP..... Request for Proposal
ROF..... Relative Objective Function
SAM..... Surface-to-Air Missile
STAMPED..... Statistical Time and Market Predictive Engineering Design
T ..... Tracer
USMCA ..... United States-Mexico-Canada Agreement

Compliance Matrix

The compliance matrix outlining the demonstrated capabilities of the Chimera and the associated location where that information can be found in the report is presented below.

Mission Requirements	Demonstrated	Compliance	Page No.
Austere Field Takeoff Distance	2,819 ft	✓	39
Austere Field Landing Distance	1,928 ft	✓	39
Payload: 3,000 lb armament	3,000 lb	✓	61
Integrated Gun	M197 Electric Cannon	✓	35
Service Ceiling: > 30,000 ft	43,000 ft	✓	38
Crew: 2 with zero-zero ejection seats	2 with zero-zero ejection seats	✓	58
Design Requirements	**Demonstrated**		**Page No.**
Wing and Powerplant Sizing	W/S: 80 lb/ft^2 T/W: 0.31	✓	23
Configuration Down Selection	LO High Mounted Twin Jet	✓	23
Performance Analysis	Figure 21.1, Figure 21.2	✓	67
V-n Diagram	Figure 14.1	✓	36
Materials Selection	Chapter 23: Bill of Materials	✓	72
Scaled Three-Views	Figure 22.1	✓	69
Aircraft Weight Statement	Table 19-I	✓	60
Propulsion System Description	Chapter 6: Wing and Powerplant Sizing	✓	21
Stability and Control Characteristics	Chapter 20: Class II Stability and Control	✓	62
Cost Estimates	Chapter 25: Class II Cost Estimates	✓	75

1. Introduction, Mission Specification, and Profile

Using the RFP provided by the AIAA for the 2020-2021 Team Aircraft Design Competition found in Ref. 2, the following mission specification seen below in Table 1-I was created to lay out the requirements and aid in the design of a light attack aircraft. The objective of the project is to design an affordable light attack aircraft that can operate from short, austere fields near the front lines to provide close air support to ground forces at short notice and complete some missions currently only feasible with attack helicopters [2].

Table 1-I: Light Attack Mission Specification [2]

General Design Requirements	
Crew	Two, both with zero-zero ejection seats
Service Life	15,000 hours over 25 years
Entry into Service	2025
Certification Base	Military MIL-STD-516C & Joint Service Specification Guides
Performance Requirements	
Takeoff/Landing	Takeoff and landing over a 50 ft obstacle in ≤ 4,000 ft when operating from austere fields at density altitude up to 6,000 ft with semi-prepared runways such as grass or dirt surfaces with California Bearing Ratio of 5
Service Ceiling	≥ 30,000 ft
Design Mission Range	100 nmi combat radius, 4 hours on station
Ferry Mission Range	900 nmi
Payload Requirements	
Payload	3000 lbs. of armament
Weapon	Integrated gun for ground targets
Additional Considerations	
Survivability	Consideration for survivability, such as armor for the cockpit and engine, reduced infrared and visual signatures, and countermeasures (chaff, flares, etc.)
Armament	Provisions for carrying/deploying a variety of weapons, including rail-launched missiles, rockets, and 500 lb. (maximum) bombs
Flexibility	Maximize mission use flexibility without undue cost
Best Value	"Best Value" meeting performance objectives over 25-year service life

Also provided in the RFP are mission profiles for a design combat mission and a long-range ferry mission. Figure 1.1 and Figure 1.2 depict these mission profiles and runway requirements in graphical form.

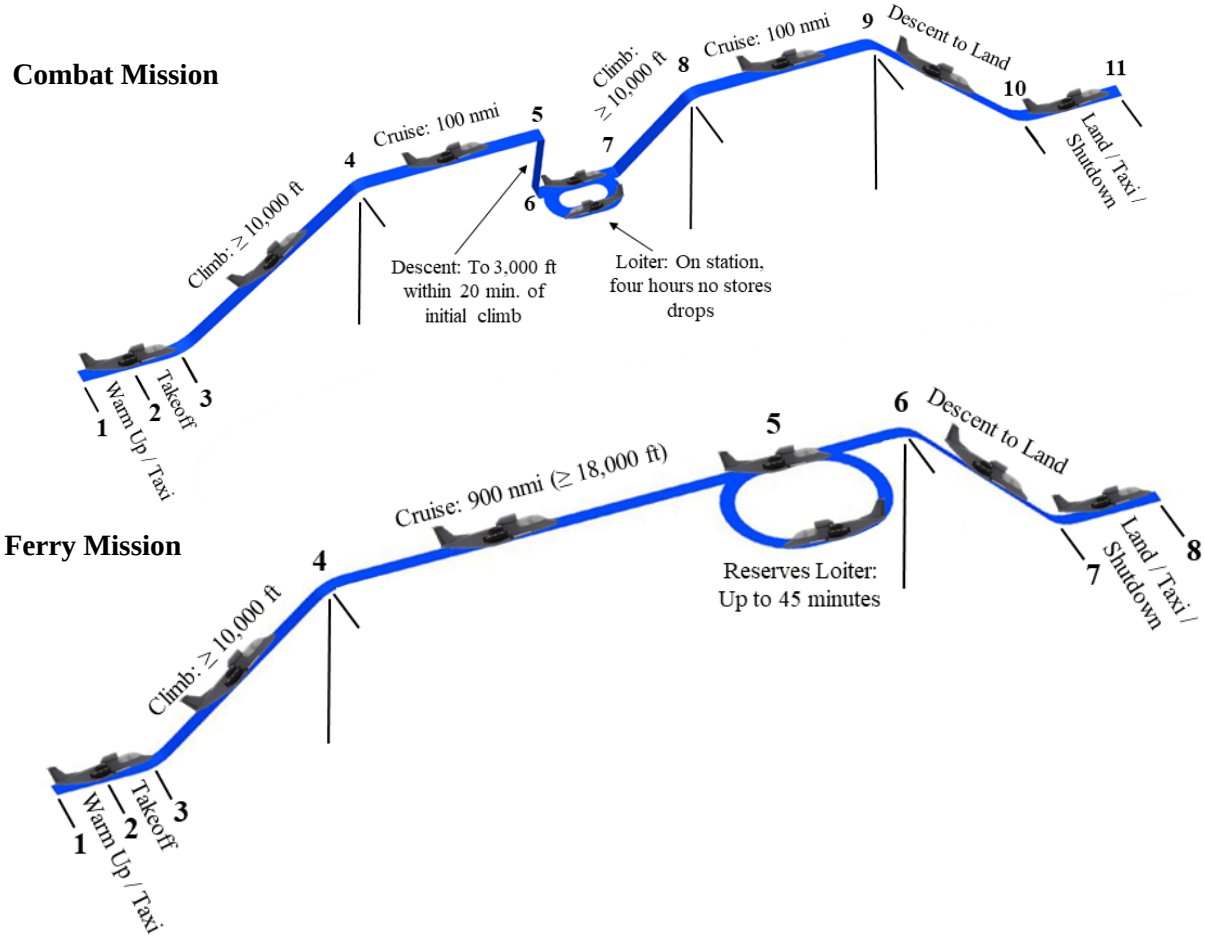

Figure 1.1: Design Combat and Ferry Missions [2]

Figure 1.2: Austere Field Length Requirements [2]

2. Historical Review of Light Attack Aircraft

This section will outline a number of the most effective historical and current light attack aircraft. An analysis of the configurations, concept of operations (ConOps) and munitions was conducted to assess the most important qualities to consider in the following proposal.

2.1 Historical Review and Competition in the Market

The Junkers JU-87 Stuka, shown in Figure 2.1, was a very effective light attack aircraft that played a large role in the German's early success in WWII. The design philosophy was to be simplistic in configuration while still implementing advanced technologies like automatic dive brakes. The success of the Stuka notes the importance of not over-designing and limiting use of technologies that have not been proven to have rugged reliability. The biggest issue the Stuka faced was its vulnerability to air-to-air attacks. It was slow, had low maneuverability, and limited air-to-air armaments. This required it to be accompanied by heavy fighter support during missions.

Figure 2.1: Junkers JU-87 [3]

The A-1E Skyraider came into service in 1946 and saw action through the 1980's. The piston powered aircraft was so effective that it stayed in service even when newer jet powered attack aircraft became available. The Skyraider had great low speed maneuverability which caters to ground-attack missions. Maneuverability along with substantial armoring and seven hardpoints on each wing for armaments gave it its advantage over other fighters. The Skyraider also had a large combat radius and superior loiter time due to the key design emphasis on limiting non-essential weight. The A-1 Skyraider can be seen in Figure 2.2.

Figure 2.2: A-1 Skyraider [4]

The A-4 Skyhawk was first flown in 1954 and retired by the US Navy in 2003, but they are still actively used by the Argentinian Air Force and Brazilian Navy. The aircraft is a subsonic single seat light attack aircraft capable of launching from a naval aircraft carrier. The Skyhawk was heavily used in service during the Vietnam, Yom Kippur, and Falklands wars. This aircraft prioritized a low empty-to-takeoff weight ratio, with the empty weight being just 40% of the takeoff weight. The A-4 Skyhawk, shown in Figure 2.3, used a turbojet engine placed in the rear of the fuselage. It had five hardpoints to deploy weaponry from. It could carry nuclear weapons using a loft delivery and a low altitude bombing system.

Figure 2.3: A-4 Skyhawk [5]

The OV-10 Bronco was introduced in 1969 and retired by the U.S. military in 1995. The aircraft is a Light Armed Reconnaissance Aircraft (LARA). The LARA designation was created to denote a new style of aircraft with high versatility and effectiveness in unpredictable environments. Some of the Bronco's main mission roles were operating as a close ground support, reconnaissance, or transport aircraft. The dual engine twin boom configuration, seem in Figure 2.4, allowed the Bronco to take off in austere field conditions with a short takeoff roll. The aircraft could also operate in forward bases with minimal ground crew support. The dual engines give improved survivability in the case of engine damage or failure. The wing mounted engine design also allowed for superior cockpit visibility compared to current light attack aircraft like the AT-6 and A-29 Super Tucano.

Figure 2.4: OV-10 Bronco [6]

Another particularly effective attack aircraft is the Fairchild Republic A-10, seen in Figure 2.5. This twin turbofan aircraft has provided close air support of friendly troops for the US Airforce since 1976. Due to its high maximum takeoff weight, the A-10 cannot be properly defined as a light attack aircraft, however it is relevant due to its unparalleled success at providing close air support. Several design elements have allowed the A-10 to serve as the premier ground attack aircraft, including its pylon spacing, engine location, and overall survivability. The pylon spacing underneath the wings allows for a large variety of weaponry to be fitted on this plane, allowing for mission flexibility. The engine location above and slightly aft of the main wing simultaneously protects the engines from ingesting debris and lowers the planes infrared and acoustic signatures. The infrared signature is reduced due to the engine exhaust being forced over the horizontal stabilizer. Survivability is high for this aircraft due to its triply redundant flight control system. Due to its effectiveness, the A-10 is still the premier ground attack airplane on the market after nearly half a century in service.

Figure 2.5: Fairchild Republic A-10 Thunderbolt II [7]

Similar to the A-10, the Boeing AH-64 Apache attack helicopter does not directly relate to the goal laid out in the RFP. However, due to the storied success of this design, its design and past success were analyzed. The AH-64 Apache, shown in Figure 2.6, incorporates two twin-turboshafts and a nose mounted sensor. Armed with a 30 mm machine gun, the Apache is lethal as a close air support and attack vehicle. This helicopter was first flown in 1975, but not introduced into service with the United States Army until 1986. It still currently serves as a close range attack helicopter with the Army. The helicopter has four hardpoints that typically carry AGM-114 Hellfire missiles or Hydra 70 rocket pods. The Apache was designed for an

Figure 2.6: AH-64 Apache Helicopter [8]

anti-armor attack mission under United States Army command. The airframe of the Apache consists of approximately 2,500 lbs of armor. The proposal for this design desired a longer range, so the Apache can carry fuel tanks on its hardpoints. This helicopter is still the primary attack helicopter of multiple nations.

Moving into the modern market, the Beechcraft AT-6, Embraer Super Tucano, Yakovlev Yak 130, and Alenia Aermacchi M-346 Master were researched. These three planes exemplify what is currently in the market, as they were all first introduced within the century and are still currently used in various militaries. The AT-6 Wolverine, shown in Figure 2.7, is a single-engine turboprop aircraft used as both a trainer and a light attack plane. The design of the AT-6 is based off the Beechcraft T-6 Texan II, which is a trainer used by the Canadian, Greek, Israeli, and Iraqi forces, as well as the United States Navy and Marine Corps [9]. The AT-6 can perform light precision attack, reconnaissance, training, counter insurgency, civil support, and maritime patrol missions. Recently, it underwent operational testing with the US Air Force under the Light-Attack/Armed Reconnaissance (LAAR) program. This program was ultimately canceled following the release of the Pentagon's FY 2020 budget request, as the Air Force announced it would not move forward with the LAAR program.

Figure 2.7: Beechcraft AT-6 [10]

The Embraer A-29 Super Tucano, displayed in Figure 2.8, is another modern light attack aircraft, and is primarily used by the United States, Brazil, Colombia, and Ecuador. The Super Tucano was designed to be a low-cost system that is operated in low-threat environments [11]. Similar to the AT-6, this plane was evaluated by the US Air Force under the LAAR program. These two planes were the finalists for the LAAR program prior to its cancellation.

Figure 2.8: Embraer A-29 [12]

The Yak 130 and M-346 Master are both twin engine trainer and light attack aircraft. A single plane was originally going to be developed by Yakovlev and Alenia Aermacchi, but this partnership dissolved in 2000 [13]. The Yak 130, shown in Figure 2.9, has two wingtip hardpoints, six under-wing hardpoints, and one under-fuselage hard point. Presently, this plane is used primarily by the Russian Air Force. The M-346 Master is primarily used by the Italian and Israeli Air Forces. It only has seven hardpoints, two less than the similar Yak 130 [14]. The M-346 Master can be seen in Figure 2.10. Both of these aircraft are used as trainers to lead pilots into flying jet aircraft. They were both designed to replicate fourth generation jet aircraft while still functioning as light attack aircraft.

Figure 2.9: Yakovlev Yak 130 [15]

Figure 2.10: Alenia Aermacchi M-346 [16]

2.2 Comparison of Concepts of Operation

There are three main combat scenarios that modern light attack aircraft could fulfill: strafe running, orbiting, and glide bombing. Each scenario will be described individually, along with a relevant concept of operation graphic for each scenario. In a strafe run, the aircraft will fly directly towards the target at a low altitude and fire its machine guns and cannons. The aircraft may also commonly fire air-to-ground rockets if it has the capability. After the aircraft has hit the target it will pull up and look to loop around for another pass at the target if needed. Using several aircraft in combination can keep the target suppressed for long periods of time, as each aircraft can perform a strafe during the down time of another aircraft. A concept of operation for a strafe run is shown below in Figure 2.11.

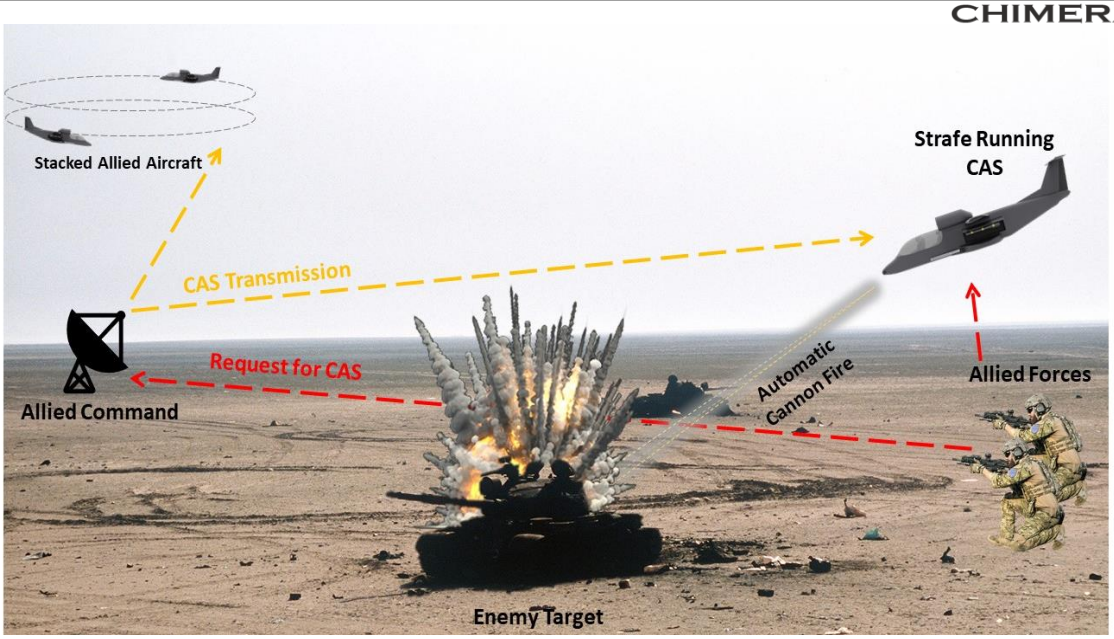

Figure 2.11: Strafe Run ConOps

While orbiting a target, the aircraft will have a weapon capable of firing to the side of the aircraft. The gun can constantly shoot at the target with little to no downtime. This would allow the aircraft to act in a very similar manner to the AC-130, circling the battlefield and eliminating targets as they appear. Since an aircraft that is orbiting can constantly fire at the target, one aircraft can constantly suppress the enemy for long periods of time. A concept of operation for an orbiting attack is shown below in Figure 2.12.

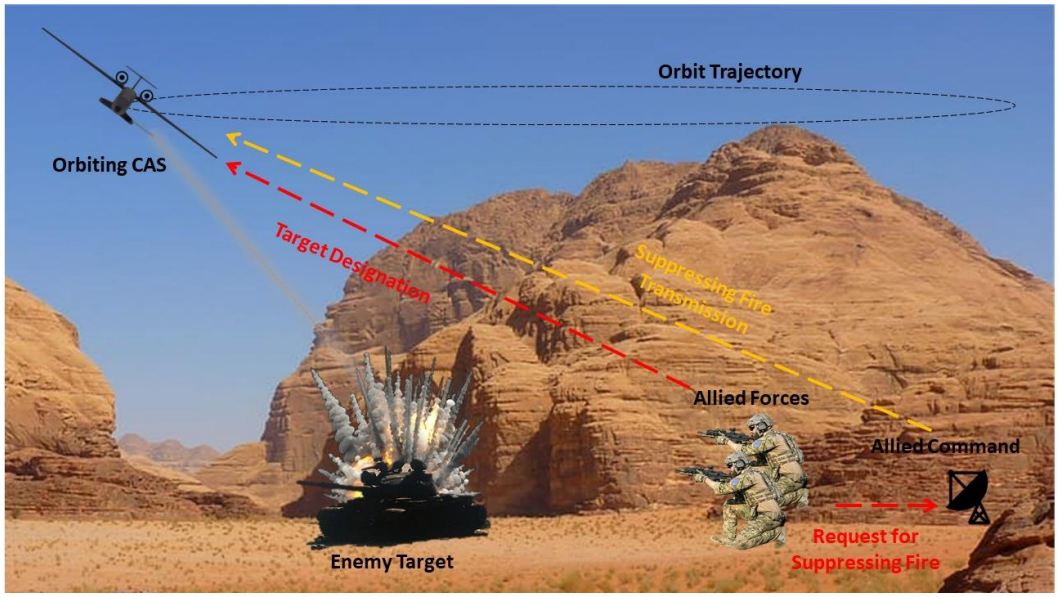

Figure 2.12: Orbiting ConOps

Lastly, glide bombing, shown in Figure 2.13, involves an aircraft dropping bombs from a high altitude and far away from the target. Glide bombs can travel very far due to their low drag profile and high lift characteristics. Modern bombs are also able to be guided and controlled to accurately reach a designated target. Since the aircraft is bombing from outside of engagement range, it is safe from any threats the enemies may possess.

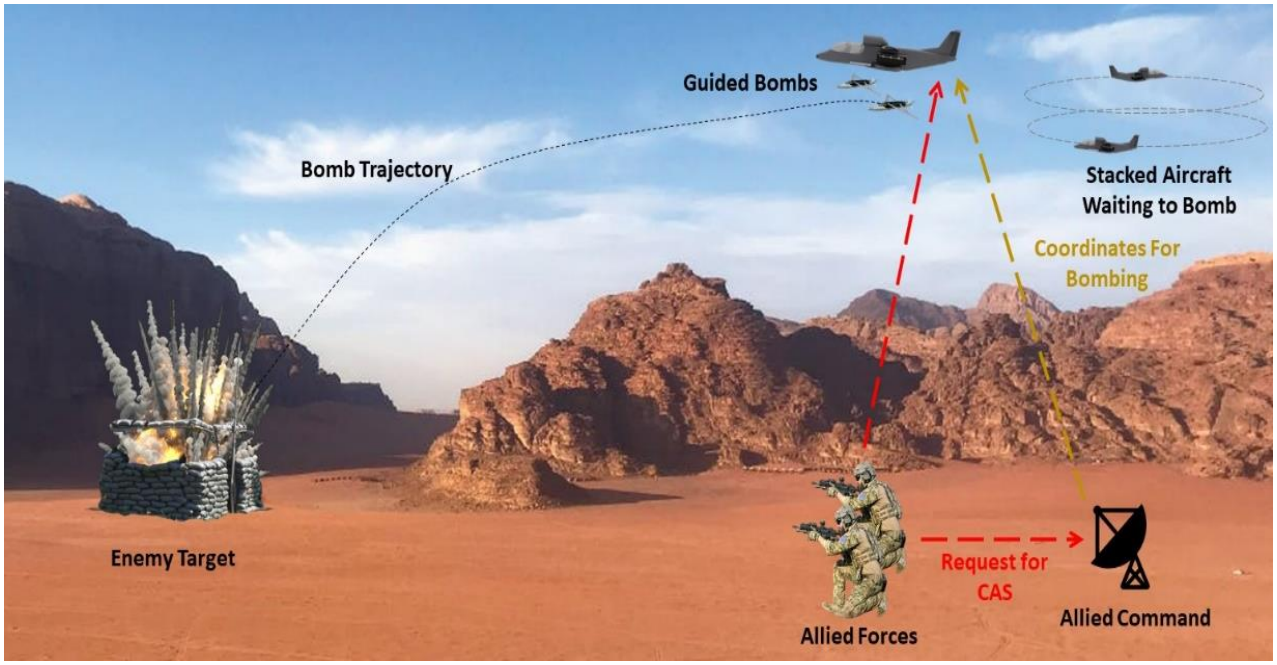

Figure 2.13: Glide Bombing ConOps

While each operation in Section 2.2 is unique and requires a certain armament configuration, a modern attack aircraft should be versatile enough to perform all three of the ConOps discussed.

2.3 Review of Relevant Ordnance and Delivery Methods

Light attack aircraft are equipped with a variety of weapons for means of completing the desired mission. The main duty of light attack aircraft is to use weapon systems for the intentions of close air support for troops on the ground. This ranges from hard launched munitions using a machine gun system, guided and unguided gravity weapons, as well as rail/tube launched missiles.

Table 2-I gives a sweep of viable options for the deliverance of hard launched ordnance. The first classification of this type of delivery method is the single barrel gun. The FN M3P is a common single

barrel heavy machine gun typically mounted on either wing. This gun fire .50 caliber bullets and is found on the AT-6. The FN M3P is housed by the HMP 400 pod [17]. The next classification of hard ordinance delivery methods is the Gatling gun. Weapons that have a caliber of 20 mm and above reside in the classification and have a varying number of barrels. These types of weapons are generally placed in the centerline of the fuselage and are used in strafing runs. In light attack aircraft applications, the recoil force is pertinent to assure the firing of these weapons will not affect the control of the aircraft. Figure 2.14 features the FN M3P, M61A1 Vulcan, GAU-12, then the GAU-8 in order from left to right. This figure shows the variable size differences between the .50 caliber, 20 mm, 25mm, and 30mm gun systems. The M3P is the smallest of the machine gun systems and features a single barrel. The GAU-8 is the behemoth of the gatling guns, as it is larger than a Volkswagen Beatle. For the purpose of the mission requirements, the Chimera will aim for a lower caliber machine gun that has similar capabilities to that of a 30 mm cannon.

Table 2-I: Aircraft Gun Systems

Name/Type	Caliber (mm)	Empty Weight (lbs)	Rate of Fire (rpm)	Recoil Force (lbs)	Aircraft
FN M3P [17]	12.7	80.5	1,100	~	AT-6, A-29
M61A1 [18]	20	248	4,000	2,133	Kai T-50
M61A2 [18]	20	202/228	6,000	3,200	F-22
M-197 [18]	20	132	1,500	1,300	AH-1, OV-10
XM301 [18]	20	80.5	1,500	800	Comanche
GAU-12/U [18]	25	270	4,200	5,000	AC-130
GAU-22/A [18]	25	230	3,300	3,700	F-35
GAU-8/A [18]	30	620	4,200	10,000	A-10

Figure 2.14: Machine Gun System Size Comparison [17,18,19]

With reviewing the type of aircraft gun systems, the ordnance shot through these weapons needs to be compared. Hard launched ordnance varies from as small as a 7.62 bullet to a 30 mm cannon shell in the light attack applications. Table 2-II gives descriptions of the applicable ammunitions. Figure 2.15 gives a scaled size comparison of the range of ordnance calibers featured on light attack aircraft.

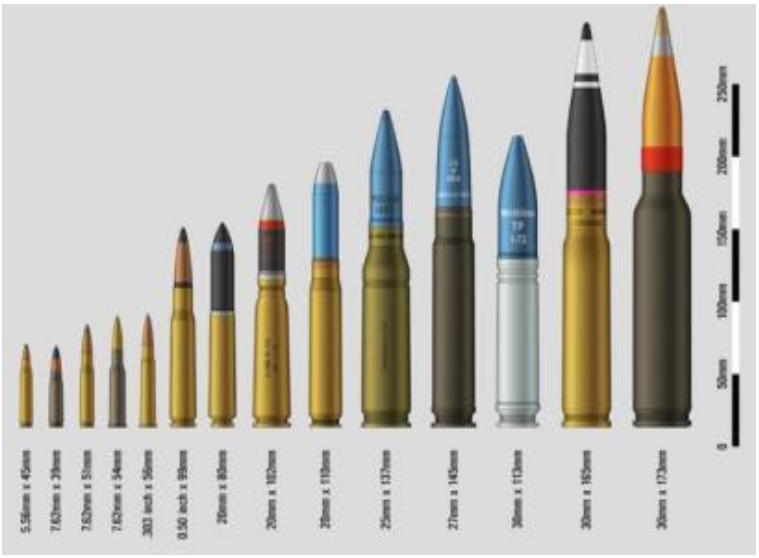

Figure 2.15 Bullet/Cannon Shell Sizing [20]

Table 2-II: Hard Launched Ordnance Review [21]

Name/Caliber	Type	Aircraft
.50 BMG (12.7 mm)	Heavy Machine Gun Rounds	AT-6, A-29
20 mm PGU-28 A/B	Semi-Armor Piercing High Explosive Incendiary	F-15, F-16, AH-1
20 mm PGU-30 A/BTP-T	Target Practice - Tracer	F-15, F-16, AH-1
25 mm PGU-47 APEX	Armor Piercing with Explosive	F-35
30 mm PGU-13/B HEI	High Explosive Incendiary	Apache
30 mm PGU-14/B API	Armor Piercing Incendiary	A-10

The second type of ordnance used on light attack aircraft are gravity weapons. Commonly known as bombs, these weapons can be guided or unguided. Table 2-III gives a summary of relevant gravity weapons used in military operations concerning light attack aircraft. Classic unguided bombs are categorized as general-purpose bombs and can be air dropped from aircraft. The Mark (MK) 80 series is the most common of this type and Table 2-III includes the MK-81 and MK-82, as bombs weighing more than 500 lbs are not typically fielded on light attack aircraft. Unguided bombs were revolutionized into laser guided bombs. Such gravity weapons are equipped with a laser homing systems to pinpoint the detonation location of the bomb. Table 2-III shows the types of guided bombs that are fielded on current light attack aircraft.

Table 2-III: Gravity Weapons

Unguided General-Purpose Bombs	
MK-81 Bomb [22]	W = 250 lbs L = 6.2 ft d = 9 in 
MK-82 Bomb [22]	W = 500 lbs L = 7.3 ft d = 10.8 in 
Smart Bombs	
GBU 58 Paveway [23]	W = 250 lbs (MK-81) Laser Guided Bomb Fielded on AT-6, A-10 
GBU 39/B [24]	W = 285 lbs LxW = 5.9 ft x 7.5 in Laser Small Diameter Bomb Max Range (standoff distance): 60 nmi Fielded on F-22,F-35, B-2, A-10 

The final type of ordnance fielded on light attack aircraft are rockets. A missile is classified as a rocket since it is propelled by a rocket engine with some type of bomb/warhead attached. This classification has either unguided or guided missiles. Table 2-IV, 2-V and 2-VI depict various types of rockets fielded in modern day light attack aircraft.

Table 2-IV: Air to Ground Guided Rockets

Air to Ground Guided Rockets	
AGM-65 Maverick [29]	W = 459 lbs Operational Range: 0.1 – 13 nmi Fielded on A-29 
AGM-114 Hellfire [30]	W =100 lbs Operational Range: 0.3 – 6 nmi Laser Guided Homing Missile Fielded on AT-6 
AGR-20a (APKWS) [31]	W = 32 lb Operational Range: 1-6 nmi Precision Guided Munition inspired by the Hydra 70 

Table 2-V: Unguided Rockets

Unguided Rockets	
Hydra 70 [25]	70 mm diameter air to ground missile W = 13.6 lb Max Range: 5.6 nmi Fielded on A-10, F-16 

Table 2-VI: Air to Air Guided Rockets

Air to Air Guided Rockets	
AIM-9X Sidewinder [26]	W = 187 lbs IR Laser Homing Missile Range: 8.6 nmi Fielded on F-15,F-22 
MAA-1 Piranha [27]	W = 196 lbs Short Range IR Laser Homing Max Range: 3.2 nmi Fielded on A-29 
Python 5 [28]	W = 231 lbs IR + electro-optical imaging Range > 10.8 nmi 

Rockets are delivered either via a rail launching system or a tube launcher. Rail launched missiles are typically the air-to-air or air-to-ground missiles. Unguided rockets are loaded into tube launchers such as the LAU series. These launchers have a capacity of either 7 or 19 70mm rockets and are fielded on a variety of attack helicopters and light attack aircraft [32]. Figure 2.16 gives a visual of the size difference between the two common tube launchers.

Figure 2.16: Tube Launchers [32]

3. Optimization Functions and Class 1 Economics

3.1 Design Optimization Function

Table 3-I below shows the mission requirements for the Chimera as laid out in the RFP [2]. The aircraft must be able to meet these requirements or it will not be accepted as a worthwhile design. Passing aircraft will earn a one for each category, while any aircraft failing to pass will earn a zero and will not be considered.

Table 3-I: Mission Requirements

Requirement #	Description
R1	Certification Base: Military MIL-STD-516C & Joint Service Specification Guides (JSSGs)
R2	Entry into Service: 2025
R3	Critical Technologies TRL: 8+
R4	Takeoff Field Length: < 4,000ft austere field at 6,000 ft altitude, over 50 ft obstacle from grass/dirt with CBR = 5
R5	Survivability: Armored cockpit & engine(s), reduced infrared & visual signatures & countermeasures
R6	Payload: 3,000lb of armament, including missiles, rockets, 500lb bombs
R7	Gun: Integrated for ground targets
R8	Service Life: 15,000hrs over 25 years
R9	Service Ceiling: > 30,000ft
R10	Crew: 2 with zero-zero ejection seats
R11	Design Mission Range: 100 nmi combat radius, 4 hrs on station
R12	Conventional Ferry Mission Range: 900 nmi

Table 3-II below shows the objectives as described in the RFP. Possible aircraft designs will be scored comparatively for these categories. The best aircraft will earn a one and the worst will earn a zero, the aircraft in between will earn a score relative to its performance.

Table 3-II: Mission Objectives

Objective #	Description
O1	"Best Value" meeting performance objectives over 25-year service life
O2	Maximize mission use flexibility without undue cost

Lastly Table 3-III below shows the ancillary objectives that the design team believes will make the Chimera a market dominant light-attack aircraft for many years to come. The ancillary objectives are scored the same way that the designed objectives are, the best aircraft gets a one and the worst a zero, aircraft in between will be scored relative to its performance. The ancillary objectives will be worth 40% as much as the design objectives, since they are not as crucial as the design objectives. This is represented later in Equation 3.1.

Table 3-III: Ancillary Mission Objectives

Ancillary Objective #	Description
AO1	Accommodate TRL-8 gun system with rounds that are more effective than the GAU-8/PGU-14 at typical engagement ranges
AO2	Store more rounds than an A-10
AO3	Cruise faster than an A-10 (450kts)
AO4	Enable remote ferry flight range greater than an A-10 2500nmi
AO5	Smaller hangar footprint than Super Tucano and AT-6
AO6	Acquisition cost 20% < Embraer Super Tucano ($25-30M) & AT-6 ($20-30M)
AO7	Operating costs 20% < Embraer Super Tucano (~$1000/hr) & AT-6 (~$1000/hr)
AO8	Cockpit visibility profiles consistent with OV-1, OV-10 & A-10
AO9	Multi-engine for combat survivability
AO10	Capable of both strafe and gunship orbiting fire
AO11	Minimize gun gas ingestion
AO12	Allow for expansion to a variety of guns and calibers
AO13	Minimize gunnery circular errors probability (CEP)
AO14	Minimize acoustic signatures
AO15	Minimize tracer observability
AO16	Allow for indirect fire with acceptable CEP
AO17	Optically perfect glass flat panel for gunnery
AO18	Combat damage resistant flight control system

The above requirements will be used to score aircraft designs using Equation 3.1. Each category only has a maximum score of one, the highest scoring designs are the most competitive.

$$\textbf{\textit{General Optimization Function}} = \prod_{i=1}^{12} R_i * \left(\frac{1}{2}\sum_{j=1}^{2} O_j + \frac{0.4}{18}\sum_{k=1}^{18} AO_k\right) \quad \textbf{Equation 3.1}$$

3.2 Class 1 Economics Model

The current light attack market is dominated by the A-29 Super Tucano and the Beechcraft AT-6. In order to have a light attack aircraft be competitive in this market, it is important that the Chimera costs 20% less in both acquisition cost and direct operating costs of the A-29 and AT-6. Table 3-IV below shows the acquisition costs and operating costs for the Super Tucano and the AT-6.

Table 3-IV: Current Light Attack Aircraft Economics [33, 34]

Aircraft	Approximate Acquisition Cost	Direct Operating Cost Per Flight Hour
A-29 Super Tucano	$20-30M	$1,000
AT-6 Wolverine	$20-30M	$1,000

From the previous table it is evident that both the A-29 and AT-6 cost roughly the same in both acquisition cost and direct operating cost. In order to make the Chimera 20% less expensive than both aircraft, the acquisition cost needs to be around $16M with a direct operating cost of approximately $800 per flight hour.

To keep the acquisition costs low, the Chimera is designed with manufacturing in mind, each component will be easily assembled and serviceable. This will also lower the life-cycle cost as pieces can be easily replaced. At the same time, it is important to take manufacturing costs into account. While it would be good to manufacture everything within the US, domestic manufacturing costs are too high. Outsourcing manufacturing to other countries with lower costs of labor could be beneficial, but there are other factors to keep in mind when outsourcing work. It is important to consider the politics of the country as well possible trade restrictions or other factors that could either slow down or stop the trade flow altogether. The most probable country of manufacture would be Mexico as the USMCA [35] has allowed for more free trade between the United States and Mexico with smaller tariffs imposed on steel and aluminum. The agreement also stands for at least 15 more years meaning that the manufacturing would at least last through the entry into service of the Chimera.

4. STAMPED Analysis

An analysis of the light attack market was performed using the Statistical Time and Market Predictive Engineering Design (STAMPED) methodology. Many light attack aircraft, including both historical and modern aircraft, were included to show the movement of the market over time. The first useful chart in analyzing this data is a comparison of empty-to-takeoff weight ratio, shown in Figure 4.1. This chart tracks the historical average of this ratio to predict the empty weight of a new light attack aircraft. Additionally, it displays what an aggressive or conservative design for empty weight could realistically be in 2025. This chart predicts the average design of a light attack aircraft in 2025 should have its empty weight comprise about 51% of its takeoff weight. This raises to 57% for a conservative design and lowers to 45% for an aggressive design. However, lower empty weights have historically been achieved by attack aircraft like the A-4, which reached a 40% ratio in 1955.

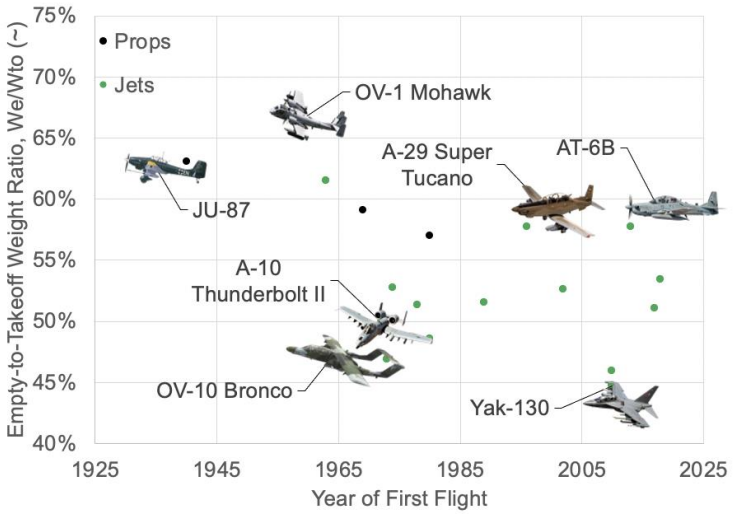

Figure 4.1: Empty-to-Takeoff Weight Ratio by Year

The payload to takeoff weight was analyzed using a similar method. This chart, in Figure 4.2, displays a clear upwards trend. Carrying payload is vital for modern

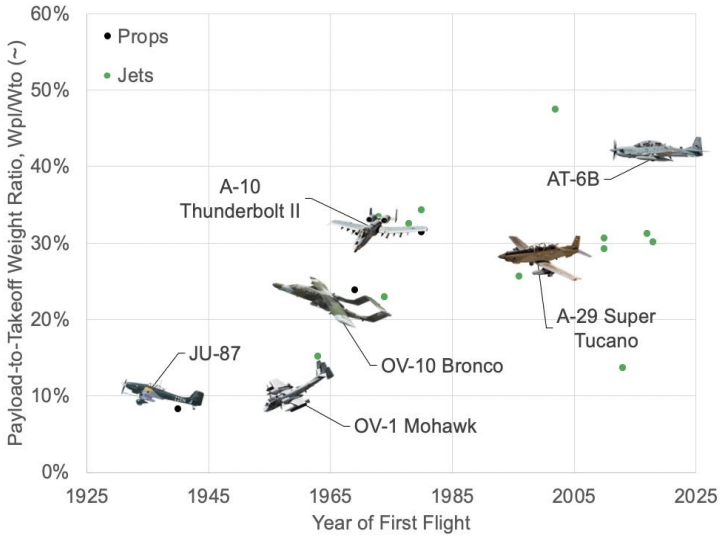

Figure 4.2: Payload-to-Takeoff Weight Ratio by Year

light attack aircraft as this impacts both the weapon capabilities and ferry range, so prioritizing this ratio is vital. The A-10, which has been a very successful attack aircraft, had a more aggressive ratio for payload-to-takeoff weight. This allowed it to carry more weaponry and be used more often. An average light attack aircraft coming out in 2025 can expect this ratio to be 37%, but this can vary by around 9% with either an aggressive or conservative design.

The span and wing loading, shown respectively in Figure 4.3 and Figure 4.4, were also analyzed by year of first flight. Attack aircraft with smaller wings, such as the A-10, had higher wing and span loads. Low level strike mission aircraft that encounter turbulence at high speed can seriously fatigue the crew or even damage the airframe, so a high wing or span loading is required to stay within stress limits. However, a large wing is ideal for other concept of operations due to its high-altitude

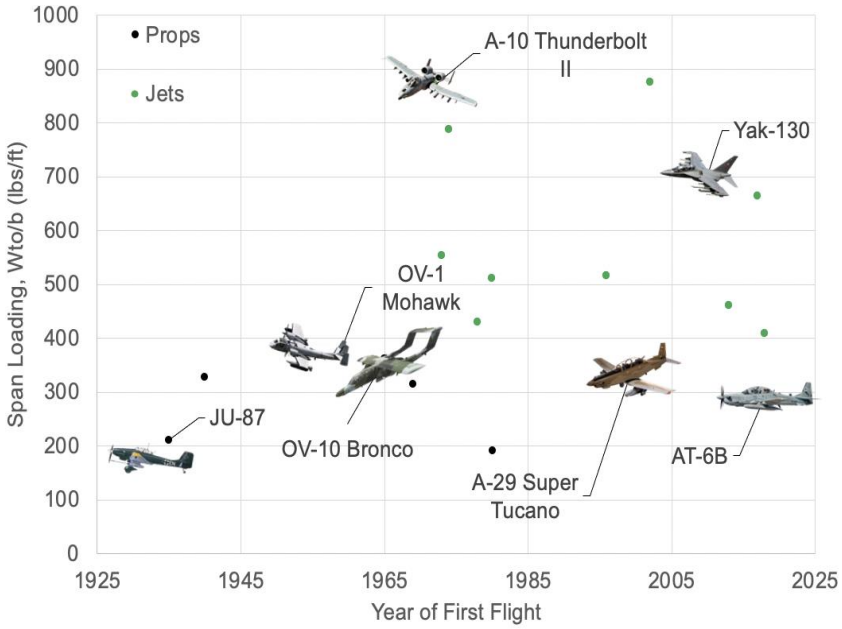

Figure 4.3: Span Loading by Year

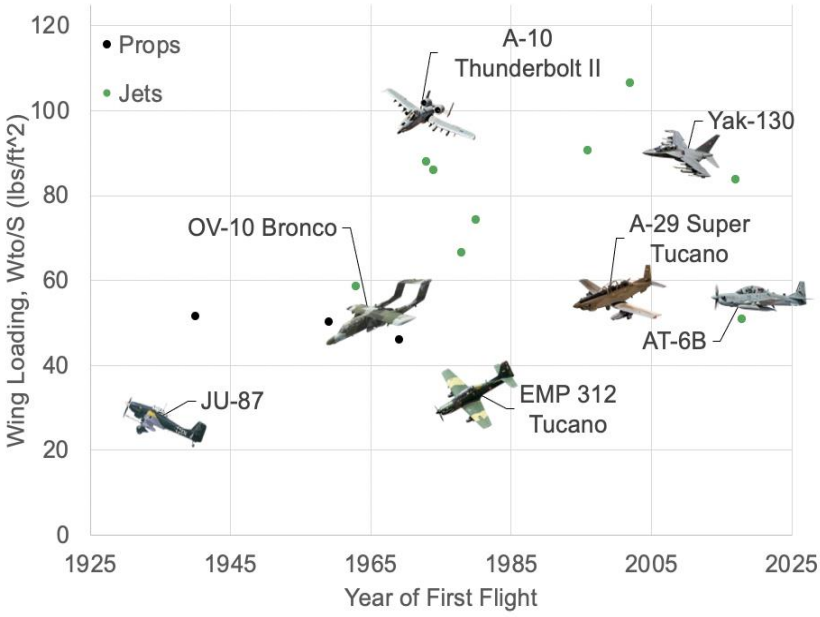

Figure 4.4: Wing Loading by Year

performance, agility, and payload carrying ability. The desired concept of operations for how this light attack aircraft performs its support missions will determine the span and wing loading.

Finally, the power and thrust at takeoff were each analyzed for the propeller and jet powered light attack aircraft. These charts are displayed in Figure 4.5 and Figure 4.6, respectively. These are each compared to the takeoff weight to express their power relative to the size of the aircraft. A higher ratio is ideal for thrust while a lower one is ideal for power, as these mean there is a more powerful engine being used without providing a detrimental impact on the maximum takeoff weight. As expected, both of these show a trend demonstrating more power at a lower weight, meaning more powerful propulsion systems are lighter with modern technology. In 2025, it can be expected that a jet engine on a light attack aircraft can provide a thrust-to-takeoff weight of 0.45.

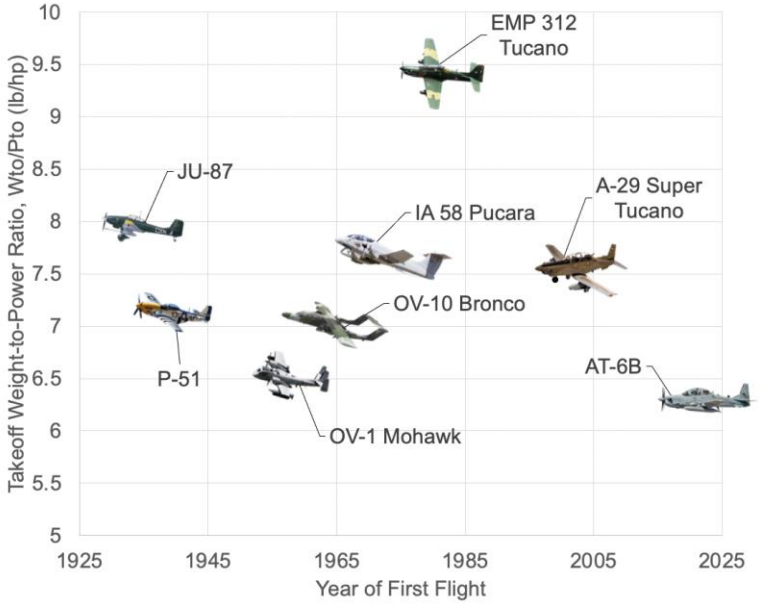

Figure 4.5: Takeoff Weight-to-Power Ratio by Year

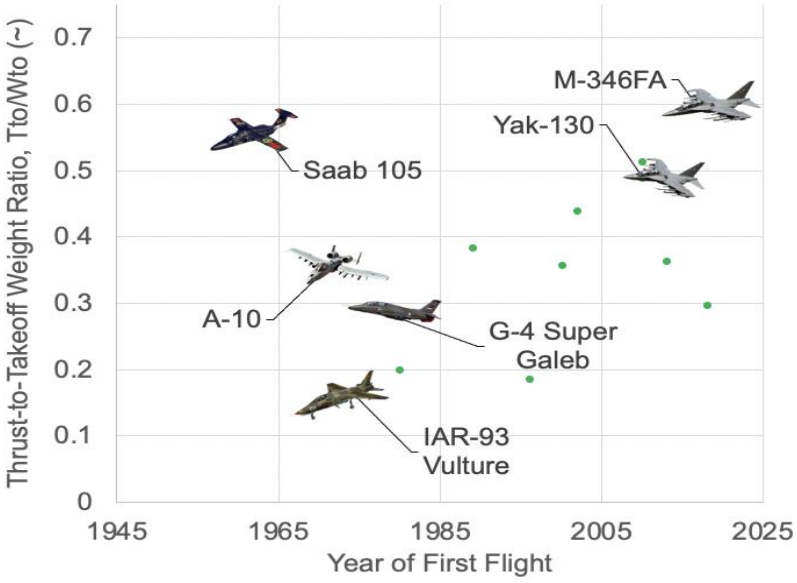

Figure 4.6: Thrust-to-Takeoff Weight Ratio by Year

5. Class I Weight Sizing

Preliminary weight sizing was completed using the methods outlined in Dr. Jan Roskam's Airplane Design Part 1 [36]. Using the mission profile found in Figure 1.1, the fuel fraction for each mission phase was calculated. For each phase except cruise and loiter, estimates for fuel fractions were made using recommendations from Table 2.1 of Ref. 36. Cruise and loiter fuel fraction were calculated using the Breguet range and endurance equations. Table 5-I shows the performance parameters used within the range and endurance calculations. These values were chosen using STAMPED analysis of current aircraft along with recommendations from our advisor, Dr. Barrett.

The takeoff weight and empty weight of the aircraft were then calculated using the iterative weight sizing method outlined in Section 2.5 of Ref. 36. The chosen empty-to-takeoff weight for calculations is set at 0.47, following the W_e/W_{TO} trend observed previously in Figure 4.1 with a slight decrease for additional weight savings. With current materials and technologies, such empty-to-takeoff weight ratio is easily achievable. The weight savings as a result of this ratio are then to be used to add armoring and increase survivability which will be further discussed in later chapters.

Future materials and technologies will allow the empty weight to takeoff weight ratio of the Chimera to lower to on the order of 0.4, matching that of the A-4 Skyhawk. First flown in 1955, this jet powered light attack aircraft, shown in Figure 5.1, was revolutionary for suppressing excess weight to lower acquisition and operational cost [37]. The preliminary design weights based on the above considerations are located in Table 5-I.

Table 5-I: Performance Parameters and Design Weights

Initial Performance Parameters	Weight
V_{cr} = 300 knots c_j = 0.43 lb/lb/hr $(L/D)_{cr}$ = 16 $(L/D)_{loiter}$ = 18 W_E/W_{TO} = 0.47	W_{crew} = 400 lb W_{pl} = 3,000 lb W_F = 2,200 lb W_{tfo} = 24 lb W_{TO} = 9,500 lb W_E = 4,000 lb

Figure 5.1: Douglas A-4 Skyhawk [37]

6. Wing and Powerplant Sizing

Using Dr. Jan Roskam's methods outlined in Chapter 3 of Ref. 36, a Sizing Chart was generated to properly size various parameters for the powerplant and the wing. Design point limitations were plotted based on takeoff, landing and cruise requirements outlined in the RFP [2]. FAR 25 climb requirements were also plotted to ensure the aircraft could operate safely in an engine out scenario. The acceptable ranges for T/W and W/S were found at a number of $C_{L,Max}$ values. To find the optimal thrust to weight ratio and wing loading, Figure 6.1 was generated to assess variations in Specific Range (SR) with cruise altitude and Aspect Ratio (AR). As can be seen, it is optimal to push AR as high as possible to achieve the highest possible efficiency. However, span, wing area, $C_{L,Max}$ are all limiting factors for AR. The wing will hold the majority of the fuel. This is because the internal bay must be able to carry all munitions due to the requirement of completely internal stores. One of the AO's from the optimization function is to match the hangar footprint of the A-29, so span is limited to 40 ft. Finally, extremely high $C_{L,Max}$ values require large span and chordwise high lift devices which eat into fuel volume. With the constraints outlined above and plotted in Figure 6.2, the maximum achievable AR was found to be 12. The balance of wing area and $C_{L,Max}$ required is found in Table 6-I, as well as the rest of the preliminary design point values.

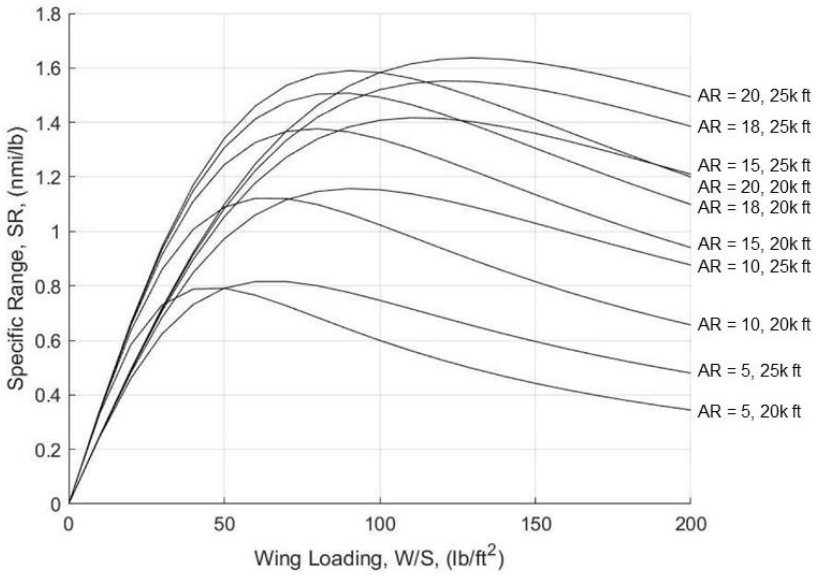

Figure 6.1: Specific Range vs. Wing Loading Optimization

Table 6-I: Design Point Summary

Parameter	Value
W/S (lb/ft^2)	80
T/W	0.31
S (ft^2)	120
b (ft)	38
Total Thrust (lb)	3,000
AR	12
$C_{L,Max,TO}$	2.5
$C_{L,Max,L}$	3.2

The blue lines in Figure 6.2 represent the cost bounds using the optimization function to satisfy the "best value" requirement. These ROF isometric lines were found using Dr. Roskam's methods outlined in the following equation: $ROF = 0.5 * (4.57 \frac{T/W_{new}}{T/W_{ref}} + 15.9 \frac{W/S_{ref}}{W/S_{new}})$ [47,48].

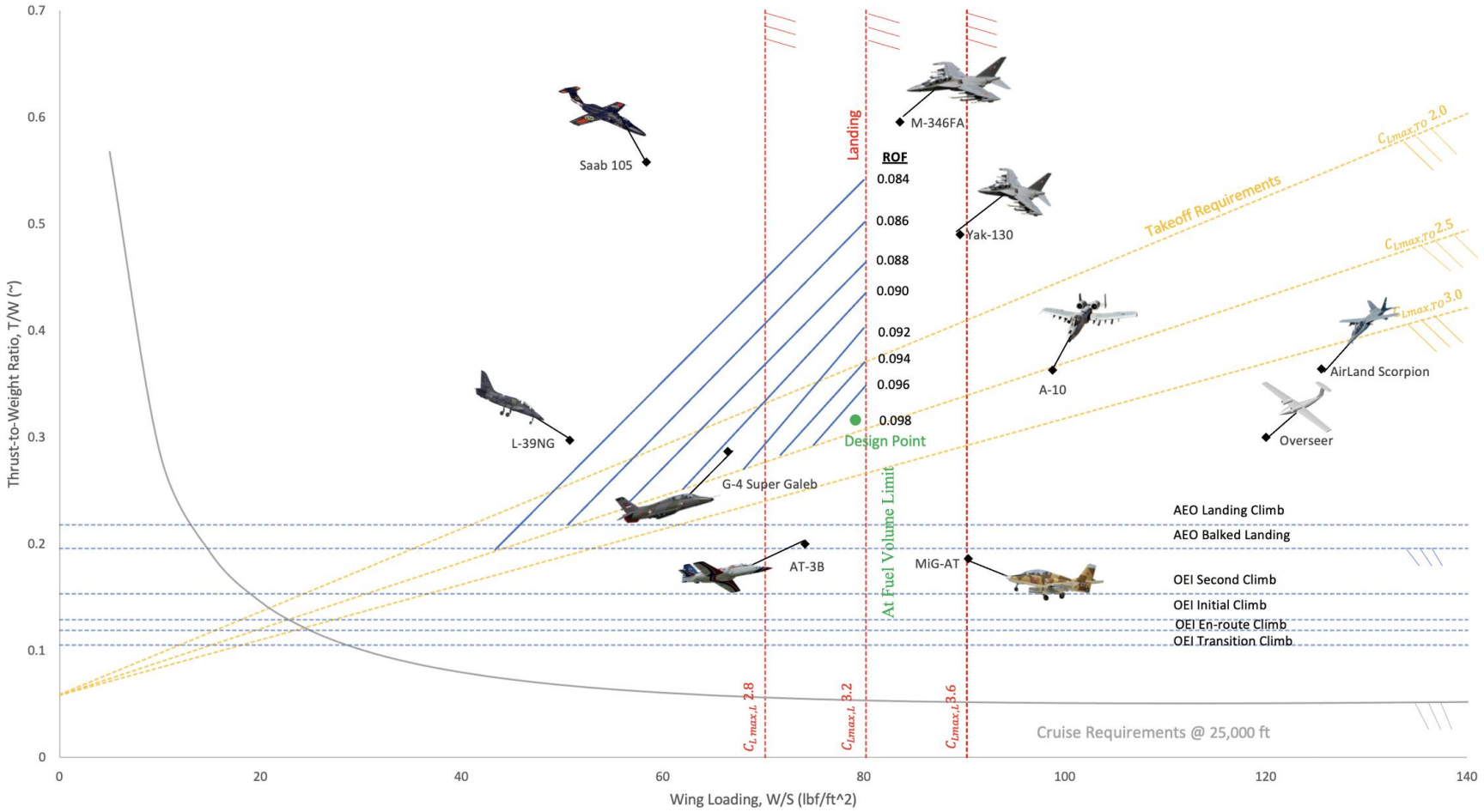

Figure 6.2: Wing and Powerplant Sizing Chart

7. Class I Configuration and Down Selection

The first step in the design process for the Chimera was the selection of a viable configuration for Class I design. A sweep of nine different configurations, seen below in Figure 7.1, were created and analyzed based on perceived characteristics. Each configuration was then rated using the optimization function created previously in Chapter 3. Table 7-I shows the final score of each aircraft, where a high score is considered to be the best, with the top three scores highlighted in green.

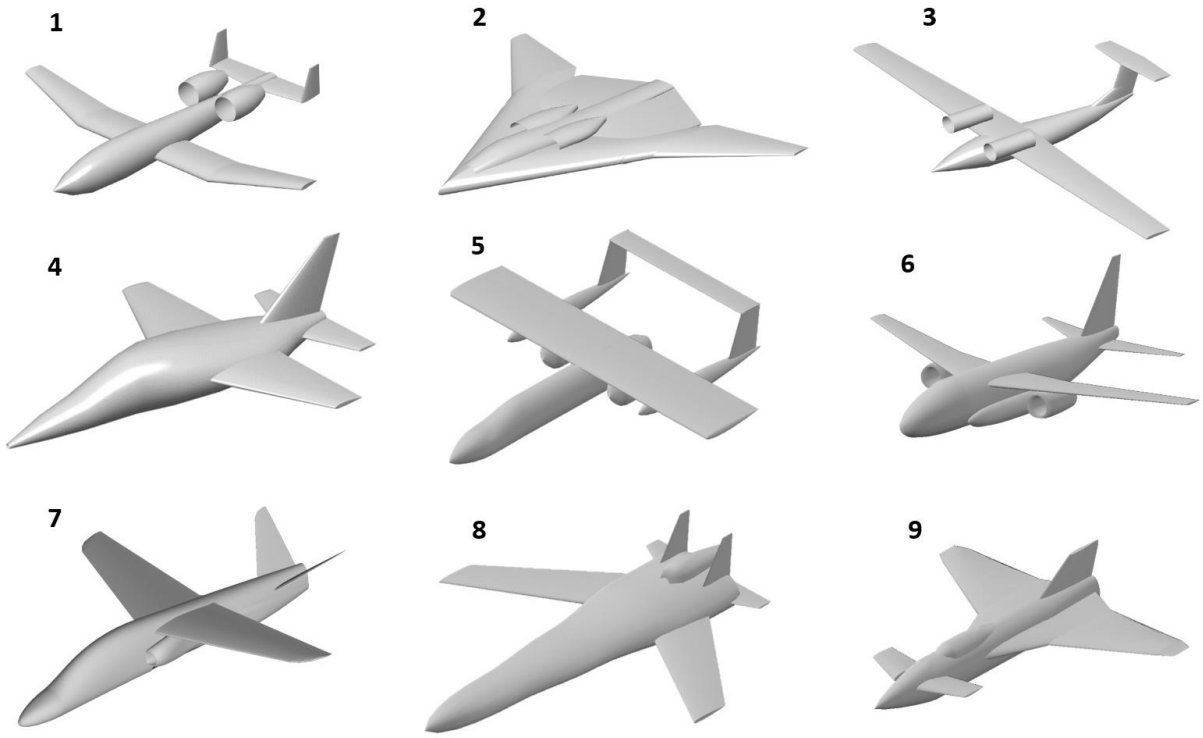

Figure 7.1: Configuration Matrix

Table 7-I: Optimization Function Scores

Number	Name	Score	Number	Name	Score
1	Aft engine	0.910	6	Conventional	0.659
2	Blended Wing	0.616	7	V-Tail	0.933
3	High Wing	1.031	8	Forward Sweep	0.605
4	Mid Wing	0.859	9	Canard	0.793
5	Twin Boom	1.028			

Additionally, each configuration was rated through a pros and cons list which can be seen on the following page. Solutions or alterations to any potential configuration's problems were not taken into account at this stage.

Configuration 1 - Aft Engines, H-Tail	Score: 0.910
+ Reliable A-10 Design	- Empennage jet wash
+ Redundant Tails	- Inlet in Downwash Field
+Engine Accessibility	- High CG Excursions
	- Gun Gas Ingestion

Configuration 2 – Blended Wing	Score: 0.616
+ Low Bending Moments	- Lateral Stability
+ High L/D	- Engine Accessibility
+ High Low Observables	- Low Cockpit Visibility

Configuration 3 – Blown High Wing	Score: 1.031
+ Stores Accessibility	- Engine Accessibility
+ Multiple Gun Locations	- Interference Drag
+ Coandă Effect	- Nacelle Weight
+ Continuous Spar	

Configuration 4 – Mid Wing, Conventional	Score: 0.859
+ Low Compressibility Drag	- Limited Stores
+ Conventional Design	- Single Engine
	- Gun Gas Ingestion

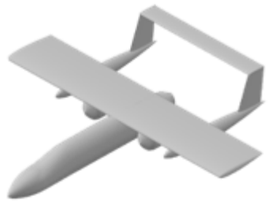

Configuration 5 – High Wing, Twin Boom	Score: 1.028
+ Reliable OV-10 Design	- Structure of Tail Prone to Failure
+ Redundant Tails	- Exposed Engines
+ Continuous Spar	- Interference Drag

Configuration 6 – Conventional Gunship	Score: 0.659
+ Conventional Design	- Exposed Engines
+ Stores Accessibility	- Low Observables
+ Continuous Spar	- Wing Weight

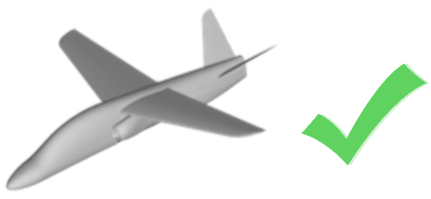

Configuration 7 – High Wing, V-Tail	Score: 0.933
+ Continuous Spar	- Foreign Object Debris
+ High Wing Stability	- Limited Stores
+ Low Compressibility Drag	- Gun Gas Ingestion

Configuration 8 – Aft Engines, Forward Swept	Score: 0.605
+ Superior Stall Characteristics	- Inlet in Downwash Field
+ Low Compressibility Drag	- Single Engine
	- Gun Gas Ingestion

Configuration 9 – Canard	Score: 0.793
+ High L/D	- Unfavorable Stall Characteristics
+ Lift Benefits From Canard	- Limited Stores
+ Landing Gear Integration	- Single Engine

The top three configurations based on the optimization function scoring were Configuration 3, 5 and 7 shown in Figures 7.2, 7.3 and 7.4, respectively. Of the aircraft considered, Configuration 3 was highest scoring based on the optimization function. Based on initial sizing estimations from Chapter 5 and 6, the aircraft must achieve a high L/D and $C_{L,Max}$. A clean configuration is required to achieve these values. This means that weaponry must be stored in internal bays. Fully internal stores also lowers the aircraft radar cross-section. Implementing a low observable design in the radar, acoustic and IR domains improves the chances of undetected entry into combat areas. This then improves the chances of a successful attack and safe return from the combat area.

Optimization Score: 1.031

Figure 7.2: Configuration 3

Optimization Score: 1.028

Figure 7.3: Configuration 5

A high wing design is also required to have internal stores on such a small aircraft. Using a low or mid wing design would have the main spar run directly through the main weapons bay which is unacceptable. While all three top configurations have a high wing, the engine placement on top of the wing for Configuration 3 is more advantageous compared to Configuration 5 and 7 for three reasons. First, the engines in Configuration 3 are far from the ground during takeoff and landing. This means the engines should be safe from FOD which is common on austere runways. Second, the engine exhaust in Configuration 3 will blow over the wing, introducing the Coandă effect, which will cause the flow to stick to the airfoil, generating a higher coefficient of lift on that section of the wing. Finally, the engines on top of the wing lowers acoustic and IR signatures with the exhaust being shielded by the wing. This further lowers the aircraft observables and enhances survivability. For these reasons,

Optimization Score: 0.933

Figure 7.4: Configuration 7

Configuration 3 was chosen as the best design to be able to achieve the high L/D and $C_{L,Max}$ required, while also having the best survivability due to its low observable design.

8. Class I Wing Layout Design

The pertinent wing dimensions are shown in Table 8-I below. The wing area and taper ratio were chosen in Chapter 6 during wing and powerplant sizing and optimization. The NACA 6718 airfoil was chosen due to the need for a thick airfoil. With such a small wing area and short wingspan, it is important that the wing is thick enough to accommodate the required fuel volume. The A-10 uses a NACA 6716 airfoil [7] which is very similar, but has a smaller T/C ratio. The NACA 6718 airfoil was analyzed using XFOIL [38] to find its characteristics at different flight regimes. This analysis can be found in Figure 8.1. The airfoil has soft stall characteristics and a wide flight envelope which is very important for a light attack aircraft.

The normal range for light attack aircraft taper ratio is between 0 and 0.5. With modern flight controllers, dihedral angle is not required as controller gains can be programmed to provide the required stability. There is no sweep angle to increase the ease of manufacturing of each wing spar. No incidence is required due to the camber of the wing creating enough lift at a zero angle of attack. The initial class I wing planform can be found below in Figure 8.2 with the main spars integrated in. The final wing has three main spars as compared to the two shown. The cross section of the NACA 6718 airfoil integrated into the wing design can be found in Figure 8.3.

Table 8-I: Salient Wing Characteristics

Wing Dimensions	
Wing Area, S	120 ft^2
Wingspan, b	37.94 ft.
Aspect Ratio, A	12
Quarter Chord Sweep Angle, Λ	0 deg.
Thickness Ratio, t/c	18%
Airfoils	NACA 6718
Taper Ratio, λ	0.5
Incidence Angle, i_w	0 deg.
Twist Angle, ε_t	0 deg.
Dihedral Angle, Γ_w	0 deg.
Root Chord, C_r	4.21 ft.
Tip Chord, C_t	2.10 ft.

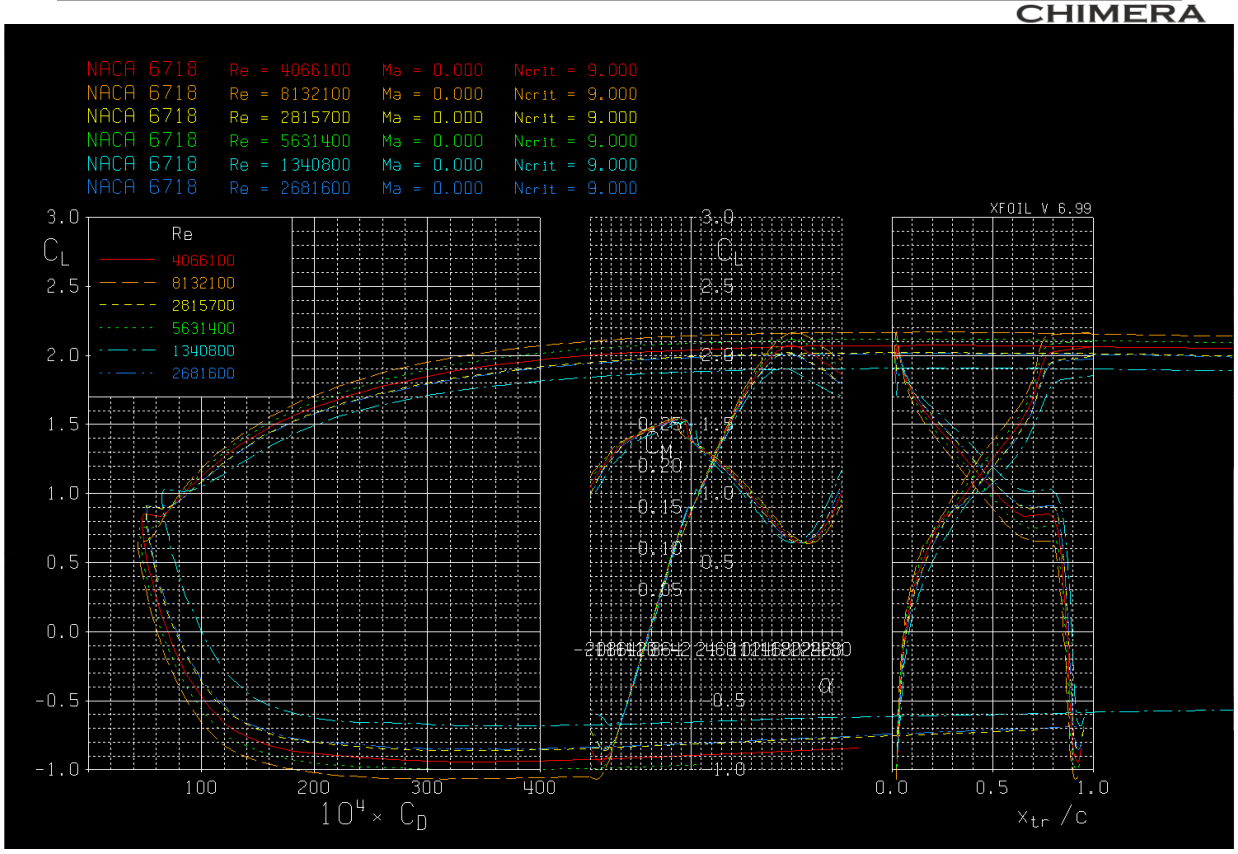

Figure 8.1: XFOIL NACA 6718 Analysis [38]

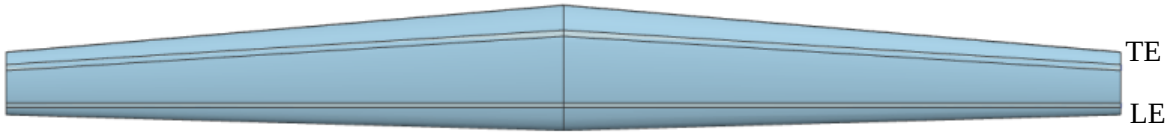

Figure 8.2: Class I Wing Planform

Figure 8.3: Class I Wing Cross Section

9. High Lift Device Sizing

Sizing the high lift devices for the Chimera followed methods described in *Airplane Design, Part II*, by Dr. Jan Roksam [40]. Initial sizing tried exclusive use of plain flaps or single slotted flaps to maintain simplicity in the airframe. Both of these flap types would require more than 100% of the wingspan, with 30% chord coverage to be covered with these flaps to meet required lift values. The flaps could not be grown to use more of the chord due to the already low fuel volume. As a result, Fowler Flaps were sized and resulted in a span coverage of 90% with 25% of the chord spanned with flaps. After this, leading edge slats were added to see how they decrease the requirement for the flap coverage. With a 4-inch gap from leading edge slats, the flap requirement only went down approximately 9%. Due to the design of the powerplant being above the wing, the Chimera is able to utilize blown over flaps which allowed the flap coverage to be decreased. The final design chosen is the use of blown-over flaps behind the engines with Fowler flaps taking up just over 45% of the span of the wing. This combination allows for the flaps to not have to fully extend at any point allowing for overhead if ever needed. Table 9-I and Figure 9.1 below show the final chosen high lift device configurations.

Table 9-I: High Lift Device Configuration

Flap Type	Wingspan Coverage
Blown Over Flaps	5-30%
Fowler Flaps	31-77%

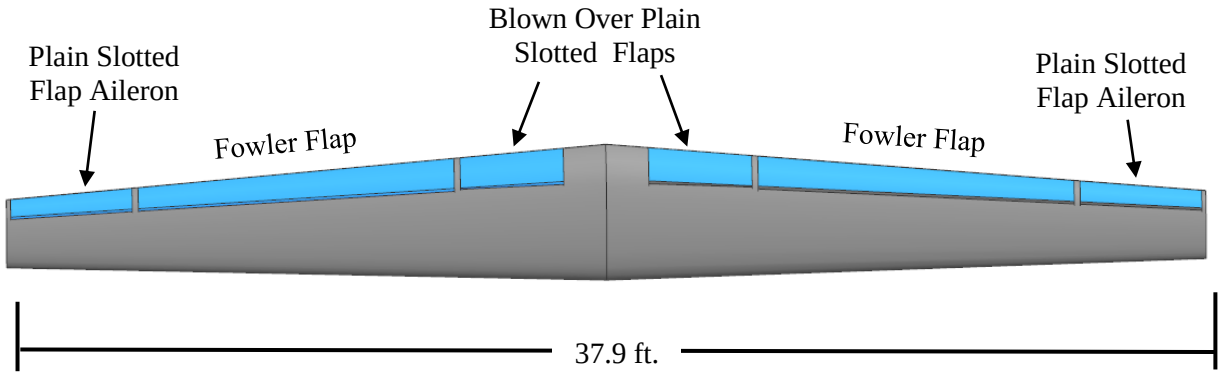

Figure 9.1: High Lift Device Layout

10. Class I Engine Specifications and Installation

The engine selected for the Chimera is the FJ44-1C, developed by Williams International. The 1C variant was chosen due to the output thrust of 1,500 lbf per engine [39] which allows the 3,000 lbf of thrust required to be met with the two installed engines. Table 10-I below depicts salient characteristics of the FJ44-1C engine.

Table 10-I: FJ44-1C Salient Characteristics [39]

Characteristic	Value
Thrust	1,500lbf
SFC	0.460 lb/lbf/h
Fan Diameter	20.9 in
Weight	460 lb
Length	41.4 in
BPR	3

Figure 10.1: Williams FJ44 Engine [39]

With the FJ44 engines mounted above the wing, the engine exhaust has natural observable suppression in both the IR and audible spectrums. Most aircraft have a more traditional engine installation location either under the wing or in line with the fuselage. This engine installation method causes the engine exhaust to be visible in IR as it heats up the fuselage or underside of the wing. Mounting the engines above the wing allows the exhaust gases to pass over the wing, making it so that the IR emission is less observable to those on the ground. A similar occurrence happens for the acoustics of the engine. Traditional engine placements cause noise to be directed towards the ground while the noise is directed upwards with the engine placed above the wing. This acoustic reflection is shown in Figure 10.2 below.

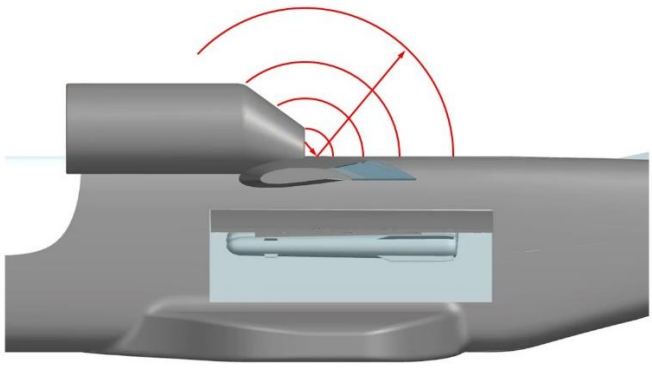

Figure 10.2: Engine Acoustic Reflection

11. Class I Empennage Sizing

The empennage surfaces were preliminarily sized using an estimate of the tail volume coefficients that were sourced from Dr. Jan Roskam's Airplane Design Part II [40]. These volume coefficients were based off the wing and fuselage sizing outlined above and the C.G. of the aircraft outlined in Class II Weight and Balance. Table 11-I outlines the horizontal tail salient characteristics. Table 11-II outlines the vertical tail salient characteristics. Figure 11.1 and Figure 11.2 show the planform of the horizontal and vertical tails, respectively.

Table 11-I: Horizontal Tail Salient Characteristics

Horizontal Tail Dimensions	
Wing Area, S	15.13 ft^2
Wingspan, b	7.59 ft
Aspect Ratio, A	4
Quarter Chord Sweep Angle, Λ	0 deg.
Thickness Ratio, t/c	12%
Airfoils	NACA 0012
Taper Ratio, λ	0.7
Incidence Angle, i_w	0 deg.
Twist Angle, ε_t	0 deg.
Dihedral Angle, Γ_w	0 deg.
Root Chord, C_r	2.35 ft
Tip Chord, C_t	1.64 ft

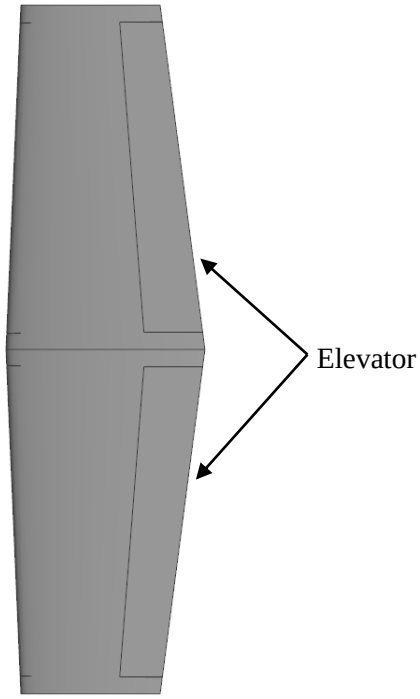

Figure 11.1: Horizontal Tail

Table 11-II: Vertical Tail Salient Characteristics

Vertical Tail Dimensions	
Wing Area, S	21.42 ft^2
Wingspan, b	5.67 ft
Aspect Ratio, A	1.5
Quarter Chord Sweep Angle, Λ	30 deg.
Thickness Ratio, t/c	12%
Airfoils	NACA 0012
Taper Ratio, λ	0.45
Incidence Angle, i_w	0 deg.
Dihedral Angle, Γ_w	90 deg.
Root Chord, C_r	5.21 ft
Tip Chord, C_t	2.35 ft

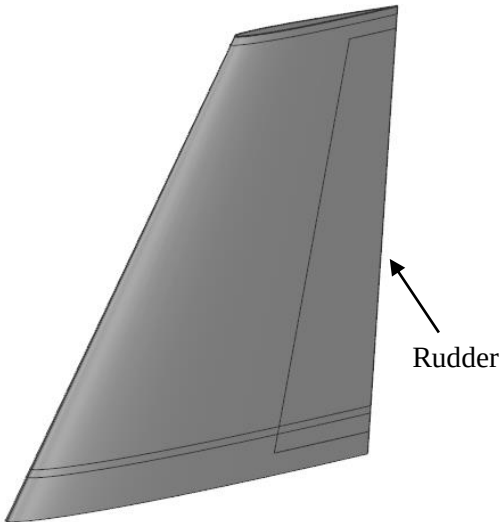

Figure 11.2: Vertical Tail

12. Ballistics Analysis of TRL-8 Flight Safe Discarding Sabot Gunnery Rounds

A hard-launch ballistics review was conducted to calculate the capabilities of different bullets and cannon shells within the light attack aircraft spectrum. Ammunition specifications were obtained from the NAMMO Ammunitions Catalog [41]. Using basic physics principles, an iterative time-stepping code was generated that would allow for the calculation of slant range, time to target, and impact energy for different bullets with a variable set of initial firing conditions. This generated code is called *Chimera Advanced Ballistics Analysis.* This allowed for a calculation of the desired variables for orbiting cover fire and strafe runs. The code was developed based on a physics model relying on three degrees of freedom. This code uses the mass, diameter, and length of any round to calculate the bullet's energy throughout its entire flight. The code relies on archival data of previous bullets to calculate the drag coefficient at every Mach number. Additionally, the air density, pressure, and temperature were modeled to accurately predict each rounds effectiveness from different heights. This can be used to find the force (F_{aero}) acting on the ballistic round at any given speed and altitude, as shown in Equation 12.1. This force can then be used to get the acceleration of the ballistic round in both the horizontal and vertical direction using Equation 12.2. This acceleration was used to calculate the velocity change over the duration of the timestep, as shown in Equation 12.3. This velocity was then used to find the new horizontal and vertical position, as well as a new flight path angle (γ) as shown in Equation 12.4 and Equation 12.5. Additionally, Figure 12.1 displays the slant range against time for various different bullets and cannon shells. Figure 12.2 displays the impact energy against the slant range for the various types of ammunition.

Equation 12.1: $$F_{aero} = .5 * \rho * v^2 * C_a * S_b$$

Equation 12.2: $$\begin{bmatrix} a_x \\ a_z \end{bmatrix} = \begin{bmatrix} \frac{F_{aero} * Cos(\gamma)}{m} \\ \frac{F_{aero} * Sin(\gamma) + m * g_0}{m} \end{bmatrix}$$

Equation 12.3: $$\begin{bmatrix} \Delta V_x \\ \Delta V_z \end{bmatrix} = \begin{bmatrix} a_x \\ a_z \end{bmatrix} * \Delta t$$

Equation 12.4:

$$\begin{bmatrix} X_{new} \\ Z_{new} \end{bmatrix} = \begin{bmatrix} X_{old} \\ Z_{old} \end{bmatrix} + \begin{bmatrix} V_x + \frac{\Delta V_x}{2} \\ V_z + \frac{\Delta V_z}{2} \end{bmatrix} * \Delta t$$

Equation 12.5: $$\gamma = \tan^{-1}\left(\frac{V_z}{V_x}\right)$$

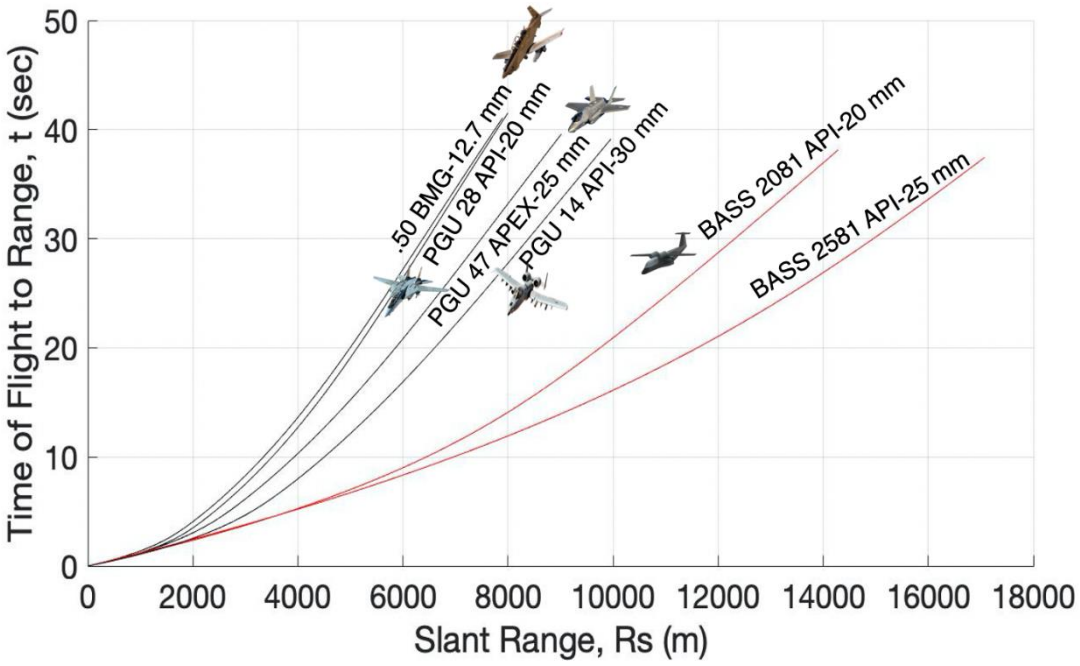

Figure 12.1: Time of Flight for each Round vs. Slant Range

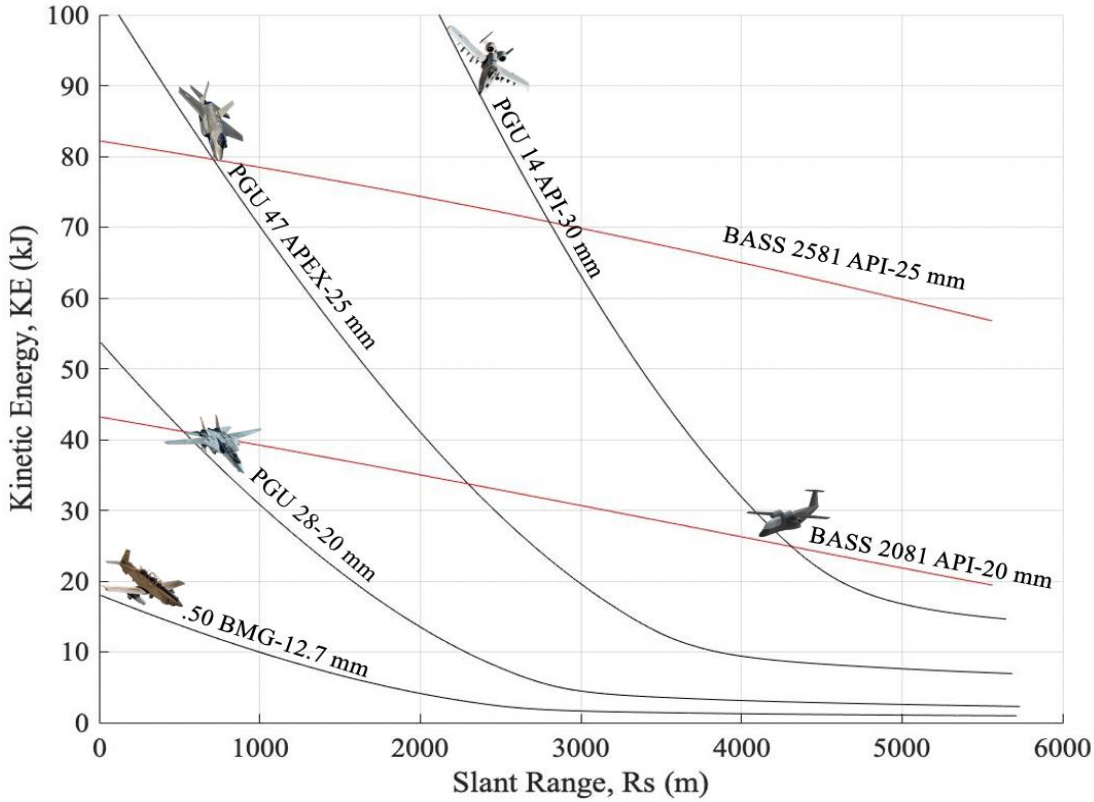

Figure 12.2: Ammunition Impact Energy vs. Distance

The Ballistically Aero-mechanically Stable Sabot (BASS) 2081 and 2581 are newly patented 20 and 25 millimeter rounds which outperform the currently used PGU rounds used by the A-10 (PGU 14) and the F-35 (PGU 47 APEX) if used at a sufficiently long range. This is due to the lower cross-sectional area and thereby lower drag coefficient for the BASS round. Being sabot rounds, they use a small diameter penetrator over their flight, allowing them to better maintain their forward velocity. This makes them highly effective in orbital strikes or any long-distance engagement with a target. Sabot rounds are commonly used in high caliber weapons; however, they are not used in aircraft due to the inability to reliably shed the sabot without it harming the aircraft. These new BASS rounds, due to their design as a "flight-safe discarding sabot," are stable in their flight [43]. The flight path of the falling sabot can be accurately predicted and is designed to fall out of the flight path of the attacking aircraft. The BASS aerial cannon shells are predicted to be much more effective when striking a target from range. The concept of operations for this round is shown in Figure 12.3.

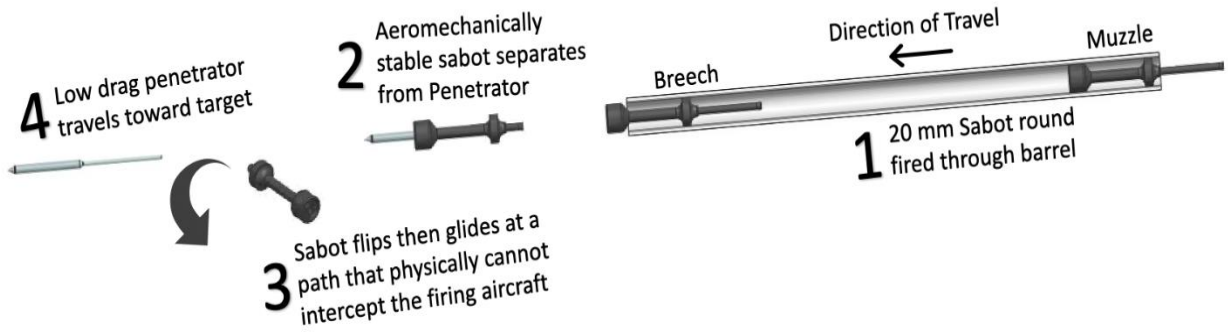

Figure 12.3: BASS Round ConOps

Additionally, a chart showing the armor penetration at each slant range is displayed in Figure 12.4. The armor penetration (AP) was calculated using Equation 12.6 [44]. This equation must then be converted to millimeters. Clearly, the BASS rounds fly much farther at a quicker rate than the other currently in-service rounds. When each of these two figures are taken together, there is clear evidence

that the currently in-service canon shell rounds are inferior to the BASS rounds that the Chimera will be equipped with.

Equation 12.6 [44]: $\mathbf{AP\ (in) = 0.000469 * \left(W_{pen}\ (lbs)\right)^{0.5506} * \left(D_{pen}\ (in)\right)^{-0.6521} * \left(V_{pen}\ \left(\frac{ft}{s}\right)\right)^{1.001}}$

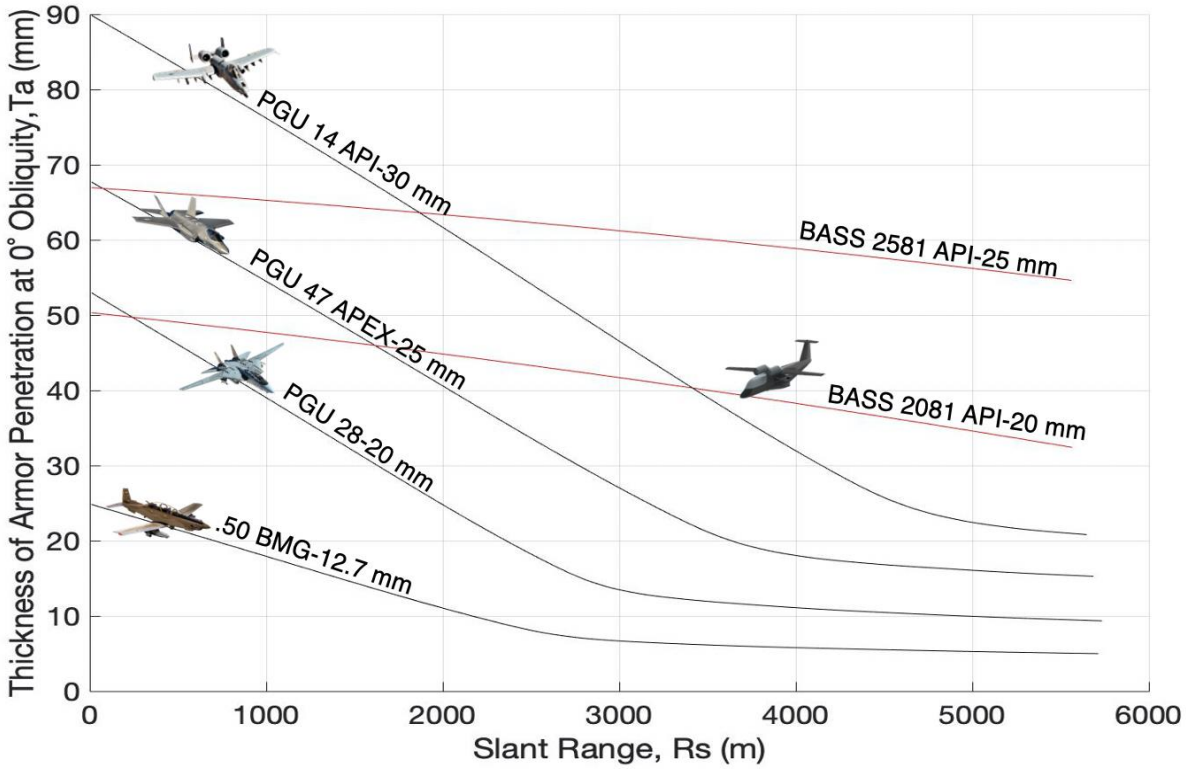

Figure 12.4: Armor Penetration Performance, showing Chimera 20 mm Outperforming the A-10 Gau-8/PGU 14 beyond 3.5 km

13. Review of Target Engagement Methods with Hard-Launched Ordnance

This section will compare the mission capabilities of conventional attack aircraft compared to the Chimera's mission capability using BASS rounds. The A-10 Warthog and the A-29 Super Tucano fire PGU-14 30mm rounds from a GAU-8 cannon and .50 cal BMG bullets from a M3P, respectively. As seen in the previous section, the BASS 2081 round outperforms conventional 30mm, 20mm, and .50 caliber rounds at high slant ranges. Using the extended range capabilities of the BASS 2081, the Chimera will be able to orbit a combat area at 15,000 ft from a slant range of 3 nmi and effectively deliver suppressive fire with a greater amount of armor penetration upon impact than any current 20, 25 or 30 mm round at

extended ranges as shown in Figure 13.1. Figure 13.2 shows an engagement scenario of the Chimera orbiting outside the range of a common SAM, the SA-25 9K333 Verba. This SAM has a slant range of 21,000 ft and service ceiling of 15,000 ft [45]. The long-range orbit keeps the Chimera out of harm's way while still effectively completing the same objective that requires the A-10 and A-29 to complete a more dangerous strafing run. The gimbaled M197 that will be used on the Chimera can also be re-oriented to face forward to allow for similar strafing runs on targets if the mission requires it as well.

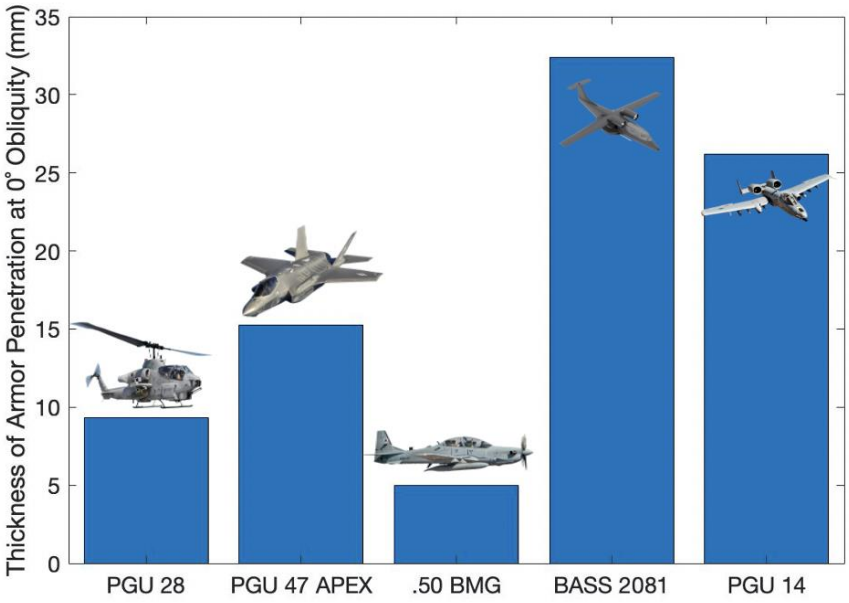

Figure 13.1: Armor Penetration at 3 nmi Range

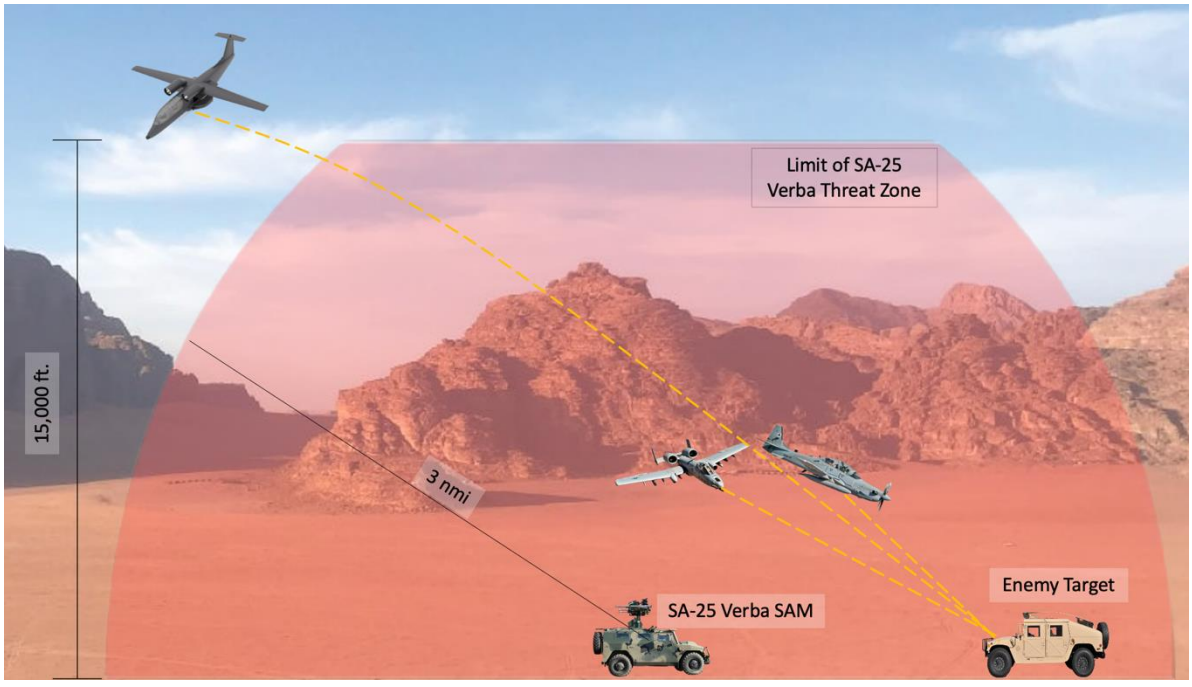

Figure 13.2: Engagement Scenario Comparison

14. Class I Performance and Drag Polar Analysis

14.1 V-n Diagram

A V-n diagram was constructed to show the limits of the Chimera's performance using methods from *Airplane Design: Part VI* [46]. Figure 14.1 shows the V-n diagram and how the load factor changes with respect to the aircraft's airspeed. The military V-n diagram only represents the maneuver limits of the aircraft with two limiting speeds. V_H is the maximum level speed and V_L is the maximum dive speed. The positive and negative load factors, n_{lim}, were +7.33 and -3.00. These values were pulled from Table 4.1 in *Airplane Design: Part V* [47]. The maximum positive load factor will be achieved at a flight speed of 172 knots and the maximum negative load factor will be achieved at a flight speed of 157 knots. The Chimera light attack aircraft will be able to operate efficiently with the bounds of load factor and the maximum design speed.

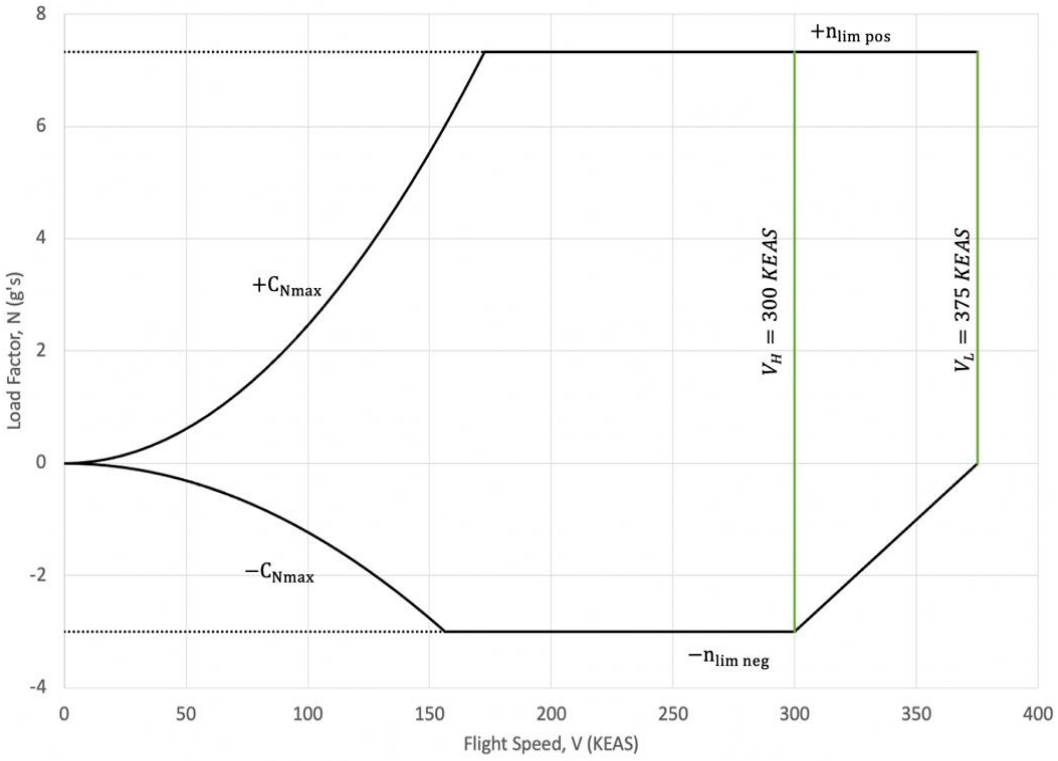

Figure 14.1: V-n Diagram

14.2 Thrust Required, Climb Rates and Doghouse Plots

In order to better characterize the performance of the Chimera, multiple other plots are required. First is the thrust required for the aircraft during different envelopes. Figure 14.2 shows the thrust required for

the aircraft based at different altitudes. Figure 14.2 also shows the thrust available from the FJ-44-1c engines.

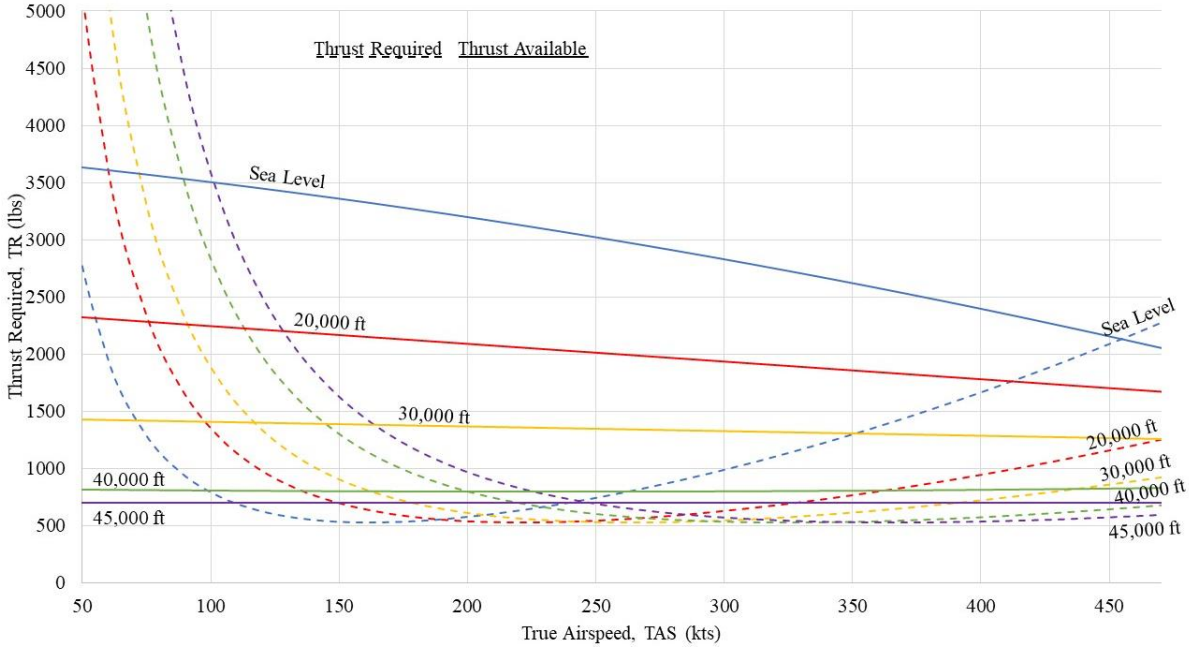

Figure 14.2: Thrust Required and Available

The next plot is the rate of climb plot. It is important that the service ceiling is known and what the performance will be at all flight envelopes. Figure 14.3 shows the rate of climb of the Chimera with increasing altitude. It is evident that as the altitude increases, the rate of climb of the Chimera decreases.

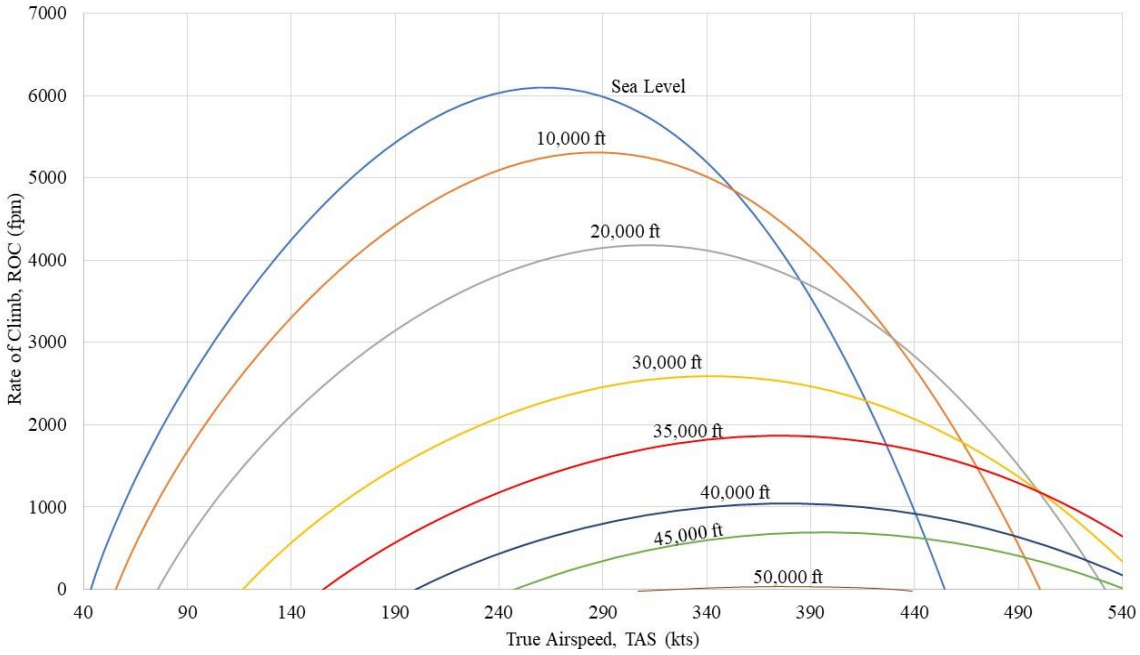

Figure 14.3: Altitude and Rate of Climb

It can also be seen that the absolute ceiling of the aircraft is about 46,000 ft, as it would no longer be able to climb at that altitude as shown in Figure 14.4. The service ceiling of the Chimera can be seen to be 43,000 ft in the same figure.

Rearranging all of these plots into one can be completed and create a doghouse plot outlining the salient characteristics of the Chimera in respect to climb performance. This plot can be seen in Figure 14.4 below.

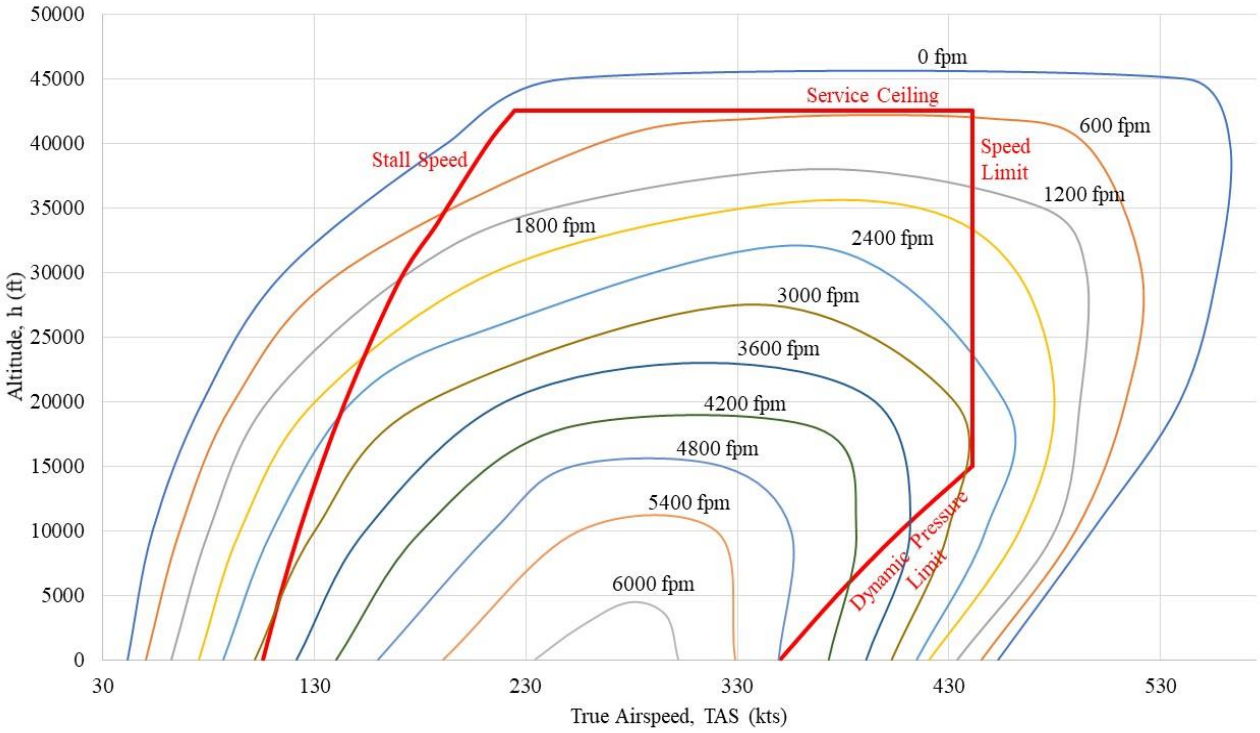

Figure 14.4: Chimera Doghouse Plot

14.3 Takeoff and Landing Field Lengths

Lastly, the takeoff and landing distances of the Chimera were found using methods described in Roskam's *Airplane Design: Part I* [36]. This was achieved using Equation 14.1 through Equation 14.5.

Equation 14.1: $$S_{TOG} = \frac{0.0447\left(\frac{W}{S}\right)_{TO}}{\rho\left[C_{L,max,TO}\left\{k_2\left(\frac{T}{W}\right)_{TO} - \mu_G\right\} - 0.72C_{Do}\right]}$$

Equation 14.2: $$k_2 = 0.75\left(\frac{5+BPR}{4+BPR}\right)$$

Equation 14.3: $$V_{stall} = \sqrt{\frac{2W}{\rho S C_L,max}}$$

Equation 14.4: $$S_{LG} = 0.265{V_{stall,L}}^2$$

Equation 14.5: $$S_L = 1.938S_{LG}$$

Plugging in known values yields laid out in prior chapters yields the following takeoff and landing distances seen in Table 14-I.

Table 14-I: Takeoff and Landing Distances

Takeoff Ground Run (ft)	Landing Ground Run (ft)
2,819	1,928

Drag polars were estimated using methods outlined in *Airplane Design, Part II* [40]. The wetted area for each aircraft component was estimated using measurement tools within CAD. These values were validated through hand calculations to make sure that the values have the right order of magnitude. The C_f is assumed to be 0.004. Table 14-II below shows the overall wetted area and the zero lift drag coefficient of the Chimera.

Table 14-II: Aircraft Component Wetted Areas

Component	Wetted Area (ft^2)
Fuselage	224.27
Wings	235.09
Empennage	69.82
Nacelles	78.54
Sponsons	49.98
Total	677.71
Parasite Area	3
C_{Do}	0.025

Incremental zero-drag lift coefficient, ΔC_{D0}, values were determined using the assistance of Table 3.6 from *Airplane Design: Part I* [36]. Flap type, flap deflection angle, and landing gear deployment status were used to determine ΔC_{D0} and Oswald's efficient factor, e, at each configuration. Table 14-III presents Class II drag polars at each flight configuration with each corresponding maximum L/D value.

Table 14-III: Chimera Drag Polar and L/D Max Values

Configuration	ΔC_{D0}	e	Drag Polar	L/D Max
Clean	0.000	0.85	$C_D = 0.025 + 0.0312C_L^2$	17.9
Takeoff Flaps, Gear Down	0.035	0.8	$C_D = 0.06 + 0.0332C_L^2$	11.2
Takeoff Flaps, Gear Up	0.015	0.8	$C_D = 0.04 + 0.0332C_L^2$	13.7
Landing Flaps, Gear Down	0.080	0.75	$C_D = 0.105 + 0.0354C_L^2$	8.2
Landing Flaps, Gear Up	0.060	0.75	$C_D = 0.085 + 0.0354C_L^2$	9.1

The drag polar at each flight configuration can then be seen graphically in Figure 14.5.

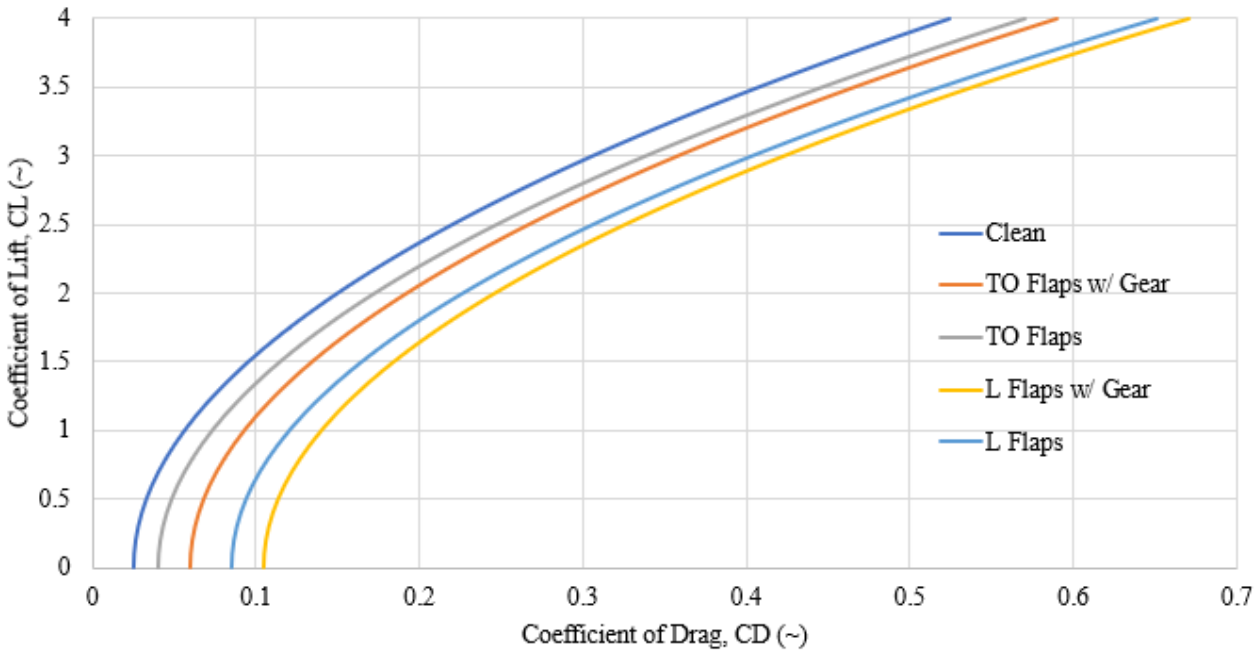

Figure 14.5: Drag Polars

Figure 14.6 below depicts a perimeter plot of the Chimera fuselage. This shows the perimeter of the fuselage with respect to fuselage station. This plot also acted as an aid to verify the fuselage wetted area value measured within CAD.

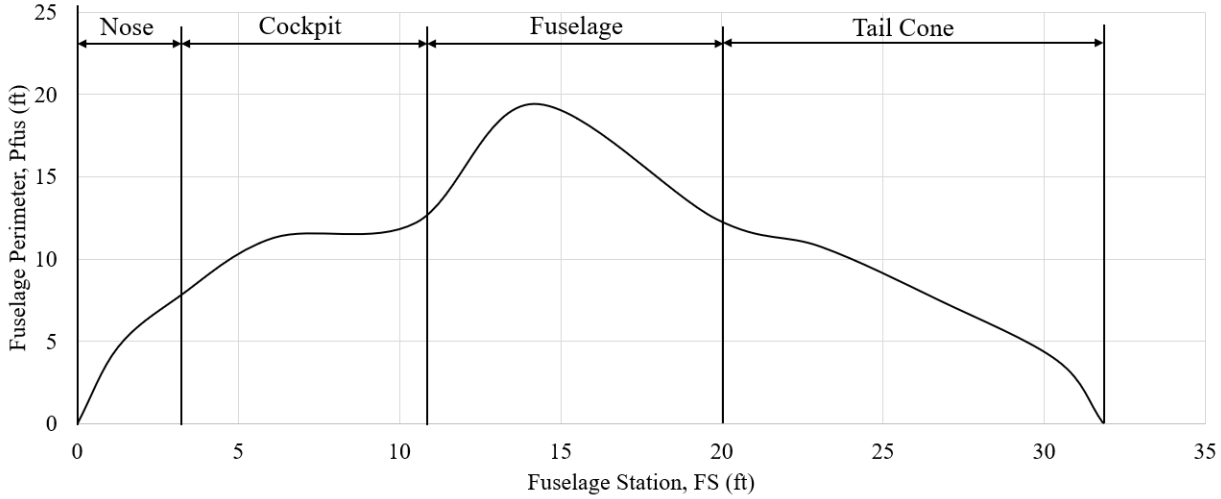

Figure 14.6: Fuselage Perimeter Plot

15. Payload-Range Diagram and Utilization Analysis

This section determines the maximum ferry range for the Chimera aircraft and analyzes the effect carrying different payloads has on the total range. The maximum range for the aircraft was found using the Breguet Range Equation, shown in Equation 15.1 below. A chart displaying the range for every payload weight that the Chimera can carry is shown in Figure 15.1.

Equation 15.1: $$\boldsymbol{R\ (nmi) = \frac{V\ (kts)}{C_j\ (lb/lb/hr)} * \frac{L}{D} * \ln\left(\frac{W_i}{W_f}\right)}$$

The maximum ferry range found, which would be when there is no payload on the aircraft just the operating empty weight. A ferry range of greater than 2,500 nmi is desired as this is nominally the amount needed to cross the Atlantic Ocean. The ability to cross the Atlantic in a ferry mission allows for greater versatility for modern and future missions as it makes the Chimera aircraft more accessible for any location. These range calculations used the full fuel volume, which occurs at the maximum takeoff

weight. A fuel reserve capable of sustaining flight for at least forty-five minutes as protection from unexpected events was maintained for these calculations.

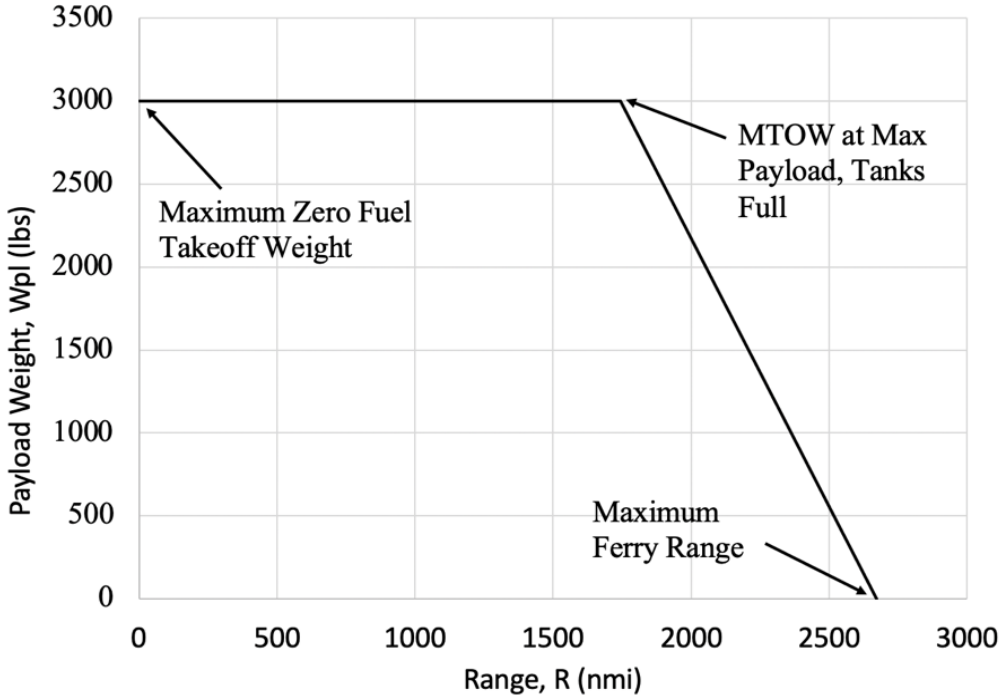

Figure 15.1: Maximum Range vs. Payload Weight

16. Class I Structures Layout

Figure 16.1 depicts the Class I structural layout for the Chimera. Table 16-I also depicts key structural characteristics.

Table 16-I: Chimera Structural Characteristics

Component	Structural Characteristic
Wing	Spar Location: 20%, 53%, 78% C_r Rib Spacing: 19 in.
Horizontal Stabilizer	Spar Location: 23%, 50%, 71% C_r Rib Spacing: 14 in.
Vertical Stabilizer	Spar Location: 14%, 40%, 65% C_r Rib Spacing: 13.5 in.
Fuselage	Frame Depth: 2 in. Frame Spacing: 16 in. Longeron Spacing: 13 in.

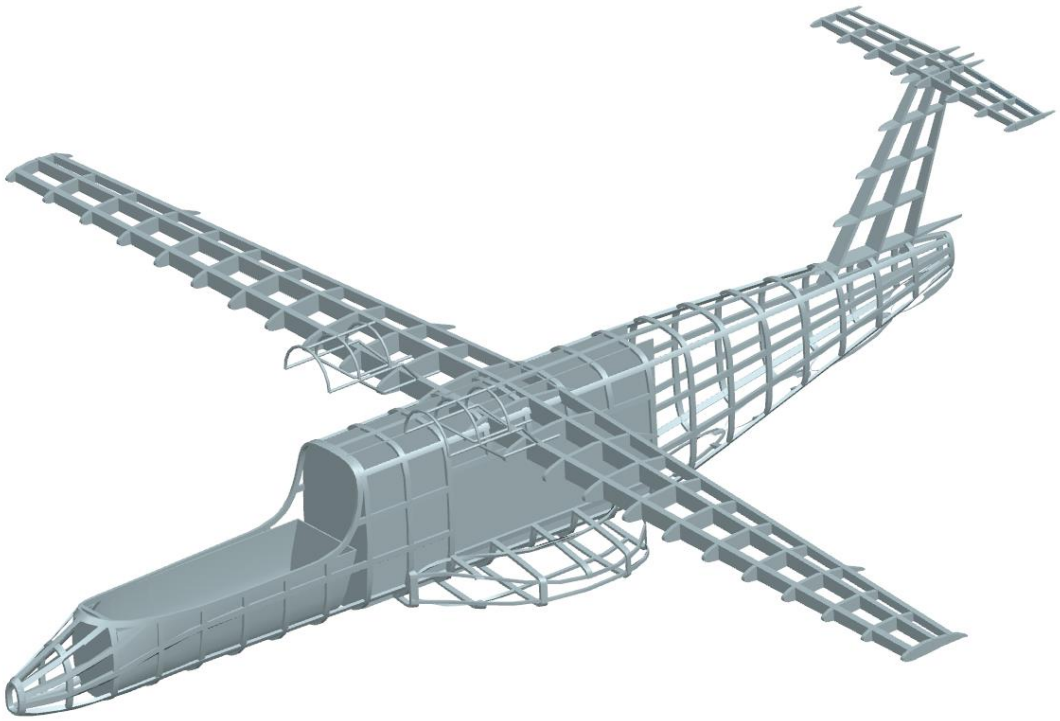

Figure 16.1: Structural Layout Overview

As evident in the previous figure, a spinal structure exists within the bomb bay. This allows torsional rigidity of the fuselage to be maintained as a result of the ring frame cutouts to accommodate the bay doors. More detail on the bay doors can be found in Chapter 18.10.

17. Class II Landing Gear Sizing and Placement

Sizing of the landing gear tires and struts followed methods presented in *Aircraft Design: Part IV* [48]. The landing gear has been sized to 1.25x the maximum landing weight of the Chimera which allows for further growth and future modifications of the aircraft. Table 17-I outlines the weight and load conditions for each of the landing gear struts. It should be noted that the main landing gear consists of two struts and the given load is per strut.

Table 17-I: Landing Gear Strut and Tire Loading

Gear	Strut Static Load (lb_f)	Strut Static Load x1.25 (lb_f)	Dynamic Strut Load (lb_f)	Maximum Tire Load (lb_f)
Main Gear	8,729	10,911	3,722	2,728
Nose Gear	771	964	2,056	2,056

From the known loading of the tires, the database of tire characteristics in Reference 48 was analyzed to find tires that would be able to adequately handle the loads. The chosen tires with their specifications are found in Table 17-II.

Table 17-II: Salient Tire Characteristics

Gear	Diameter (in)	Width (in)	Rated Load (lb_f)	Loaded Radius (in)	Rated Inflation (psi)
Main Gear	15	6	3525	6.2	110
Nose Gear	13	5	2150	5.7	88

With the tires selected, the shock absorber deflection and diameter were sized. The touchdown velocity was assumed to be 13 ft/s while the load factor was assumed to be 5g. The calculations resulted in the following strut sizing in Table 17-III.

Table 17-III: Landing Gear Strut Sizing

Gear	Strut Stroke (in)	Strut Diameter (in)
Main Gear	2.27	1.57
Nose Gear	1.033	1.61

The equation for landing gear stroke sizing adds an additional recommended one inch to the calculated value meaning that the nose may not need a shock absorber. However, it would be beneficial to keep it as the aircraft will face rough landing conditions in austere fields.

The landing gear location was decided using the methods in Aircraft Design: Part IV [48]. Figure 17.1 shows the longitudinal view of the aircraft. The location of the main gear complies with the requirement of being placed 15 degrees aft of the C.G. of the aft most ground configuration. The rotation angle from the tail to the main gear also complies with the 15 degree clearance requirement for takeoff. Figure 17.2 set the width of the main landing gear. A 35 degree half angle cone was generated at the location of the C.G. and extended to the ground. The main gear were placed outside of this radius to ensure lateral tip over compliance was met.

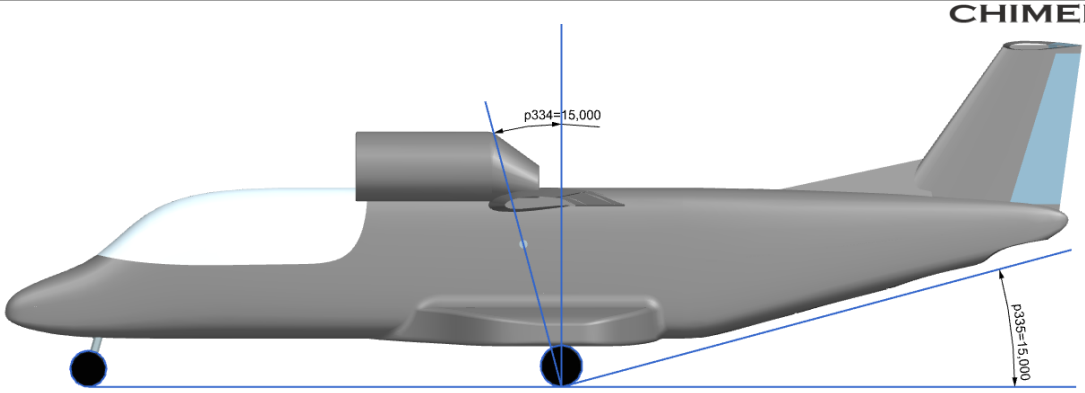

Figure 17.1: Longitudinal Tip-over and Rotation Compliance

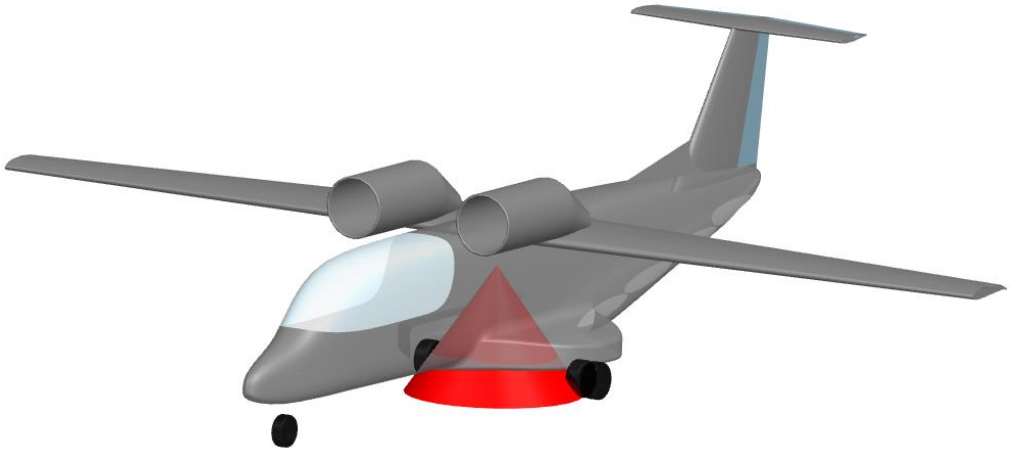

Figure 17.2: Lateral Tip-over Compliance

18. Class II Layout of Major Systems

18.1 Flight Control Systems

Given the combative nature of the mission specification for the Chimera, a flight control system with triple redundancy was implemented. Three flight computers, as shown in Figure 18.1, are used to control each control surface. This allows for complete redundancy over the single voting network. Wiring between the flight computers and the actuators, was run to minimize the possibility of more than one computer failing for any event. Optical lines were used for the wire so that the Chimera can operate in electromagnetically challenging environments. Electro-hydrostatic actuators were selected due to their

high power density and precise control when compared to electromechanical actuators. Additionally, they do not suffer from backlash issues, enabling very precise control without error caused by gaps between mechanical components.

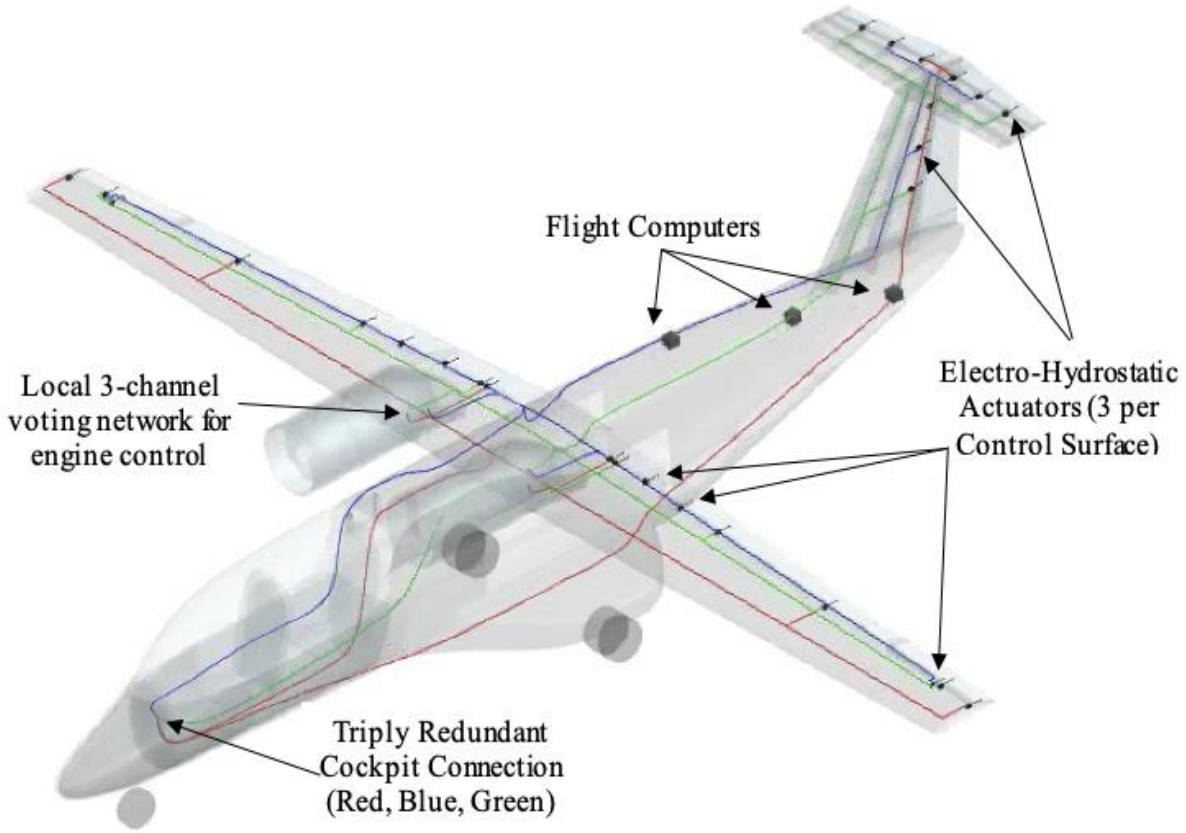

Figure 18.1: Flight Control Optical Signal Paths

18.2 Fuel System

The required fuel for the Chimera is 2,200 pounds which translates into a required fuel volume of just under 330 gallons. Due to the high aspect ratio of the wing, not all of the fuel is able to be stored in the wings. This reduction in fuel volume an required an auxiliary tank to be added in between the wings to meet the required fuel volume. This location sits right on the center of gravity of the aircraft meaning that the C.G. excursion due to fuel usage is minimized. In order to maintain usage from each fuel tank

even in the case of failure, all three fuel tanks have individual pumps and are connected with fuel pipes. The entire fuel system is shown in Figure 18.2 in orange.

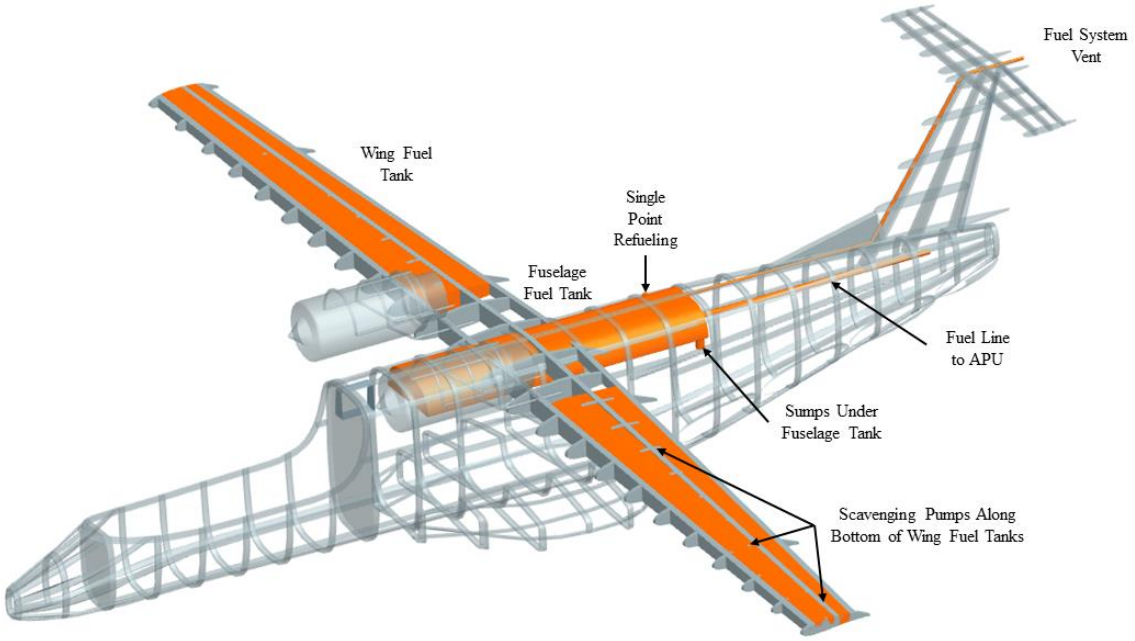

Figure 18.2: Fuel System Overview

To maximize the fuel volume available in the wings, the entire span, other than the area directly behind the engine exhaust, is occupied by fuel tanks. In order to supply fuel to the APU in the tail of the aircraft, a fuel line extends from the fuselage fuel tank to the APU. With a high wing, it is important that the refueling is taken into consideration. Due to the fact that the wing sits just under six feet off the ground, it is possible to refuel through the top of the wing. This means that the system is refueled at the highest point in the system and does not require any extra pumps to move the fuel into the tanks. The lack of either anhedral or dihedral on the wing causes the need for scavenge pumps to be located along the bottom of the wing fuel tanks as there is no natural low spot. A vent for fuel vapors runs along the top of the fuselage tank and extends to vent out of the back of the horizontal tail. The vent line has a check valve within it preventing liquid to pass through and restrict it to only vapors.

18.3 Hydraulic System

The Chimera requires hydraulic systems for both the landing gear and the bay doors for the missiles. Due to the use of electro-hydrostatic actuators for flight control, the hydraulic system can be simplified. The hydraulic system is used both for the landing gear and the Hellfire bay doors. The entire hydraulic system is double-redundant due to the nature of the dual engine design. In the case that all hydraulic systems encounter a failure, the landing gear is still able to operate. The main gear extends out of the sponson while the front gear can drop with a gravity assist. The Hellfire doors on the Chimera open in the same manner as the bay doors on the Comanche Attack Helicopter with hydraulic pistons connected to the top of the door. The entire hydraulic system can be seen in Figure 18.3 below.

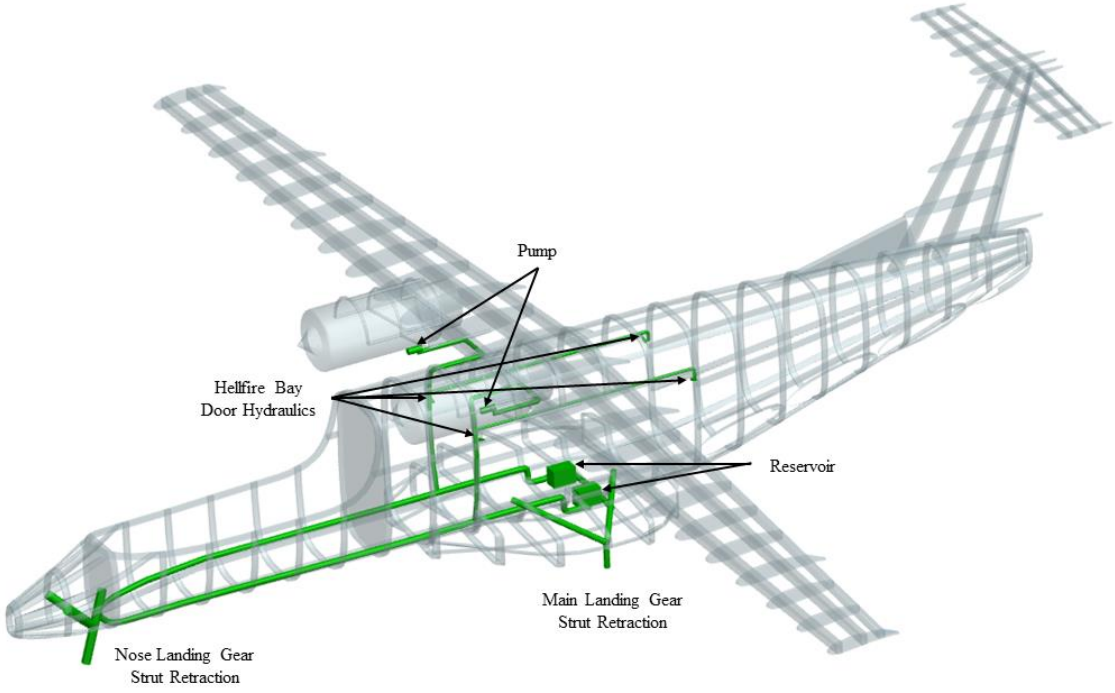

Figure 18.3: Hydraulic System Overview

18.4 Electrical System

In order to power all of the systems on the aircraft, a robust electrical system is required. For ground operation the main power comes from the APU in the aft of the aircraft while during flight all power comes from the FJ44 turbine engines. In order to maintain safety and survivability, the entire electrical system is triple-redundant to allow for any two of the three systems to fail. This includes three batteries

located around the aircraft that will be able to store and regulate power in case of damage. All three batteries are located within isolated bays with external vents. The SATCOM antenna is also wired into the power grid of the aircraft and is placed on the vertical tail to maintain unobstructed access to the satellite systems.

All weapons systems are connected to the triple-redundant power system. The bay doors have power cables running down them to power the Hellfire missiles while all of the bomb tubes have cables running to them to power the GBU 39's. The M197 gun is also wired in to the electrical system through the gimbal at the base of the gun. Finally, the Star SAFIRE targeting pod receives power as well through the same power system. The wiring and electrical system is shown in Figure 18.4 with the wires being shown in yellow.

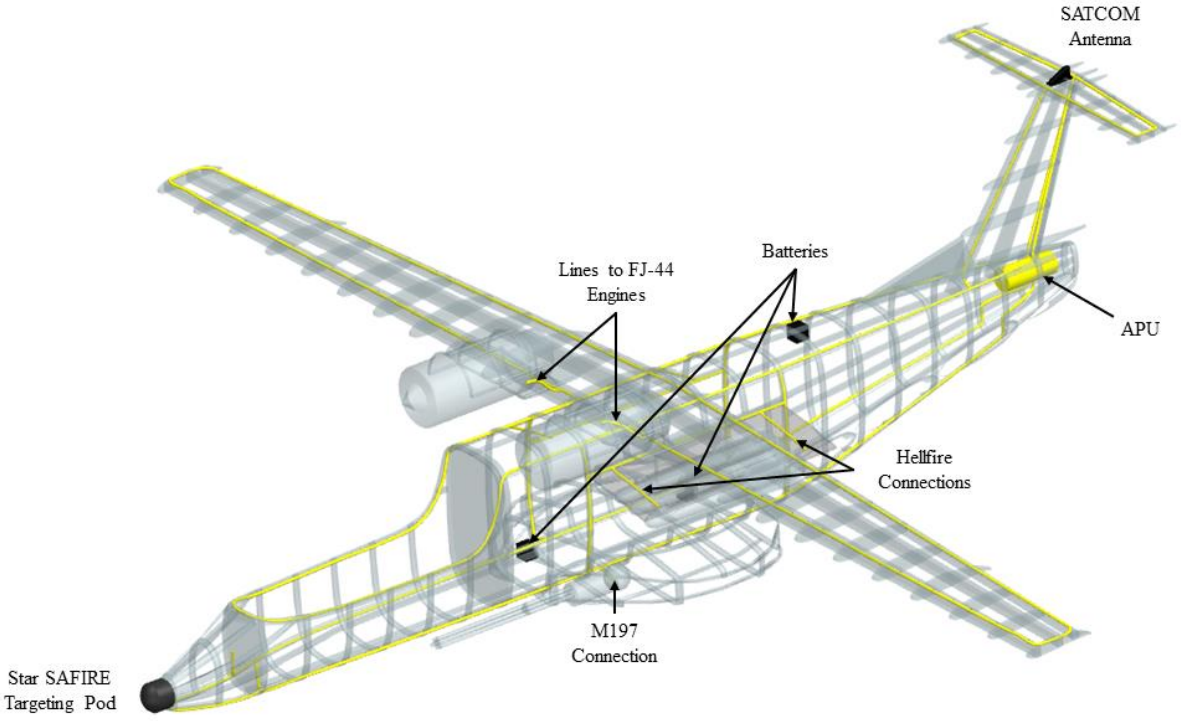

Figure 18.4: Electrical System Overview

18.5 Target Systems & Optics

The targeting/optics system that will be fielded on the Chimera will be the FLIR Star SAFIRE electro-optical/infrared sensor, designated the AN/AAQ-22, as seen in Figure 18.5. This targeting system is capable of internal navigation for precise targeting, a MWIR thermal imager, optional HD color and low-light cameras, and multiple laser payload options [49]. The Star SAFIRE system is 15 inches in diameter, 17.5 inches in height, and weighs 100 pounds. The pod will be mounted externally on the nose of the aircraft, as seen in Figure 18.6. On takeoff and landing, the camera will rotate and face aft to avoid any debris damaging the face of the camera.

Figure 18.5: Star SAFIRE [49]

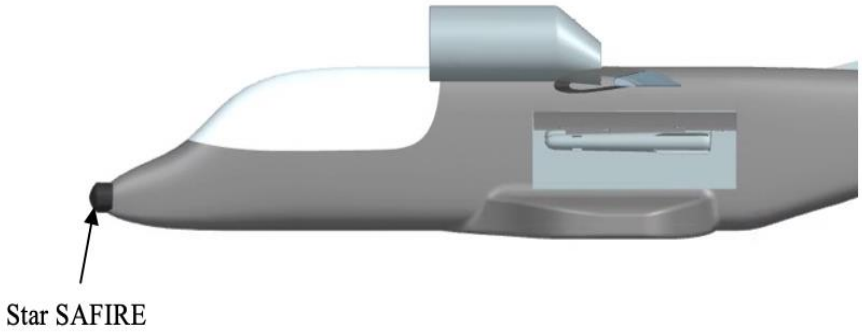

Figure 18.6: Targeting Pod Location

18.6 Cockpit Instrumentation, RF and Sat Coms

In order to have a pilot be as effective as possible, it is important that the cockpit is setup in a way that makes them comfortable with the aircraft. Due to this, the aircraft will be controlled with a side-stick style cockpit and have a glass touch cockpit similar to that of the F-35 Lightning II. The Chimera cockpit can be seen in Figure 18.7.

Along with flight controls, it is important that the pilot is able to communicate with ground troops, air traffic controllers, fighters, operations, etc. Due to this the Chimera is equipped with narrow-band

SATCOM. The antenna for this communication can be seen in Figure 18.4 above as the black triangle above the horizontal tail.

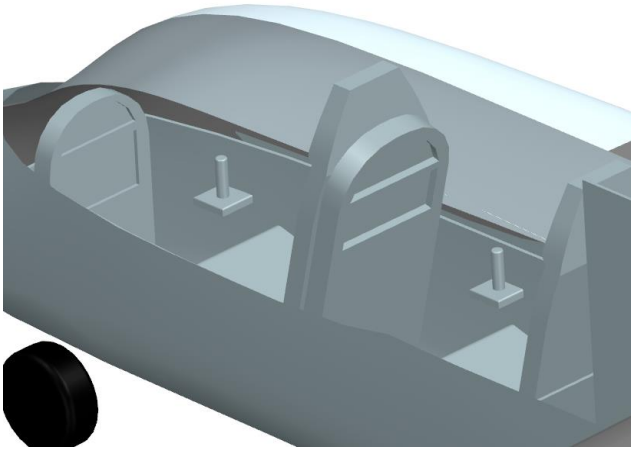

Figure 18.7: Chimera Cockpit

18.7 De-icing and Anti-icing Systems

The Chimera is capable of using bleed air from the main engines and the APU to de-ice the engine cowl inlets. Engine bleed air is run through the stators, then the hot, compressed air is pushed over the components to warm them and eliminate any ice, as shown in Figure 18.8. While this will add a slight increase in the IR observable, it is not planned to operate during combat. A shut-off valve is used to return to normal engine operations in the event that the weather does not require actively warming the cowls. The Chimera v. The electromechanical transducer element delivers a shock to the ice-covered leading edge of the wing, eliminating ice on the surface of the wing. This system was used due to its capability to eliminate ice without increasing the IR or RF spectrum observables.

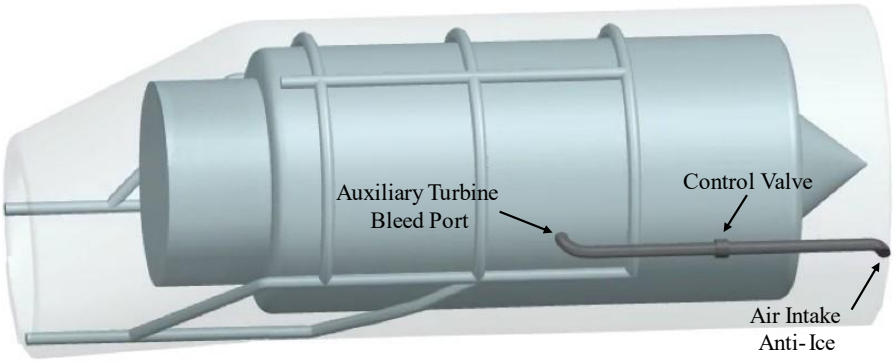

Figure 18.8: Engine Anti-Icing System

18.8 Window, Rain, Fog, and Frost Control

The Chimera is fielded with a hydrophobic coating on its cockpit to prevent the accumulation of water. This prevention is vital to maintain visibility through the cockpit in the event of rain. The hydrophobic coating causes the water droplets to bead and become spheres on contact with the chemical. These spheres are instantly blown off due to the high-speed airflow around the cockpit. Beaded water on a windshield is demonstrated in Figure 18.9.

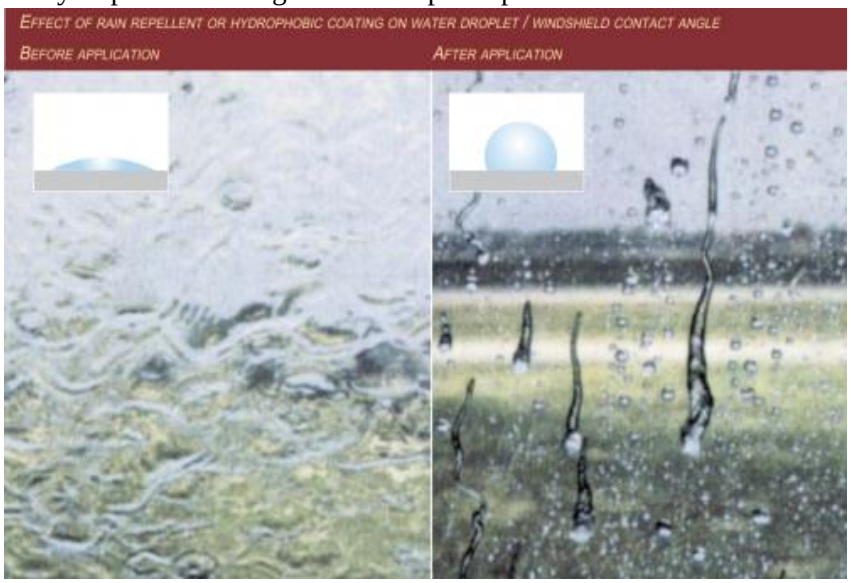

Figure 18.9: Windshield Rain Repellant [55]

Additionally, an electrical system is used to warm the glass of the Chimera. This prevents fogging and frosting of the glass during operation. This system blows hot air through a jet core running along the inside of the cockpit glass, which then directs the air along the inside of the cockpit glass to prevent fogging or frost from building. It is powered by the electrical wiring beneath the window of the cockpit. The defog system of the Chimera cockpit is shown in Figure 18.10.

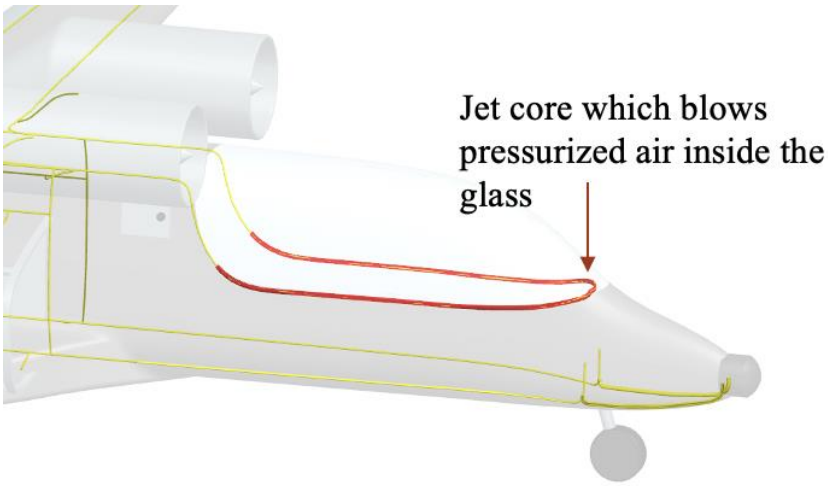

Figure 18.10: Electrical System Schematic

18.9 Gun System, Round Handling, & Loading

The Chimera is fielded with a M-197 Gatling gun which fires 20 mm rounds. This type of weapon can effectively engage ground targets for the purpose of CAS. The gun is in the left sponson, as seen in Figure 18.11. The gun will be gimbaled at the front end of the sponson such that it can perform in both strafe and orbit runs if needed. The sponson will have a cutout for the gun to be able to sweepout to achieve left-handed orbiting fire. There will be a mechanical system installed to move the gun along a track and lock into place for orbiting fire. The gun and gimbal system will be secured to the substructure of the sponson as well as the ring frames of the fuselage. The back end of the gun will need to be connected to a primary structure section to withstand the recoil. The entire barrel is outside the aircraft thus it will be air cooled as well as easily cleaned. The location of the gun minimizes the drag effect. The M-197 will have an ammo belt being fed from the ammo drum located behind the cockpit. The ammo drum and feeding system is shaded blue. The ammo being fed into the gun will be linked 20mm cannon shells and the spent shells will be cycled back into the ammo drum. There will be an access panel on top of the sponson to access the gun for maintenance. There is another access panel on the other side of the aircraft where the ammo drum lies to allow the drum to be reloaded and replenished, as seen in Figure 18.12. Figure 18.13 shows the Chimera being loaded using a standard ammo loading truck, which will be

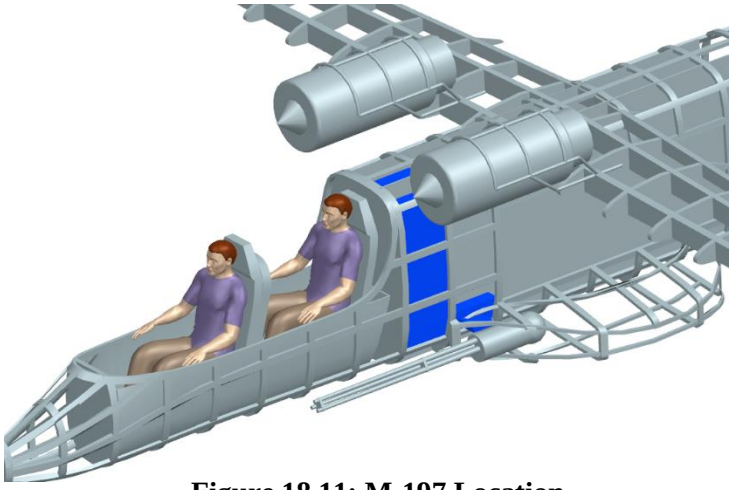

Figure 18.11: M-197 Location

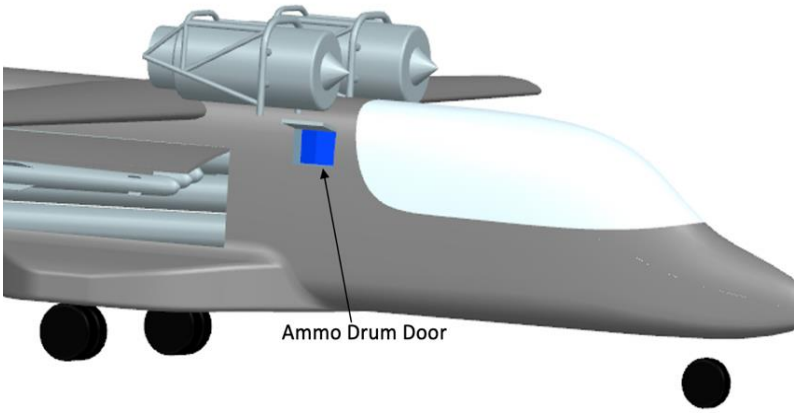

Figure 18.12: Ammo Loading Location

discussed in section 18.13. The Chimera is able to hold roughly 2,500 rounds of 20 mm ammo based on the full ammo drum weight & size, whereas the A-10 is able to hold 1,350 rounds of 30 mm ammo.

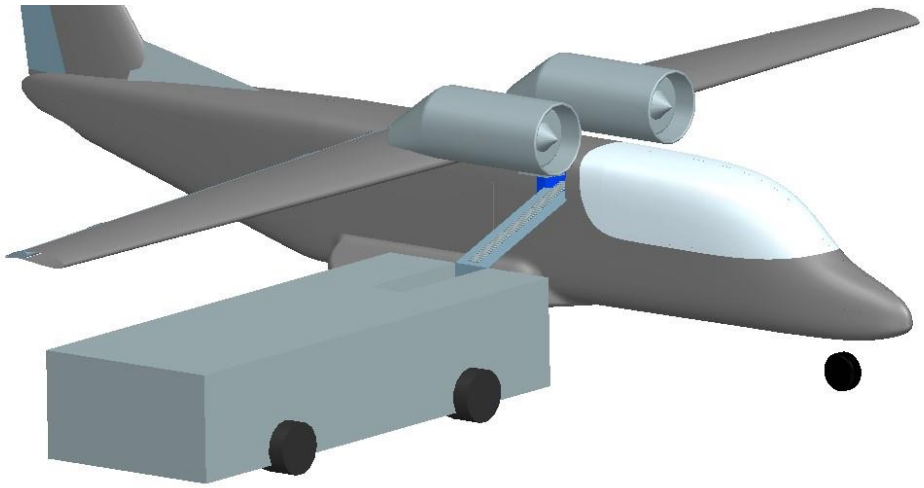

Figure 18.13 Ammo Loading

18.10 Missile Accommodation, Loading and Launch

Due to the Chimera's high L/D requirement, the missiles will be held inside the bay to keep the wings clean and to maintain the high performance that the Chimera delivers.

The Chimera has the capability of holding 3 Hellfire missiles in each bay door on the side of the fuselage. These missiles will be mounted internally on rails. When it is time to launch the missiles, the doors swing open to give the missiles an unobstructed launch forward. This system will work very similarly to how the Boeing-Sikorsky RAH-66 Comanche utilizes its doors. The Hellfire missiles will also be loaded through the bay doors, which will be opened when on the ground for maintenance and systems checks. Each Hellfire missile weighs a maximum of 110 lbs and can easily be loaded by two ground crew operators. Figure 18.14 shows the Chimera with the bay doors open and 6 Hellfire missiles loaded.

Figure 18.14: Open Bay Doors

The Hellfire missile is used due to how common it is in air-to-ground combat missions. The Hellfire comes with a variety of payloads and can be configured for different targets and environments depending on the mission requirements. The Hellfire missiles will use the FLIR Star SAFIRE for targeting prior to launching and can be guided via radar or laser designation.

If required, the Chimera can also carry two Hellfire missiles mounted at the tip of each wing. This would require a pylon be attached and it would remove the capability to have tip-mounted fuel tanks. Figure 18.15 shows a more detailed look at the bay door setup.

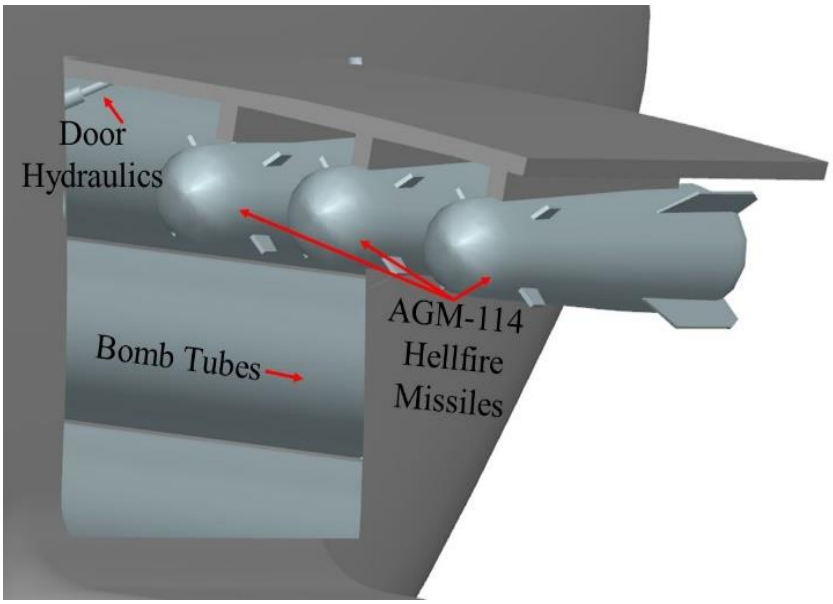

Figure 18.15: Detailed Bay Doors

18.11 Bomb

Accommodation, Loading and Launch

The bomb bay of the Chimera is inspired by the A-5 Vigilante. The Chimera is designed to drop bombs out of the rear of the aircraft instead of out the bottom through a bomb-bay door. The A-5 Vigilante had a singular tube, where its bomb was held behind two fuel tanks, all of these ejected out the rear linearly. The Chimera is designed to hold four GBU-39's and has four tubes spanning the bomb bay and the rear of the aircraft. Each bomb will sit within its own tube and will be loaded and deployed via that tube. With this system, each bomb can be dropped individually or all at the same time. This also allows other bombs to deploy if one gets jammed or fails to launch. Due to the Chimera using tubes, any bomb of a smaller diameter than the 9" tubes may be used with ease. All bombs will be placed within a 9" diameter sabot to ensure a tight fit within the tubes.

The bombs will be loaded through vacuum pressure in the tubes generated by the APU, which will suck the bomb and sabot into the aircraft's bay. The bombs will stay in the bay due to simple pins that can pop out to secure the sabot on both sides. When it is time to deploy the bombs, each tube can be pressurized by the APU to push the bomb out, the tubes are also outfitted with a small release charge that can help to push the bomb out of the tube, much like an airbag. These airbags can be accessed by crew on the ground via the bay doors on the side of the Chimera for replacement after use.

GBU-39's were chosen as the standard bomb due to their price and range. The Chimera operates best at large standoff distances, the GBU-39's have a superior range. Dumb bombs like the Mk. 82 were initially considered due to their simplicity and commonality within similar aircraft, however it is expected that dumb bombs will be used less in the near future before being abandoned altogether. Dumb bombs lack the range of glide bombs, and obviously cannot be controlled, which leads to a higher chance of collateral damage. The GBU-39's will be wired into the FLIR Star SAFIRE once they are in the tubes and will receive targeting information prior to deployment. The GBU-39's can navigate with GPS, laser designation, and inertial navigation systems.

Figure 18.16 shows how the bombs will be loaded and stored within the Chimera.

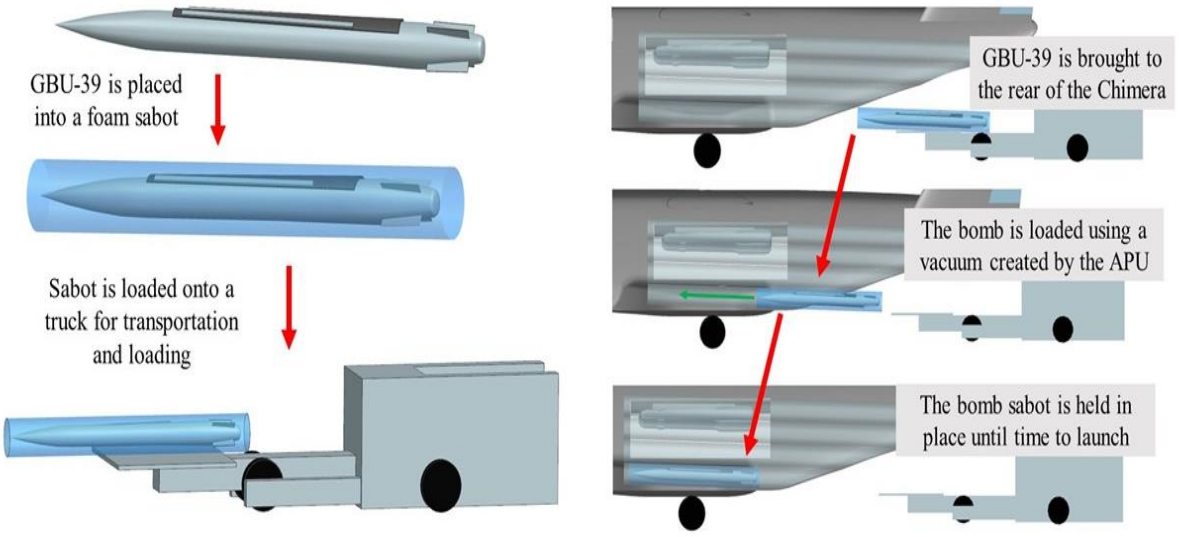

Figure 18.16: Chimera Bomb Loading and Storage

Figure 18.17 shows how the bombs will be launched from the Chimera. When the sabot clears the rear of the aircraft, the drag will peel open the sabot and it will shed from the bomb. In the case of the GBU-39, once the sabot has cleared, the wings will fold open, and the bomb will glide to its destination.

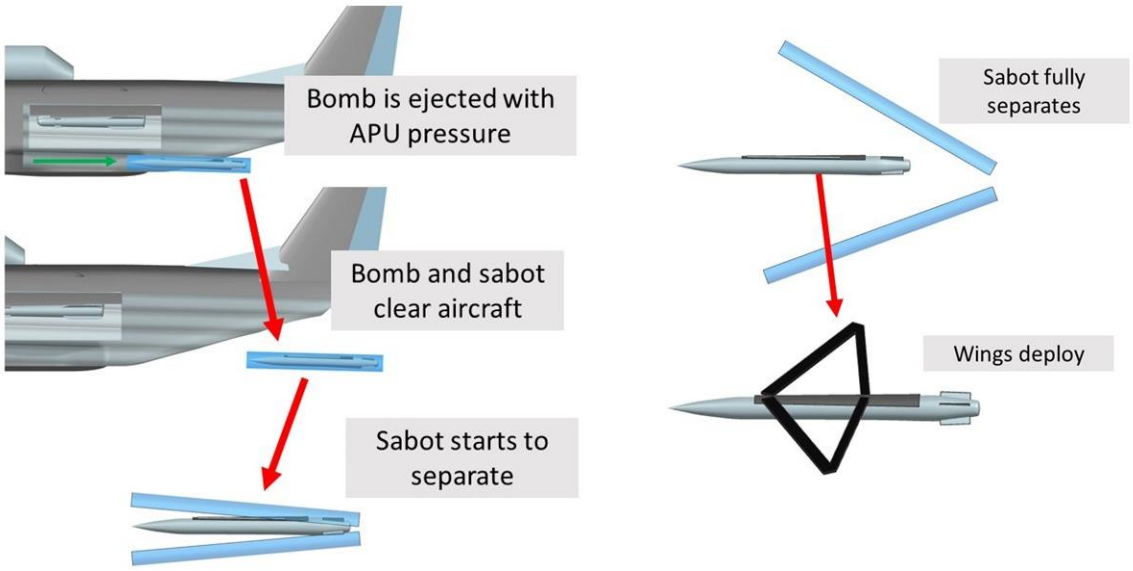

Figure 18.17 Chimera Bomb Egress

Figure 18.18 and Figure 18.19 show the rear of the Chimera and the side of the bomb bay, respectively. The bomb tubes are each covered with a rubber seal to keep airflow over the fuselage as attached as possible. These coverings are slotted much like the lid of a soft drink cup to allow the bomb to pass through easily. This allows for the tube to mostly seal when the bombs are stowed during flight, allowing the airflow over the rear of the Chimera to stay attached.

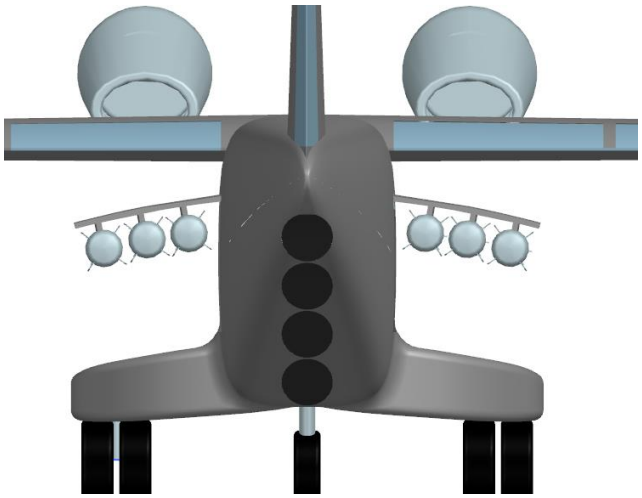

Figure 18.18 Rear of Chimera Bomb Tubes

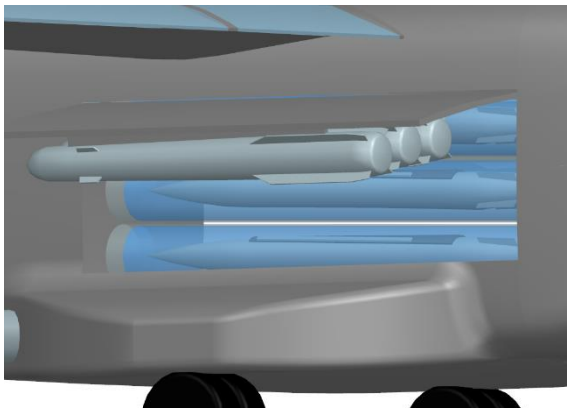

Figure 18.19 Side-View of Stowed Bombs

18.12 Ejection Seats, Crashworthiness, and Armor

The Chimera will utilize a Martin-Baker Mk. 10 ejection seat for both the pilot and the gunner. This seat is used in the Super Tucano, Sea Harrier, and Tornado. This will provide the pilot and gunner with a reliable and safe exit from the aircraft in case of an emergency. Figure 18.20 shows the Mk. 10 ejection seat.

Figure 18.20: Martin-Baker Mk. 10 [51]

In the event of a crash, the Chimera is designed for safety. The bottom half of the aircraft can act as a crumple zone to dampen the load during the crash. The main gear of the Chimera will also be exposed even when stowed, allowing for the wheels and landing gear to absorb some of the impact instead of the fuselage. In the event of an engine failure, the pilots are in front of the turbine blades and will remain clear of any shrapnel that is thrown from the engine. The fuel tanks and lines are separated from the cockpit by a solid bulkhead, meaning that any fuel fires would not spread to the pilots, and they can remain safe in the event of a fire. In the event of an ejection, the canopy will swing open from the aft side of the cockpit, blocking some of the suction from the engines, and giving the pilots a clear path upwards and away from the aircraft.

The pilots are surrounded by a Kevlar “bathtub” that lines the cockpit. This bathtub is designed to stop any shrapnel, flak, and small arms fire from harming the pilots. The canopy is also bullet-proof glass and should protect against any small arms fire. Since the Chimera is designed for orbit, the left-wing will be more heavily armored than the right wing, as will the left side of the fuselage. This should help to protect the fuel tanks and engine on the left side of the aircraft, allowing for a safer, sustained flight.

18.13 Ground Equipment, Ergonometric & Vehicles Compatibility

The ground equipment required by the Chimera is a refueler truck, an aerial stores lift truck, and an ammo loader system. As previously stated, the fuel port is on top of the fuselage and thus any aircraft refueler truck will be able to access this port. A refueler truck with a lift deck may be necessary to adequately reach the top of the fuselage. An aerial store lift truck will be needed to load both the missiles and bombs. Figure 18.21 shows the MJ-1 which is a common aerial store lift truck that can lift up to 3,000 lbs. This truck is limited by a maximum store diameter of 40 inches and a maximum length of 144 inches. The lift has a maximum height of 78 inches and a minimum clearance of the ground to the bottom of the store of 6.25 inches. The fuselage is 71 inches from the ground and thus a truck like this will be able to lift the missiles and bombs to the required height to be secured in the plane.

Figure 18.21: MJ-1 Lift Truck [52]

A Universal Ammunition Loading System (UALS) would be needed to load the ammo drum sitting behind the cockpit. Figure 18.22 shows the UALS. The UALS provided by General Dynamics can load up to 2,100 rounds at 400 rounds a minute. The system comes with both a loader and a replenisher. The UALS loader is 181” long, 68” wide, and 37” tall. This type of UALS will adequately be able to reach the ammo door on the Chimera.

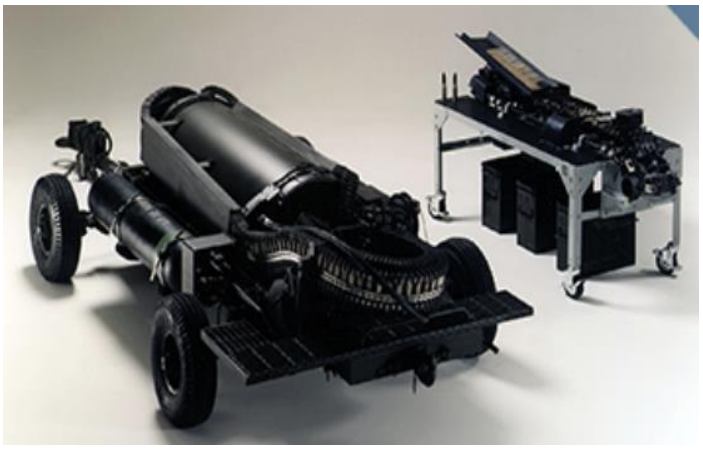

Figure 18.22: UALS Ammo Loader [53]

19. Class II Weight and Balance

The following section outlines the Class II weight and balance calculations completed using Advanced Aircraft Analysis (AAA) software. The component breakdown itemizing the weight and C.G. location of each component can be found in Table 19-I. Figure 19.1 further shows the C.G. location of each of the numbered components found in Table 19-I in a sideview of the Chimera.

Table 19-I: Weight Breakdown

#	Component	Weight (lb)	Weight Fraction (~)	X_{CG} (in)	Y_{CG} (in)	Z_{CG} (in)
	Structural					
1	Wing	757	0.081	311	0	159
2	Horizontal Tail	58	0.006	490	0	216
3	Vertical Tail	62	0.007	481	0	185
4	Fuselage	707	0.075	306	0	138
6	Engine Nacelles	97	0.010	275	0	172
7	Nose Landing Gear	41	0.004	150	0	100
8	Main Landing Gear	230	0.025	320	0	100
	Powerplant					
9	Engines	920	0.098	272	0	172
10	Fuel System	150	0.016	336	0	156
11	Air Induction System	4	0.000	282	0	172
12	Propulsion System	49	0.005	288	0	172
	Fixed Equipment					
13	Flight Control System	87	0.009	348	8	138
14	Hydraulic and Pneumatic System	36	0.004	288	10	120
15	Instruments/Avionics	50	0.005	222	0	133
16	Electrical System	128	0.014	420	9	159
17	2 Ejection Seats	242	0.026	216	0	133
18	Air Conditioning/Anti-Icing Systems	40	0.004	408	0	160
19	Oxygen System	26	0.003	252	0	120
20	APU	78	0.008	480	0	148
21	Battery	30	0.003	480	0	155
22	Gun	132	0.014	296	-23	115
23	Hellfire Hardpoints	300	0.032	320	0	135
24	Optical Ball	100	0.011	125	0	120
	Empty Weight	4324	0.461	287	3	148
25	Crew 1	200	0.021	194	0	133
26	Crew 2	200	0.021	238	0	133
27	Trapped Fuel and Oil	64	0.007	302	0	164
	Operating Empty Weight	4788	0.511	296	3	148
28	Fuel Weight	2200	0.235	303	0	159
29	4 GBU 39's	1140	0.122	320	0	132
30	6 Hellfire Missiles	648	0.069	320	0	135
31	Full Ammo Drum	600	0.064	263	0	138
	Takeoff Weight	9376	1.00	300	0	147

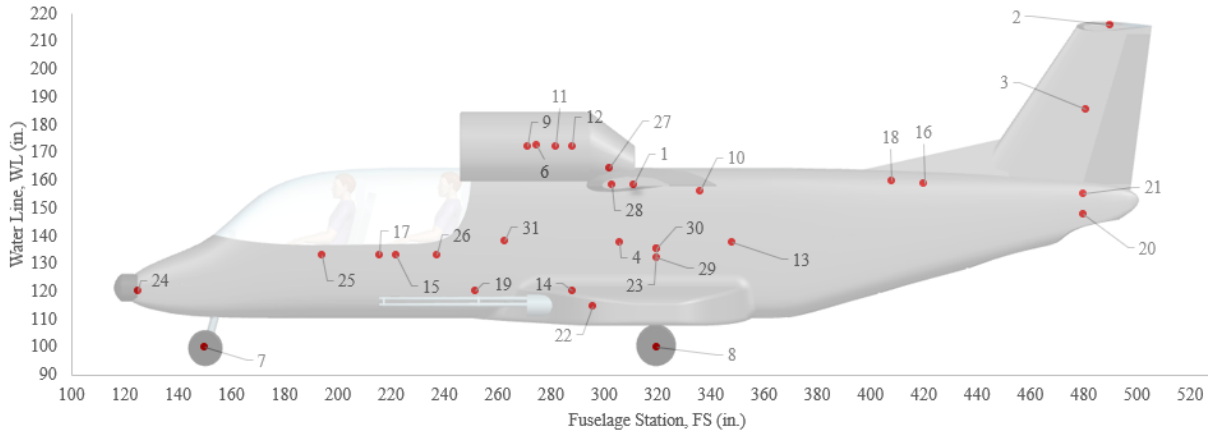

Figure 19.1: Component Center of Gravity Locations

The aircraft C.G. Excursion chart can be found in Figure 19.2. Each possible ground loading configuration is shown in as the blue lines. The C.G. excursion of the ground configurations is 11%. The possible C.G. ranges while in the flight condition is shown as the orange lines. The flight configuration C.G. excursion is 10%. Figure 19.3 shows the relative contribution to takeoff weight of each aircraft component based on the weight breakdown shown above.

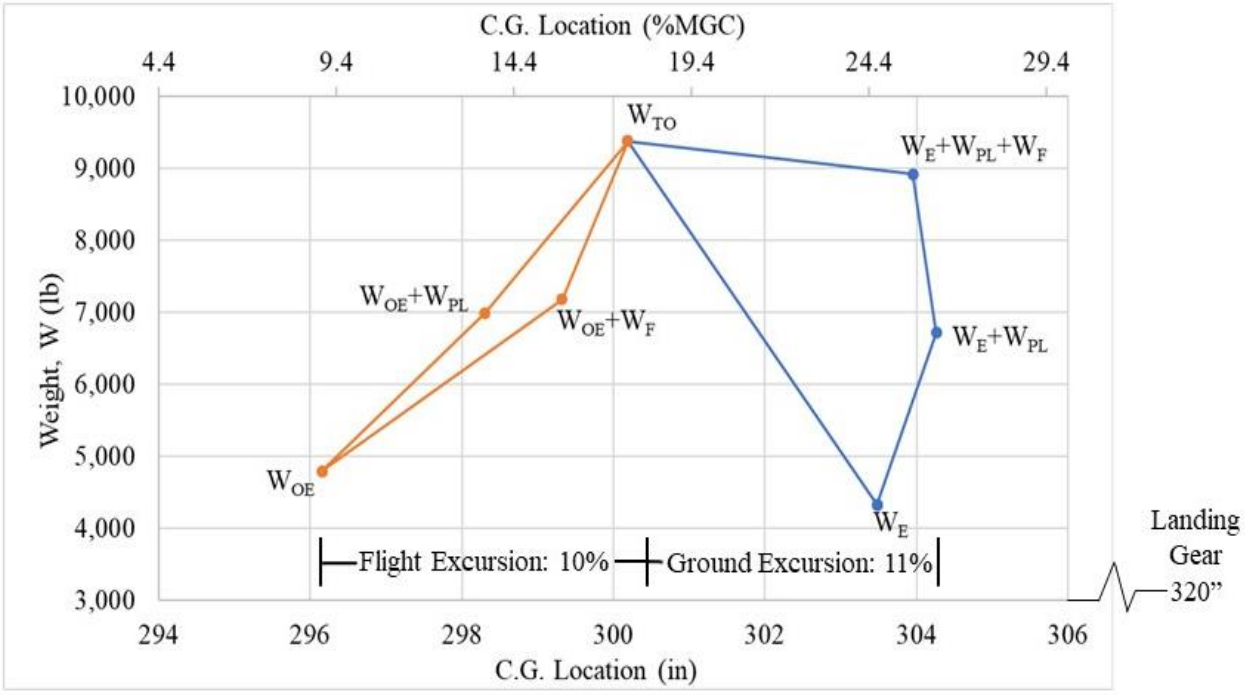

Figure 19.2: C.G. Excursion Chart

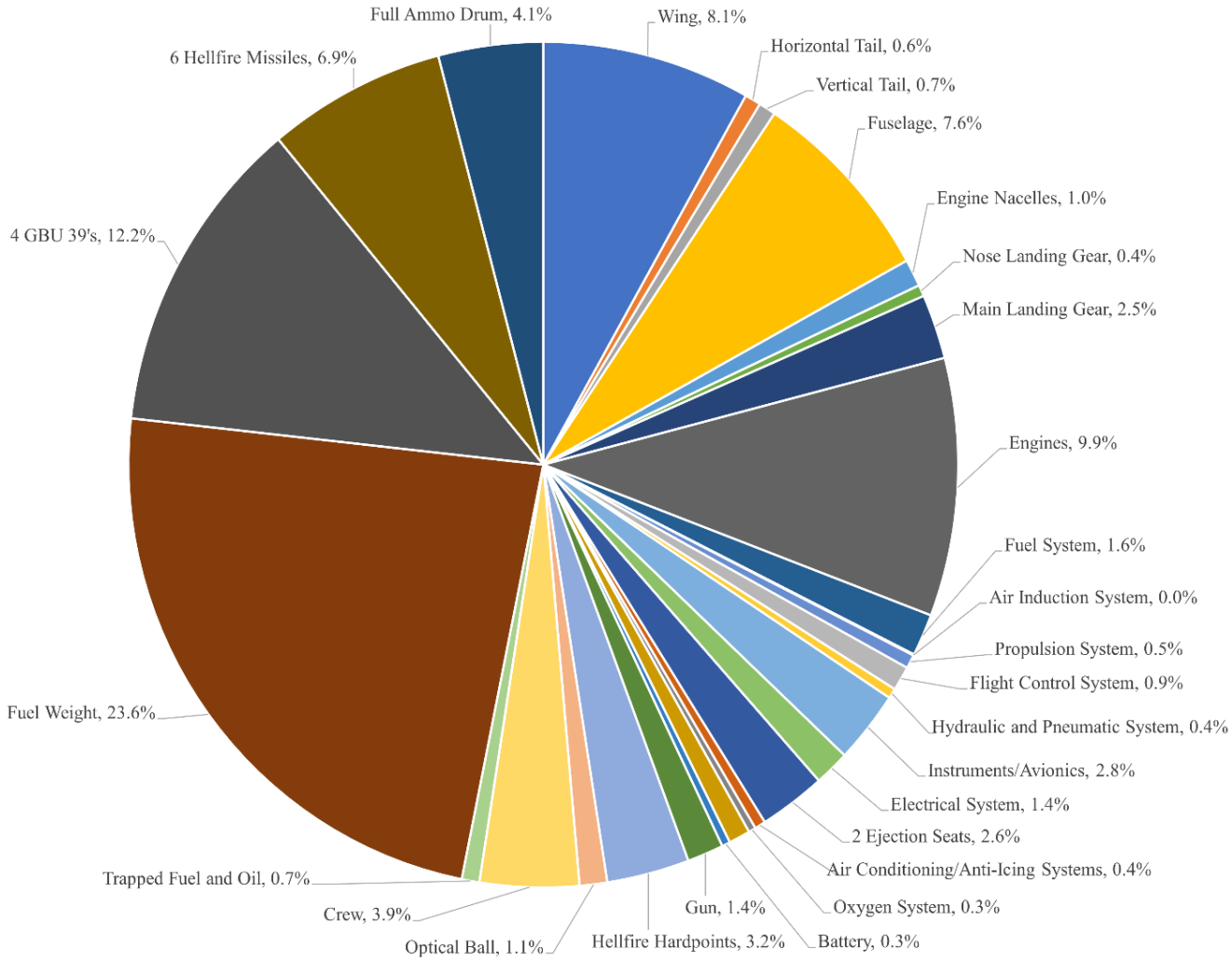

Figure 19.3: Takeoff Weight Breakdown

20. Class II Stability and Control

20.1 Longitudinal and Lateral X Plots

The X-Plot defining the static margin of the aircraft can be found in Figure 20.1. The aerodynamic center of the aircraft is located at 18% of the MGC. The static margin varies in flight from 2% to 14%. The current static margin can be augmented using a variable k_α gain to achieve the ideal 10% static margin for the pilot.

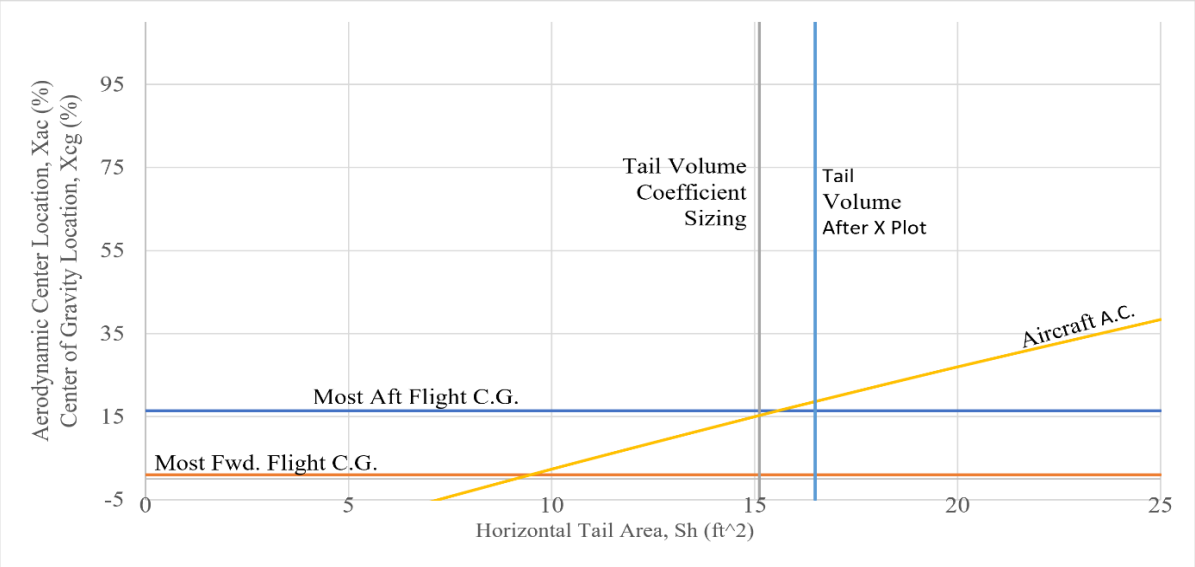

Figure 20.1: Longitudinal X-Plot

The directional X-Plot for the aircraft can be seen below in Figure 20.2. With the current vertical tail area of 21.42ft, the $C_{n\beta}$ value is approximately 0.0018/deg. The desired $C_{n\beta}$ value for a stable aircraft is anything larger than 0.001/deg which is met with the current vertical tail area. Yaw control must be maintained in a one engine out scenario. Using *Airplane Design Part V* [46] the required rudder deflection to maintain steady heading with one engine out was calculated as 22°. This is within the acceptable required range of rudder deflections.

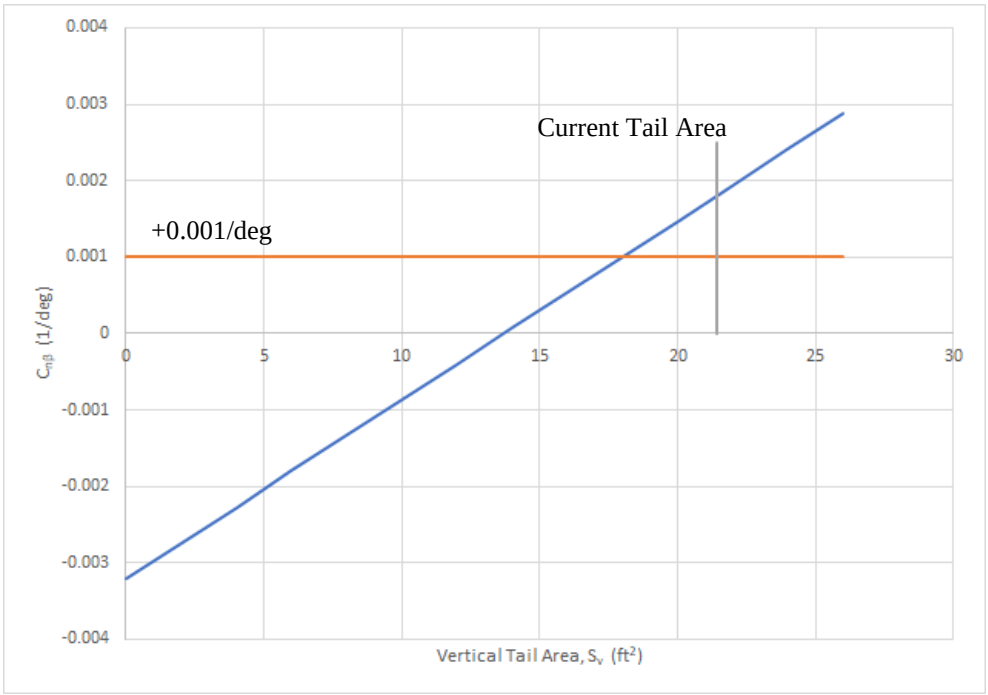

Figure 20.2: Directional X-Plot

20.2 Stability and Control Derivatives

AAA was used to complete the Class II stability and control analysis for the cruise condition. Table 20-I tabulates the static stability and control derivatives for the aircraft in the longitudinal and lateral directions. Table 20-II and Table 20-III tabulate the dynamic stability and control handling qualities in the longitudinal and lateral directions, respectively. The handling capabilities are all at or above the required levels for attack aircraft.

Table 20-I: Stability and Control Derivatives

Longitudinal Control Derivatives		Lateral Control Derivatives	
$C_{L,u}$	0.13375	$C_{y,\beta}$	-0.5682 (rad^{-1})
$C_{m,u}$	0.01613	$C_{l,\beta}$	-0.061 (rad^{-1})
$C_{D,\alpha}$	0.159 (rad^{-1})	$C_{n,\beta}$	0.00428 (rad^{-1})
$C_{L,\alpha}$	5.14023 (rad^{-1})	$C_{y,p}$	-0.0044 (sec/rad)
$C_{m,\alpha}$	-0.7258 (rad^{-1})	$C_{l,p}$	-0.5125 (sec/rad)
$C_{L,\dot{\alpha}}$	1.15535 (sec/rad)	$C_{n,p}$	-0.0527 (sec/rad)
$C_{m,\dot{\alpha}}$	-5.3169 (sec/rad)	$C_{y,r}$	0.29298 (sec/rad)
$C_{L,q}$	8.1355 (sec/rad)	$C_{l,r}$	0.14899 (sec/rad)
$C_{m,q}$	-22.781 (sec/rad)	$C_{n,r}$	-0.1075 (sec/rad)
$C_{D,ih}$	0.01884 (rad^{-1})	$C_{l,\delta a}$	0.01567 (rad^{-1})
$C_{L,ih}$	0.51699 (rad^{-1})	$C_{n,\delta a}$	-0.0013 (rad^{-1})
$C_{m,ih}$	-2.3792 (rad^{-1})	$C_{y,\delta r}$	0.16336 (rad^{-1})
$C_{D,\delta e}$	0.00498 (rad^{-1})	$C_{l,\delta r}$	0.01313 (rad^{-1})
$C_{L,\delta e}$	0.14652 (rad^{-1})	$C_{n,\delta r}$	-0.0698 (rad^{-1})
$C_{m,\delta e}$	-0.6743 (rad^{-1})		

Table 20-II: Longitudinal Handling Qualities

$\omega_{n,SP}$ (rad/s)	ζ_{SP} (~)	$\omega_{n,P,Long}$ (rad/s)	$\zeta_{P,Long}$ (~)	n/α (g/rad)	Level Phugoid Stability	Level Short Period Damping	Level Short Period Frequency
1.97	0.315	0.0984	0.059	12.52	1	1	1

Table 20-III: Lateral Handling Qualities

T_R (s)	ζ_D (~)	$T_{1/2,S}$ (s)	Level Roll Time Constant	Level Roll Performance	Level Dutch Roll Frequency	Level Dutch Roll Damping	Level Spiral Stability
0.41	0.32	14.73	1	1	1	1	1

Figure 20.3 and Figure 20.4 depict the outputted design point against handling quality levels from AAA.

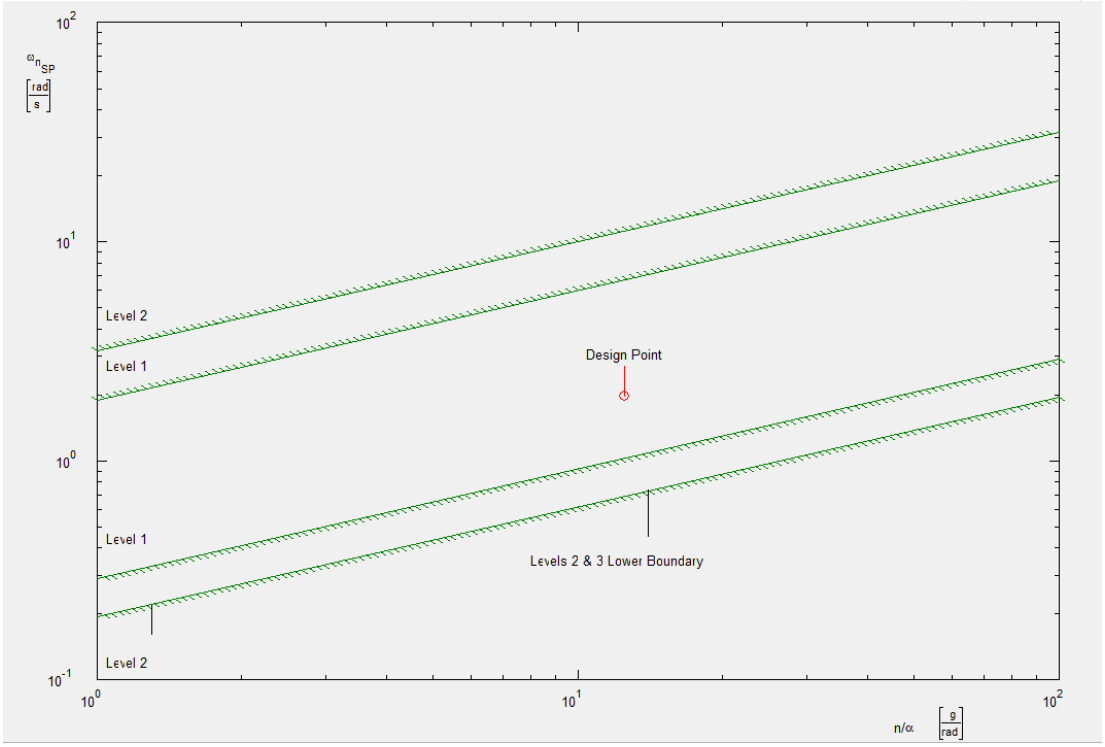

Figure 20.3: Longitudinal Handling Quality Level from AAA

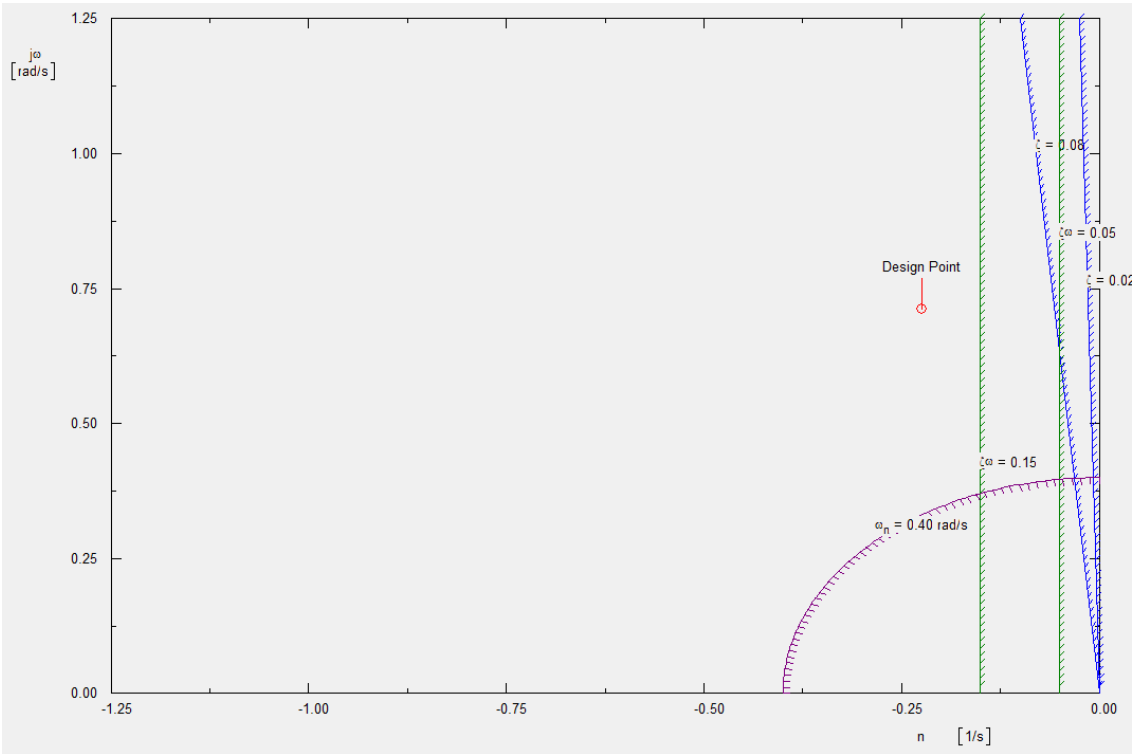

Figure 20.4: Lateral Handling Quality Level from AAA

Figure 20.5 outlines the trim diagram in the cruise condition for the Chimera. This was generated using AAA software based on Class II stability and control inputs.

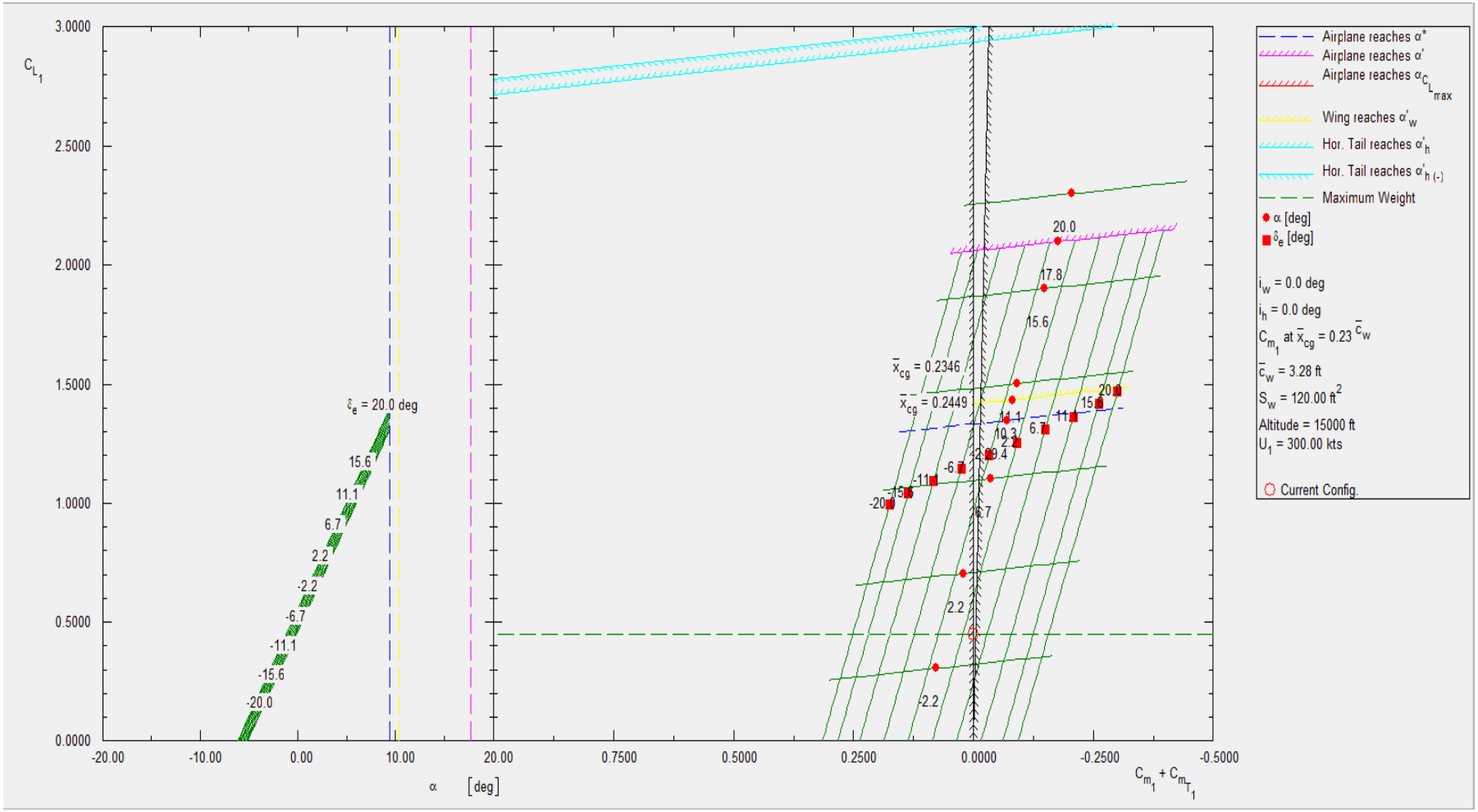

Figure 20.5: Chimera Cruise Trim Diagram from AAA

21. Class II Performance Analysis

A Class II performance analysis was performed on the Chimera to assess its flight envelope. First, the rate of climb for the Chimera was assessed for various possible weights. This analysis is shown in Figure 21.1. Multiple weights were assessed to show how the performance could vary for the mission. The service ceiling was determined as the altitude where climb could reach a minimum of 100 feet per minute. The cruise ceiling is the altitude where the Chimera can climb at a minimum of 300 feet per minute. The combat ceiling is the altitude at which the Chimera can climb at a minimum of 500 feet per second.

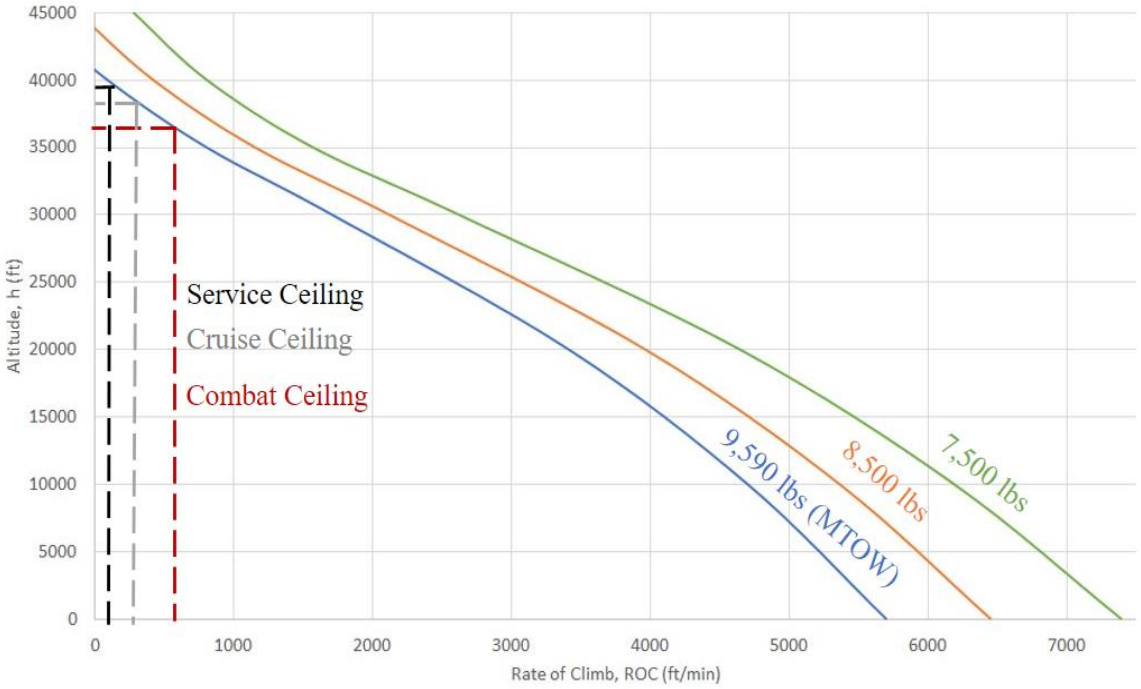

Figure 21.1: Chimera Rate of Climb at Various Altitudes

Next, the turn radius of the Chimera was analyzed and compared to available data. The turn radius for the T-6, T-34C, and Chimera are shown against airspeed in Figure 21.2. The data for the T-6 and T-34C were taken from Reference 56. The Chimera is very comparable to the T-6 and the T-34C in terms of maneuverability. The analysis of the Chimera was performed using Equation 21.1 through

Equation 21.4 to derive the relevant boundaries of the chart. These provide the limits of the rates for which the Chimera can turn.

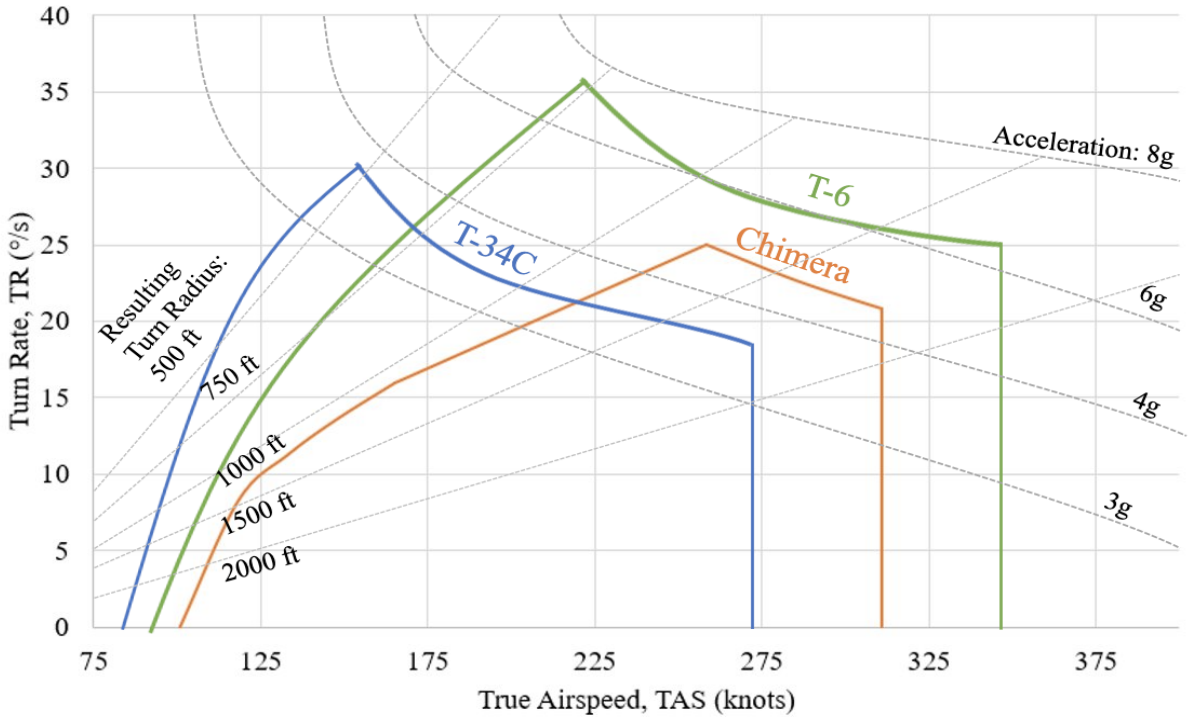

Figure 21.2: Turn Rate vs. Airspeed

Equation 21.1: $TR = \frac{g\sqrt{n^2-1}}{U_1}$

Equation 21.2: $TR = \frac{U_1}{r}$

Equation 21.3: $TR = \frac{g\sqrt{\frac{C_{Lmax,clean}\bar{q}}{W/S}-1}}{U_1}$

Equation 21.4: $TR = \frac{g}{U_1}\left[\left(\frac{\bar{q}}{W/S}\right)^2\left[\frac{T_{av}}{\bar{q}S} - C_{D0}\right]\pi Ae - 1\right]$

22. Class II 3-View, Advanced CAD, and Exploded Views

Figure 22.1 and Figure 22.2 below show the Class II 3-View and exploded views of the Chimera respectively. Overall dimensions can be seen in the 3-view below.

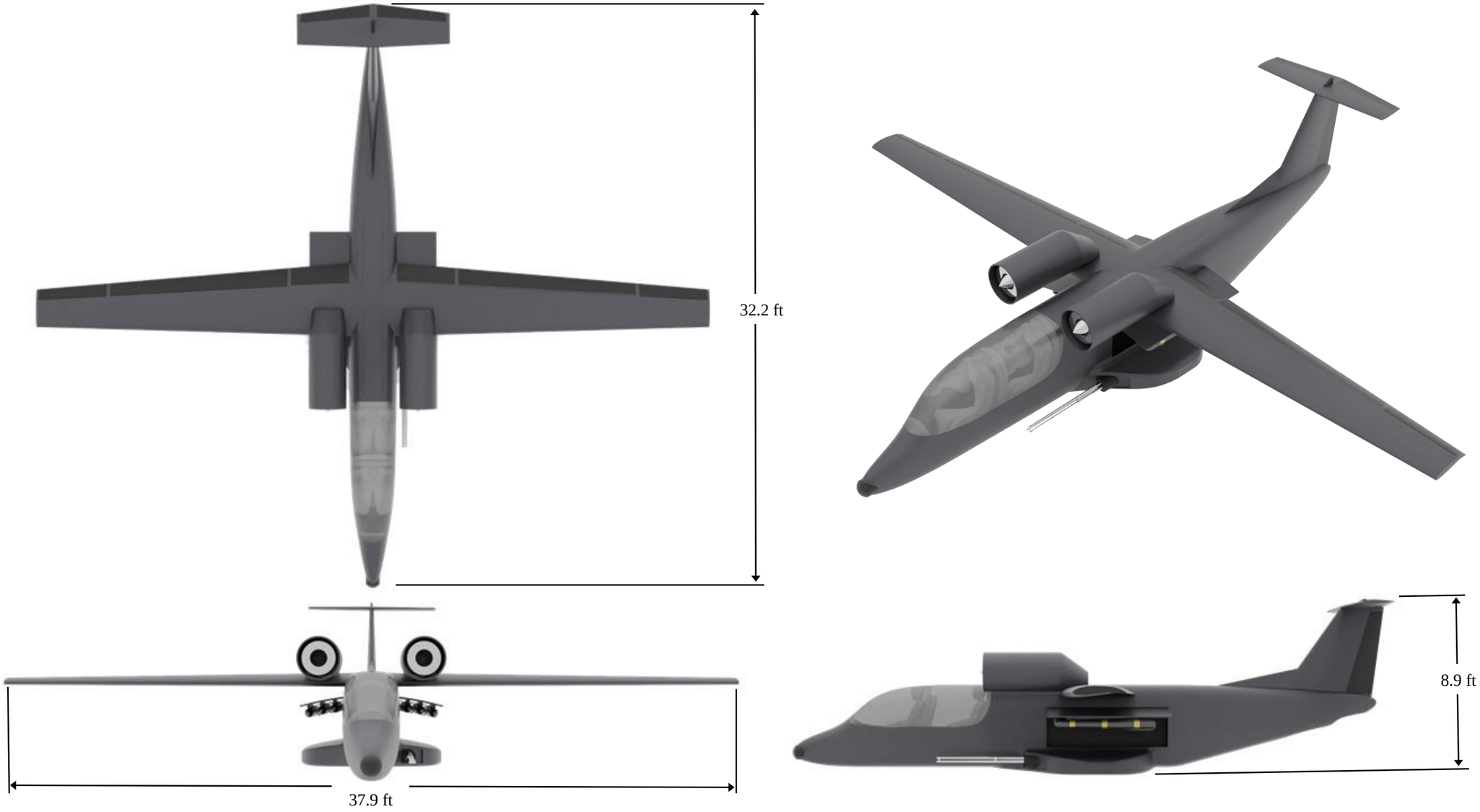

Figure 22.1: Chimera 3-View

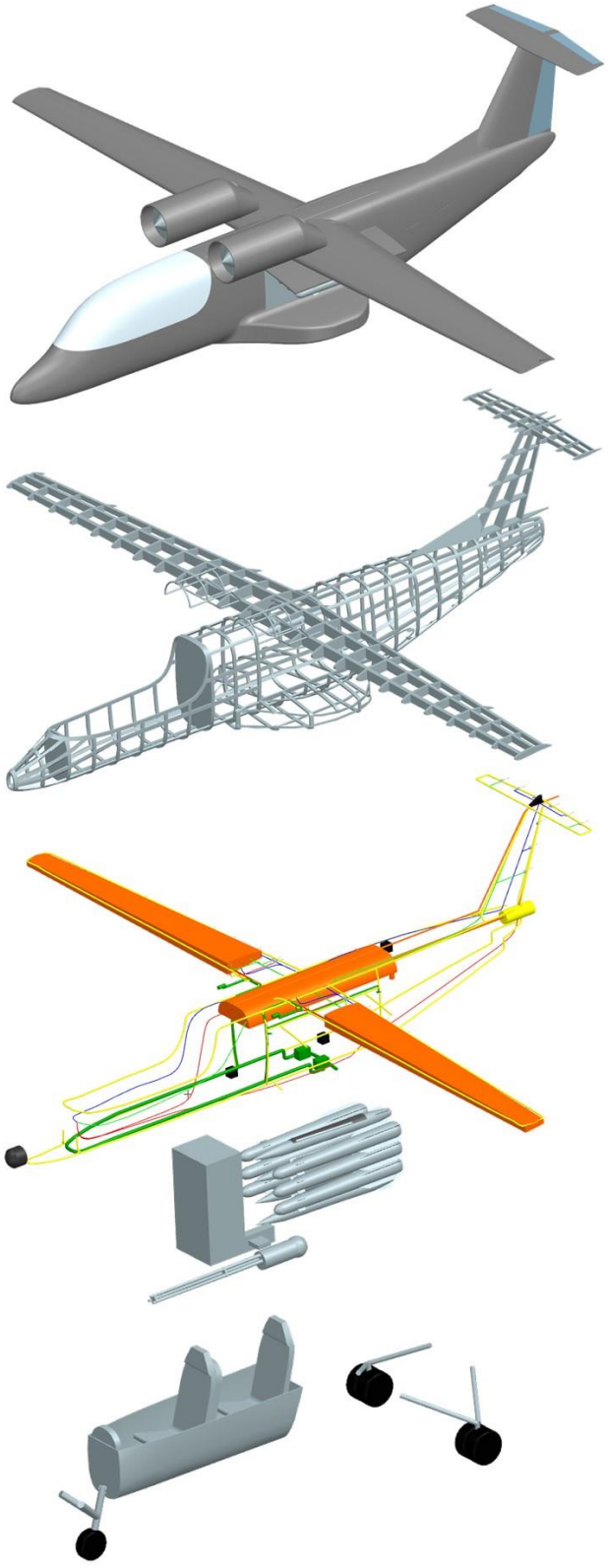

Figure 22.2: Chimera Exploded View

Shown in Figure 22.3 and Figure 22.4 below are the side and top views of the Chimera with the CG and AC locations included in them. The red dot is the aircraft mean C.G. location during flight operations while the yellow dots are the AC locations of different parts of the aircraft. The tail moment arms are also included in the figures.

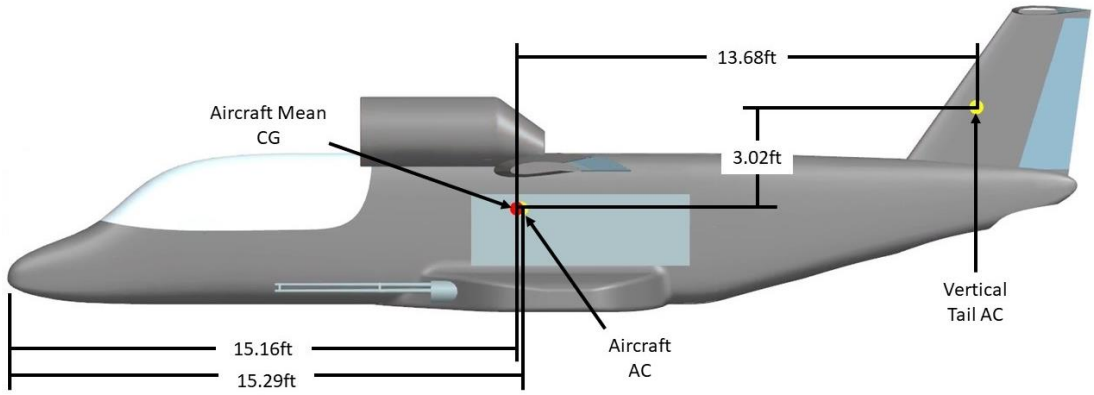

Figure 22.3: Chimera Aerodynamic Side View

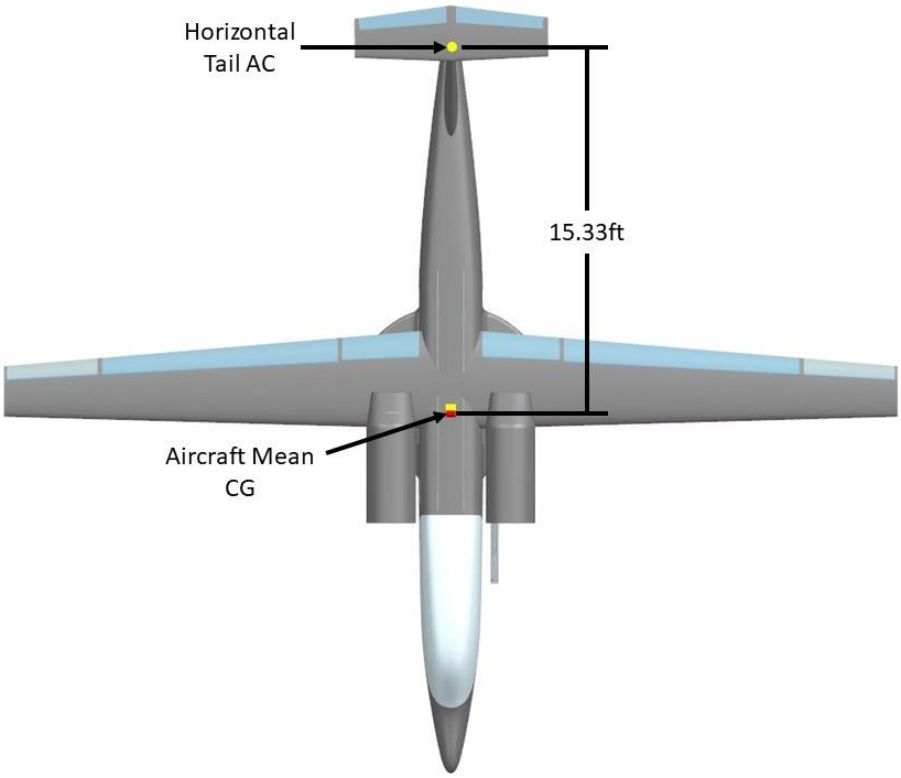

Figure 22.4: Chimera Aerodynamic Top View

23. Bill of Materials

The bill of materials for the Chimera is shown below in Table 23-I. The Chimera will be primarily made of composite materials to keep the maximum weight of the aircraft low. The blown over flaps behind the engine are required to be titanium since they will be exposed to the hot exhaust. The main structure of the Chimera will be made of aluminum-lithium composite to be very strong, but also keep the Chimera lightweight.

Table 23-I: Bill of Materials

Part Number	Part Name & Info	Material	Quantity Required (per Aircraft)	Source/Supplier	Approximate Component Weight (lbs)
1	Main Gear Tires 15 x 6	n/a	4	BFGoodrich	55
2	Nose Gear Tires 13 x 5	b/a	1	BFGoodrich	6
3	Main Gear Strut	Stainless Steel	2	n/a	230
4	Nose Gear Strut	Stainless Steel	1	n/a	41
5	Gear Retraction Actuator	n/a	3	Textron Actuator Division	40
6	Ailerons and Fowler Flaps	Kevlar	4	GKN Composites Inc.	6
7	Blown Over Flaps	Titanium	2	TMS Titanium	3
8	Elevator	Kevlar	2	GKN Composites Inc.	6
9	Rudder	Kevlar	1	GKN Composites Inc.	5
10	FJ44 Powerplants	n/a	2	Williams International	460
11	Mk10 Ejection Seat	n/a	2	Martin Baker	80
12	Upper Wing Skin	APC-2 PEEK/graphite composite	1	GKN Composites Inc.	200
13	Lower Wing Skin	APC-2 PEEK/graphite Composite	1	GKN Composites Inc.	180
14	Fuselage Skin	APC-2 PEEK/graphite Composite	1	GKN Composites Inc.	580
15	Aircraft Structure	Aluminum Lithium Composite	1	Arconic	1000

24. Advanced Technologies and Program Risk Mitigation

The Chimera has been designed to accommodate new, advanced technology throughout its minimum 25-year service life. If critical new technology is developed, the Chimera is meant to be flexible in its munitions and sensors. The ability to readily accept new technology will help the Chimera provide the best value to the purchaser over the lifetime of the platform. The modularity of the Chimera will also help to mitigate the risk to purchaser by ensuring the Chimera can adapt when new weaponry overmatches what is currently available.

Figure 24.1: Northrop Grumman Sky Viper Chain Gun [57]

The Chimera is currently designed with an M197 electric cannon, which has been fielded since 1967 and has been used in the AH-1W and AH-1Z gunships. While the M197 is reliable and meets the needs of the Chimera's mission, new cannons are being developed. Northrop Grumman announced recently that they are building a new 20mm cannon that is supposedly more accurate than the AH-64's 30mm chain gun [8]. The gun will be called the Sky Viper and is expected to be of a similar size to the M197 and is shown in Figure 24.1.

The Chimera will also be able to accommodate larger caliber cannons, however the ammo system will also need to be changed to allow for the larger BASS rounds. These larger cannons may adjust some of the aircraft's performance, as the C.G. location will move, and the recoil will be different, but the Chimera has plenty of rudder authority to handle the recoil, and the cannon is mounted very close to the current design's C.G.

The Chimera currently holds 4 GBU 39 glide bombs. In the future, the Chimera can be modified easily to hold any bombs of the same or smaller size just by fitting them into a new foam sabot, this will easily allow for the GBU 53 to fit in the Chimera in its current design, and possibly any newly developed small-diameter bombs. If a larger bomb like the Mk. 82 is desired, then the aircraft bay can be modified

to have larger bomb tubes, however, as the diameter of the bomb grows, the number of bombs held will have to decrease.

It is expected that two pilots will not be needed in order for the Chimera to successfully complete most of its missions. While most similarly sized light-attack aircraft utilize two pilots, planes like the A-10, F-35, and F-16 all conventionally have one pilot and perform missions successfully. The RFP calls for an aircraft to have two pilots, and the Chimera delivers on that, however the Chimera has also been designed with idea in mind that one pilot can complete the mission. If needed a remote gunner may be utilized like how the MQ-9 uses a remote pilot/gunner. The space required for the second seat can be used for communications infrastructure and the fuselage could also be shortened if the second seat is removed. The MQ-9 control room is shown below in Figure 24.2.

Figure 24.2: Current MQ-9 Virtual Cockpit [58]

25. Class II Cost Estimates

The purpose of this chapter is to present the costs associated with the Chimera program. Each value presented in this chapter was estimated using the cost module in AAA. It should be noted each of the cost values are for 50 or 1,000 aircraft with 1,200 flight hours per year along with six separate aircraft dedicated for the research and development phase. Table 25-I depicts cost breakdowns for each phase of the Chimera program.

Table 25-I: Chimera Cost Breakdown

	Item	50 Units Cost ($)	1000 Units Cost ($)
Research, Development, Test, and Evaluation	Airframe Engineering and Design	$26.5 M	$26.5 M
	Development, Support, and Testing	$7.8 M	$7.8 M
	Flight Test Airplanes	$148.5 M	$148.5 M
	Flight Test Operations	$2.1 M	$2.1 M
	Test and Simulation Facilities	$53.6 M	$53.6 M
	Financing	$29.8 M	$29.8 M
	Profit	$29.8 M	$29.8 M
	Total R.D.T.E Cost	**$298.2 M**	**$298.2 M**
Acquisition Costs	Airframe Engineering and Design	$13.4 M	$41.3 M
	Program Production	$490.8 M	$3,686.2 M
	Flight Test Operations	$11.2 M	$11.2 M
	Financing	$57.3 M	$439.0 M
	Profit	$57.3 M	$439.0 M
	Manufacturing	$572.7 M	$4,390.2 M
	Total Acquisition Cost	**$630.0 M**	**$4.8 B**
	Price per Airplane	**$18.5 M**	**$5.2 M**
Operating Costs	Fuel, Oil, Lubricants (1,200 flight hours/yr)	$42.5 M	$1.35 B
	Consumable Materials	$286.4 M	$9.1 B
	Direct Maintenance Personnel	$1.9 M	$62.9 B
	Indirect Personnel	$477 M	$15.1 B
	Spare Parts	$366.9 M	$11.6 B
	Maintenance Depot	$366.9 M	$11.6 B
	Miscellaneous Items	$146.8 M	$4.6 B
	Total Operating Cost	**$3.7 B**	**$116.6 B**
	Operating Cost per Hour	**$2795/hr**	**$2795/hr**
Life Cycle Cost	Research, Development, Test, and Evaluation	$298.2 M	$298.2 M
	Acquisition Cost	$30.0 M	$4.8 B
	Operating Costs	$3.7 B	$116.6 B
	Disposal	$46.4 M	$1.3 M
	Life Cycle Cost	**$4.6 B**	**$122.7 B**

An estimated price per airplane based on the number of airplanes in the Chimera program is shown in Figure 25.1. It is evident that as the total amount of aircraft produced increases, the price per airplane decreases. It should be noted this figure depicts a constant production run of 50 aircraft.

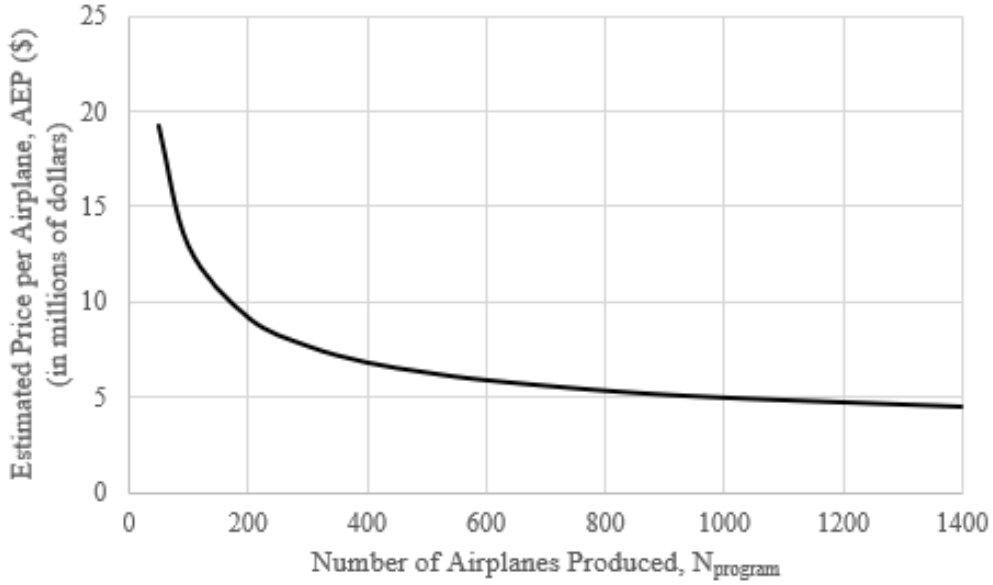

Figure 25.1: Estimated Price per Airplane

Lastly, the estimated number of manhours for the development and production of the Chimera program can be seen in Table 25-II. Similar to the price trend observed in Figure 25.1, as the number of aircraft produced increases, the total manhours spent per aircraft will decrease as a result of worker experience in the manufacturing process.

Table 25-II: Chimera Program Required Manhours

Item	50 units (Hrs)	1000 units (Hrs)
Manufacturing Manhours Required in RDTE Phase	799,977.3	799,977.3
Tooling Manhours Required in RDTE Phase	515,672.6	515,672.6
Total Engineering Manhours Required in RDTE Phase	197,981.8	197,981.8
Total Engineering Manhours Required in the Entire Program	376,966.7	505,474.4
Manufacturing Manhours Required in Manufacturing Phase	2,803,683.8	11,713,528.8
Tooling Manhours for the Whole Program	804,966.7	1,171,865.4

26. Chimera Head-to-Head Comparison to AT-6 Wolverine

The following section will outline a head-to-head comparison between the Chimera and the current light attack market leader, the AT-6 Wolverine. The ferry range of the Chimera is 2,650 nmi while the ferry range of the AT-6 is 1,725 nmi [9]. The enhanced ferry range of the Chimera allows it to cross the Atlantic Ocean without the need to refuel. This ability allows it to be rapidly deployed from the continental U.S. without any ferry assistance. This much more rapid response time is not possible with the AT-6 as the ferry range does not allow it to cross the Atlantic.

The gun system of the Chimera greatly outmatches the AT-6. The Chimera uses the M197 to fire 20 mm BASS rounds at 1,500 rounds per minute while the AT-6 fires .50 cal rounds at only 1,025 rounds per minute. The use of BASS rounds on the Chimera also allows for much better armor penetration to be achieved at all slant ranges compared to the AT-6. The Chimera's gimbaled M197 and aero-mechanically stable, long-range BASS rounds also allows for orbit fire to be achieved. No current light attack aircraft fields this capability. The orbit ability allows the Chimera to consistently fire on a target providing constant suppressive fire for ground troops. This can be much more effective than requiring stacked AT-6's to complete successive strafe runs to provide the same amount of time on target. The orbit fire also keeps the Chimera out of the threat zone while orbiting compared to the much higher risk of taking damage while strafing. A rendering of the Chimera orbit firing can be seen in Figure 26.1. A reiteration of the advantages of the Chimera's combat capabilities compared to the AT-6 Wolverine can be found in Figure 26.2.

Figure 26.1: Chimera Orbit Firing

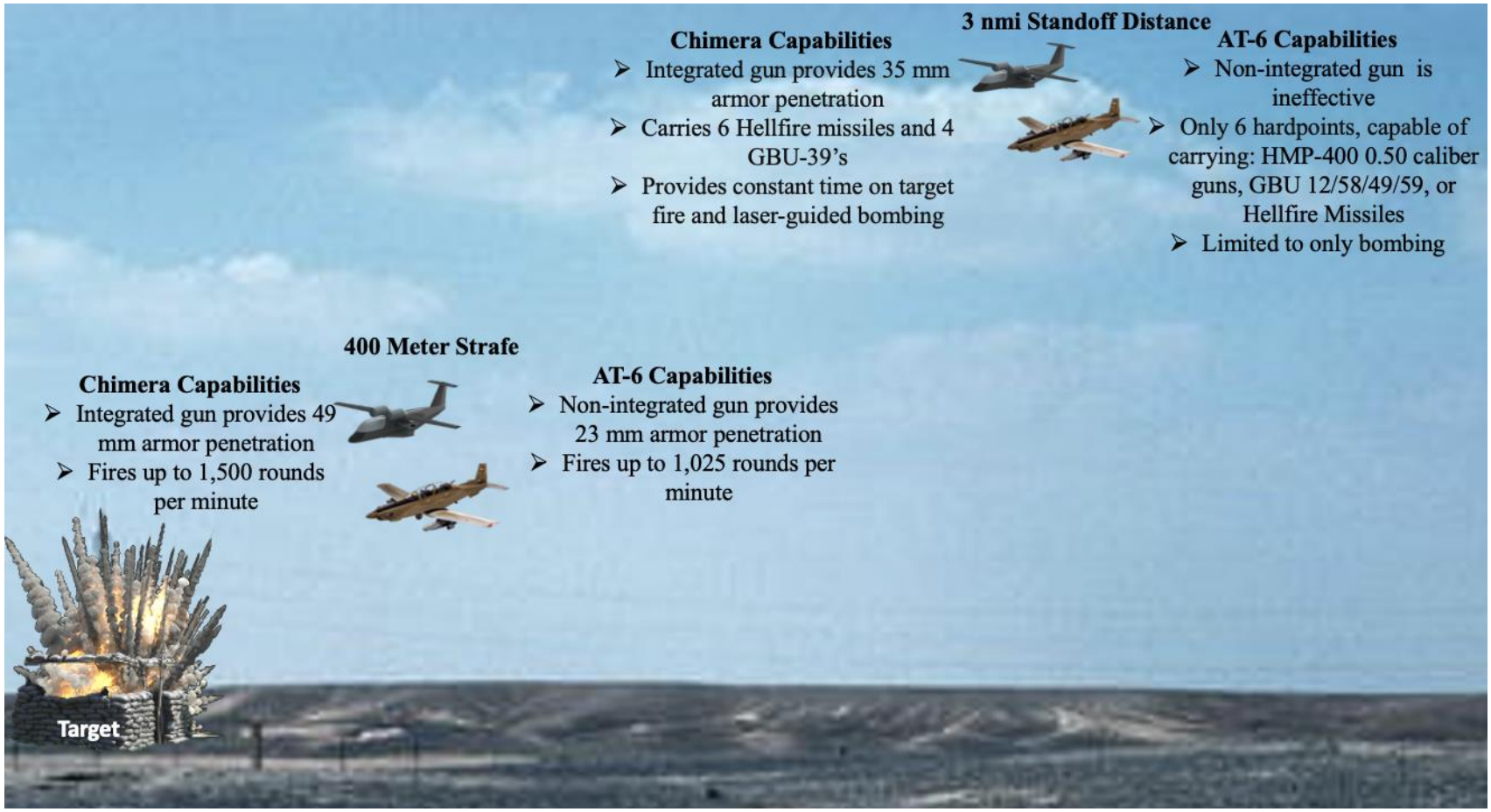

Figure 26.2: Chimera and Wolverine Head-to-Head Comparison

27. Conclusions and Expert Testimonials

While the Chimera does not look like any historical or current conventional light attack aircraft. It was designed with the intent to provide capabilities no current light attack aircraft can offer while being adaptable to the ever changing and advancing combat environment. The fully internal stores and high engine mount facilitate an LO design in the acoustic and thermal regimes. This LO design provides the Chimera with superb survivability by allowing it to enter the combat area, complete its mission, and exit the combat area before excessive enemy fire can be taken. The superb survivability helps to limit lifetime costs of the program by minimizing aircraft damage and total loss. More importantly, it helps improve the safety of the U.S. warfighter while flying in enemy territory.

The Chimera's weapon system also allows for extreme variability and optionality when choosing how to engage a target. The M197 firing 1,500 20 mm BASS rounds per minute provides enhanced armor penetration and energy upon target impact. The Chimera can also not only strafe run like a conventional attack aircraft, but also orbit fire on targets. The gimbaled gun allows for long range orbiting that provides constant suppressive fire on a target while being outside of the threat zone. The 6 Hellfire missiles and 4 GBU-39 bombs allow the Chimera to deal with more heavily armed targets and buildings as well.

Finally, the Chimera's modular design allows it to be updated with more advanced technology that becomes available over the 25-year service life to ensure it remains an effective attack aircraft.

Expert testimonials from a range of aircraft designers to combat pilots have been gathered discussing the Chimera's design and are provided below.

Figure 27.1: Chimera Final Rendering

References

1. "Chimera Logo," Chimera Investment Corporation, Available: https://www.chimerareit.com/websites/chimera/English/1000/investor-relations.html 2019.
2. "Request for Proposal; Austere Field Light Attack Aircraft," 2020-2021 AIAA Foundation Undergraduate Team Aircraft Competition, pp. [online RFP], Available: https://www.aiaa.org/designcompetitions.
3. "Junkers Ju 87," Wikipedia, Available: https://en.wikipedia.org/wiki/Junkers_Ju_87.
4. "Douglas A-1 Skyraider," Wikipedia, Available: https://en.wikipedia.org/wiki/Douglas_A-1_Skyraider.
5. "Douglas A-4 Skyhawk," Top Aces, Available: https://www.topaces.com/our-fleet/douglas-a-4-skyhawk
6. "North American Rockwell OV-10 Bronco," Wikipedia, Available: https://en.wikipedia.org/wiki/North_American_Rockwell_OV-10_Bronco.
7. "Fairchild Republic A-10 Thunderbolt II," Wikipedia, Available: https://en.wikipedia.org/wiki/Fairchild_Republic_A-10_Thunderbolt_II.
8. "Boeing AH-64 Apache," Wikipedia, Available: https://en.wikipedia.org/wiki/Boeing_AH-64_Apache
9. "Beechcraft T-6 Texan II," Wikipedia, Available: https://en.wikipedia.org/wiki/Beechcraft_T-6_Texan_II#Variants.
10. Tritten, Travis., "The Air Force wants a cheaper plane to fight terrorists. Will it survive on the battlefield?" Washington Examiner, Available: https://www.washingtonexaminer.com/policy/defense-national-security/the-air-force-wants-a-cheaper-plane-to-fight-terrorists-will-it-survive-on-the-battlefield, 17 July 2018.
11. "Embraer EMB 314 Super Tucano," Wikipedia, Available: https://en.wikipedia.org/wiki/Embraer_EMB_314_Super_Tucano.
12. "Modern Attack Aircraft Resembles WWII Fighters," Web Aviation, Available: http://webaviation.blogspot.com/2012/08/modern-attack-aircraft-resembles-wwii.html, 30 Nov. 2013.
13. "Yakovlev Yak-130," Wikipedia, Available: https://en.wikipedia.org/wiki/Yakovlev_Yak-130.
14. "Alenia Aermacchi M-346 Master," Wikipedia, Available: https://en.wikipedia.org/wiki/Alenia_Aermacchi_M-346_Master.
15. Hawk, Kitty., "Yakovlev Yak-130 'Mitten' – Review," Scalespot, Available: https://www.scalespot.com/reviews/kits/yak130-kh/review.htm, 18 Feb. 2019.
16. "The Aermacchi M-346FA: multirole master," Leonardo, Available: https://www.leonardocompany.com/en/news-and-stories-detail/-/detail/focus-aermacchi-m346fa-multirole, 08 July 2018.
17. "FN® M3P," *FN®* Available: https://fnamerica.com/products/weapon-systems/fn-m3p/#:~:text=The%20FN%C2%AE%20M3P%20is,out%20to%20nearly%201%2C850%20meters.
18. "Aircraft Guns and Gun Systems - 20-30mm Gatling Gun Systems," *General Dynamics Ordnance and Tactical Systems* Available: https://www.gd-ots.com/armaments/aircraft-guns-gun-systems/.
19. Walker, J., *GAU-8 Avenger* Available: https://www.fourmilab.ch/documents/gau-8/.
20. "Ammunition Size Chart," *DeviantArt* Available: https://www.deviantart.com/claveworks/art/Ammunition-Size-Chart-199844276.
21. *General Dynamics Ordnance and Tactical Systems* Available: https://www.gd-ots.com/.

22. "General-purpose bomb," *Wikipedia* Available: https://en.wikipedia.org/wiki/General-purpose_bomb.
23. "Paveway," *Deagel* Available: https://www.deagel.com/Defensive%20Weapons/Paveway/a001151.
24. "Laser SDB," *Boeing* Available: https://www.boeing.ca/products-and-services/defense-space-security/laser-sdb.page.
25. "Hydra 70," *Wikipedia* Available: https://en.wikipedia.org/wiki/Hydra_70.
26. "AIM-9X Sidewinder Air-to-Air Missile," *Airforce Technology@2x* Available: https://www.airforce-technology.com/projects/aim-9x-sidewinder-air-to-air-missile/.
27. "MAA-1 Piranha", *Deagle* Available: https://www.deagel.com/Defensive%20Weapons/MAA-1%20Piranha/a000953.
28. "Python (missile)," *Wikipedia* Available: https://en.wikipedia.org/wiki/Python_(missile).
29. "AGM-65b Maverick", *Deagle,* Available: https://www.deagel.com/Offensive%20Weapons/AGM-65%20Maverick/a001167.
30. "AGM-114 Hellfire," *Wikipedia* Available: https://en.wikipedia.org/wiki/AGM-114_Hellfire.
31. "Advanced Precision Kill Weapon System," *Wikipedia* Available: https://en.wikipedia.org/wiki/Advanced_Precision_Kill_Weapon_System.
32. "Products & Services," *Arnold Defense* Available: https://www.arnolddefense.com/products-and-services/.
33. Gouré, D., "The A-29 Super Tucano Is The International Market Leader For Light Attack Aircraft," Lexington Institute Available: https://www.lexingtoninstitute.org/the-a-29-super-tucano-is-the-international-market-leader-for-light-attack-aircraft/#:~:text=The%20Super%20Tucano%20costs%20around,for%20budget%20constrained%20partner%20nations.
34. Pierson, S., "Textron Aviation Defense announces $70.2M U.S. Air Force contract award for two Beechcraft AT-6 Wolverine aircraft, training and support services," Textron Inc - Investors Available: https://investor.textron.com/news/news-releases/press-release-details/2020/Textron-Aviation-Defense-announces-702M-US-Air-Force-contract-award-for-two-Beechcraft-AT-6-Wolverine-aircraft-training-and-support-services/default.aspx.
35. "Agreement between the United States of America, the United Mexican States, and Canada 7/1/20 Text," United States Trade Representative Available: https://ustr.gov/trade-agreements/free-trade-agreements/united-states-mexico-canada-agreement/agreement-between.
36. Roskam, Jan, "Airplane Design: Part I, Preliminary Sizing of Airplanes," DARcorporation, Lawrence, KS, 1997.
37. "Douglas A-4 Skyhawk," Wikipedia, Available: https://en.wikipedia.org/wiki/Douglas_A-4_Skyhawk.
38. Anon., "XFOIL Subsonic Airfoil Development System," *MIT Software*, Available: https://web.mit.edu/drela/Public/web/xfoil/ December 23, 2013.
39. "Williams FJ44," *Wikipedia,* Available: https://en.wikipedia.org/wiki/Williams_FJ44
40. Roskam, Jan, "Airplane Design: Part II, Preliminary Configuration Design," DARcorporation, Lawrence, KS, 2004.
41. Anon., "Ammunition Handbook," *NAMMO* Available: [https://www.nammo.com/wp-content/uploads/2020/05/nammo_ammo_handbook_aw_screen_updated.pdf] 5th Ed., 2018.
42. Schumacher, L., "The Development of Design Requirements and Application of Guided Hard-Launch Munitions on Aerial Platforms." Ph. D. University of Kansas, 2016.
43. Barrett, R, Schumacher, L., "Maneuvering Aeromechanically Stable Sabot System," WO/2020/217227, University of Kansas, October 10, 2020.
44. Preistle, J., "The Garzke and Dulin Empirical Formula for Armor Penetration." *NavWeaps* Available: http://www.navweaps.com/index_tech/tech-109.pdf

45. "9K333 Verba," *Wikipedia* Available: https://en.wikipedia.org/wiki/9K333_Verba.
46. Roskam, Jan, "Airplane Design: Part VI, Preliminary Calculation of Aerodynamic Thrust and Power Characteristics," DARcorporation, Lawrence, KS, 2008.
47. Roskam, Jan, "Airplane Design: Part V, Component Weight Estimation," DARcorporation, Lawrence, KS, 2010.
48. Roskam, Jan, "Airplane Design: Part IV, Layout of Landing Gear and Systems," DARcorporation, Lawrence, KS, 2010.
49. "Star SAFIRE® 380-HD," *Star Safire 380-HD Single LRU HD EO/IR Imaging System | FLIR Systems* Available: https://www.flir.com/products/star-safire-380-hd/.
50. Anon., "Dassault Falcon Ice and Rain Protection," *Smart Cockpit*., Available: https://www.smartcockpit.com/docs/DASSAULT_FALCON_000DX-EX-Ice_and_Rain_Protection.pdf
51. "Products," Martin-Bake Website, https://martin-baker.com/products/
52. "Aerial Stores Lift Truck," *Hydraulics International Inc.*, Available: http://megmar.pl/wp-content/uploads/2016/09/MJ-1C.pdf
53. "UALS - 20mm Universal Ammunition Loading System," *General Dynamics Ordnance and Tactical Systems* Available: https://www.gd-ots.com/armaments/aircraft-platform-systems/uals/.
54. Roskam, Jan, " Advanced Aircraft Analysis," DARcorporation, Available: https://www.darcorp.com/advanced-aircraft-analysis-software/, 2021.
55. "Aircraft Rain Protection," *SKYbrary*, Available: https://www.skybrary.aero/index.php/Aircraft_Rain_Protection
56. Nordlund, Robert "Energy–Maneuverability (E–M) Plot," *MATLAB Central File Exchange.* Available: https://www.mathworks.com/matlabcentral/fileexchange/42632-energy-maneuverability-e-m-plot, 2021.
57. Tegler, E., "Northrop Grumman's Sky Viper Chain Gun," *Forbes Online:* [https://www.forbes.com/sites/erictegler/2021/03/24/northrop-grummans-sky-viper-chain-gun-may-get-a-shot-at-the-armys-fara-helicopter/?sh=22b6dded1f05] March 24, 2021.
58. Subbaraman, N., "In the Virtual Cockpit," *NBC News Online:* [https://www.nbcnews.com/technolog/virtual-cockpit-what-it-takes-fly-drone-1c9319684] April 13, 2013.